Localization and Density of States of Disordered Low-Dimensional Systems in a Magnetic Field

Dissertation
zur Erlangung des Doktorgrades
des Fachbereichs Physik
der Universität Hamburg

vorgelegt von

Riccardo Mazzarello

aus Genova (Italien)

Hamburg
2004

Gutachter der Dissertation:

1. Prof. Dr. Bernhard Kramer

2. PD Dr. Stefan Kettemann

Gutachter der Disputation:

1. Prof. Dr. Bernhard Kramer

2. Prof. Dr. Hajo Leschke

Datum der Disputation:

09.06.2004

Vorsitzender des Prüfungsausschusses:

Prof. Dr. Douglas Fay

Vorsitzender des Promotionsausschusses:

Prof. Dr. Roland Wiesendanger

Dekan des Fachbereichs Physik:

Prof. Dr. Günter Huber

In this work we investigate the influence of magnetic fields on the localization and the density of states of fermions in some low-dimensional disordered systems.

The first part is concerned with the localization of electrons in thick, disordered wires in the presence of a constant magnetic field. The second part deals with some properties of Composite Fermions in the Fractional Quantum Hall Effect and with the related problem of free fermions moving in a 2D static, random magnetic field.

In part 1 we investigate the averaged localization length of fermions in a quasi 1D system as a function of a magnetic field applied perpendicular to the wire. We show that the localization length increases with the magnetic field by calculating the autocorrelation function of spectral determinants. For strong fields, the localization length saturates at twice its value without magnetic field, in agreement with previous analytical and numerical work. The crossover behaviour of the localization length is shown to be governed by the magnetic phase shifting rate. We derive this quantity analytically in a general, closed form. We compare our results with recent experimental work.

In part 2, chapter 5, we investigate the spin polarization of the FQHE ground states at fixed filling factors within a model of spinful, non-interacting Composite Fermions. We show that transitions between differently polarized ground states as a function of the magnetic field occur, in agreement with recent experiments. We also investigate the effect of temperature, disorder and spin-orbit scattering on the transitions.

In chapter 6 we consider the problem of a fermion subject to a static random magnetic field with large mean. This problem is also important for the Composite Fermion description of the Fractional Quantum Hall Effect. We investigate the properties of the localized states which determine the spectrum in the tails of the density of states. We calculate the Density of States in the tails as a function of the energy and the mean value of the RMF within the framework of the Optimum Fluctuation Method. We show that, near the centres of Landau bands, the DOS is a Gaussian function of the energy, whereas the energy dependence of the DOS is non-analytic near the band edge.

In dieser Arbeit untersuchen wir den Einfluß von Magnetfeldern auf das Lokalisierungsverhalten und die Zustandsdichte von Fermionen in niedrigdimensionalen Systemen.

Der erste Teil beschäftigt sich mit der Lokalisierung von Elektronen in dicken, ungeordneten Drähten in einem konstanten Magnetfeld. Der zweite Teil handelt von einigen Eigenschaften von *Composite Fermions* im Fraktionalen Quantenhalleffekt(FQHE) und dem zugehörigen Problem von sich in einem statischen, zweidimensionalen Zufallsmagnetfeld bewegenden, freien Fermionen.

In Teil 1 untersuchen wir die gemittelte Lokalisierunglänge von Fermionen in einem quasi-eindimensionalen System als Funktion des senkrecht zum Draht angelegten Magnetfeldes. Wir berechen die Autokorrelationsfunktion der Spektraldeterminanten und zeigen, dass die Lokalisierungslänge mit dem Magnetfeld ansteigt. Für starke Felder sättigt die Lokalisierungslänge beim zweifachen ihres Wertes im Fall ohne Magnetfeld, in Übereinstimmung zu bestehenden analytischen und numerischen Arbeiten. Es wird gezeigt, dass das Übergangsverhalten von der magnetischen Phasenverschiebung bestimmt wird. Wir leiten dies analytisch in allgemeiner, geschlossener Form her, und vergleichen unsere Ergebnisse mit jüngsten experimentellen Arbeiten.

In Teil 2, Kapitel 5 untersuchen wir die Spinpolarisation des FQHE Grundzustands bei festen Füllfaktor in einem Modell von nicht-wechselwirkenden, spinbehafteten *Composite Fermions*. Wir zeigen in Übereinstimmung mit jüngsten Experimenten, dass Übergänge zwischen verschieden polarisierten Grundzuständen als Funktion des Magnetfeldes auftreten. Wir untersuchen ebenfalls den Einfluß der Temperatur, Unordnung und Spinbahnwechselwirkung auf die Übergänge.

In Kapitel 6 behandeln wir das Problem eines Fermions in einem statischen Zufallsmagnetfeld mit grossen Mittelwert. Dieses Problem ist ebenfalls wichtig für die *Composite Fermion*-Beschreibung des FQHE. Wir untersuchen die Eigenschaften der lokalisierten Zustände, welche das Spektrum in den Schwänzen der Zustandsdichte bestimmen. Wir berechnen die Zustandsdichte in den Schwänzen als Funktion der Energie und des mittleren Wertes des Zufallsmagnetfelds im Rahmen der *Optimum Fluctuation* Methode. Wir zeigen, dass nahe dem Zentrum der Landaubänder die Zustandsdichte eine Gaußfunktion der Energie ist, wohingegen die Energieabhängigkeit der Zustandsdichte an den Bandrändern nicht mehr analytisch ist.

Contents

Introduction

The physics of disordered systems with reduced dimensionality has been the subject of intense theoretical and experimental research in the past 30 years.
Until recently, disorder was always assumed to be of electrostatic nature and connected with the presence of impurities and imperfections in the crystal.
Quantum interference effects in a disordered electrostatic potential drastically affect the properties of the electronic wavefunctions. According to the celebrated scaling theory of localization, disordered, non-interacting one-dimensional (1D) and two-dimensional (2D) systems at the absolute zero of temperature are insulators since all the one-particle wave functions are localized, no matter how weak the disorder is. The exponential localization of all the eigenstates has been proven rigorously for 1D and quasi 1D systems. The 2D case is more difficult to tackle since it lies at the edge between metallic and insulating. On the contrary, three-dimensional systems exhibit a disorder induced metal-insulator transition (MIT). In the 2D and 3D case, the only available rigorous results concern the exponential localization of electrons in the tails of quantum-mechanically allowed energy bands.

The application of a magnetic field induces changes in the phase of the wave functions and thus affects interference effects. Roughly speaking, such effects are reduced due to the breaking of time reversal symmetry. As a consequence, in the presence of a strong magnetic field, the localization length of electrons in quasi 1D systems is doubled. As far as 2D systems are concerned, the interplay of disorder and high magnetic fields is responsible for the Integer Quantum Hall Effect. In this regime, Landau levels are broadened into bands and states are localized in the tails of the bands. Near the centres of Landau bands, there are singularities in the localization length as a function of the energy and thus localization-delocalization transitions induced by the magnetic field occur.

In the above scenario, electron-electron interactions enter only at non zero temperature as a dephasing source which upsets quantum interference and localization. However, their effects can be more dramatic. For instance, it is well known that Coulomb interactions alone can induce a MIT, the so called Mott-Hubbard transition. An understanding of many experimentally observed MITs, especially in highly doped semiconductors, is not possible without taking both

disorder and interactions into account.

As regards 2D systems in a strong magnetic field, the interplay of Coulomb interactions and disorder leads to the Fractional Quantum Hall Effect. In this regime, due to interactions and high magnetic fields, electrons form new, collective ground states. Until recently, much of our understanding of this effect was based only on the study of trial ground state wavefunctions and not on any systematic perturbative approach.

Recently, a new theory of the FQHE has been developed, the so called Composite Fermion theory. Within the framework of this theory, a new object, the Composite Fermion (CF), made out of one electron and an even number of flux quanta attached to it, is introduced. It turns out that CFs behave in many respects like weakly correlated fermions with strongly renormalized quasiparticle effective parameters due to CF-CF interactions. At the noninteracting CF quasiparticle level, the FQHE of electrons is mapped onto the IQHE of CFs. Many important features of the FQHE can be addressed at this level.

Due to their composite nature, CFs experience a fictitious random magnetic field (RMF) in addition to the external one and to the scalar disorder potential due to impurities. Owing to its relevance in this effective description of the FQHE, the problem of a fermion moving in a 2D RMF has attracted considerable interest recently. Furthermore, stochastically inhomogeneous magnetic fields can now be experimentally realized in various ways.
This problem is directly amenable to the theory of noninteracting particles and it has been shown that a 2D electron gas in a static RMF belongs to the conventional unitary universality class. Therefore, all the states are expected to be localized in such systems when the RMF has zero mean value and the Quantum Hall Effect ought to occur when the average value of the RMF is large.

In this thesis we investigate the localization of electrons in quasi 1D wires in the presence of a magnetic field and the localization of fermions in 2D subjected to a random magnetic field with large mean value in the tails of Landau bands. We calculate the leading exponential factor of the density of states in these tails. We also study the spin polarization of the FQHE ground states in terms of non interacting spinful CFs.

In chapter 1, we give an introduction to some of the most successful approaches to localization in disordered systems. After discussing the weak localization corrections to the transport properties of such systems, we turn to the scaling theory of localization and then to a field-theoretic approach, the supersymmetric non-linear σ-model.

In chapter 2 we investigate the influence of a magnetic field on the localization properties of electrons in quasi 1D systems by means of a spectral correlation function, the autocorrelation of spectral determinant. The averaged localization length is derived as the crossover length scale from correlated to uncorrelated energy level statistics. This approach enables us to calculate the localization

length in the crossover region between the orthogonal ensemble (no magnetic field) and the unitary ensemble (moderately strong magnetic field). We derive the magnetic phase shifting rate analytically in a very general, closed form. This quantity is shown to govern the crossover behaviour of the localization length. For strong fields, we show that the localization length saturates at twice its value without magnetic field, in agreement with previous analytical work. Direct quantitative comparison with recent experiments is given.

In chapter 3 we discuss the general theory of the IQHE and the FQHE while in chapter 4 we introduce the theory of spinless Composite Fermions. In the latter chapter we also calculate explicitly the correlator of the random magnetic field experienced by CFs.

In chapter 5 we investigate the spin polarization of the FQHE ground states at fixed filling factors within a model of spinful, non-interacting Composite Fermions. We show that transitions between differently polarized ground states as a function of the magnetic field occur, in agreement with recent experiments. The effect of the fictitious, static RMF on the spin polarization transitions is also investigated, as well as the effect of temperature and spin-orbit scattering.

In chapter 6 we consider a fermion (electron or Composite Fermion) in 2D subject to a static RMF with large mean value and we investigate the properties of the localized states which determine the spectrum in the tails of the density of states. This analysis enables us to calculate the dependence of the Density of States on the energy and the mean value of the RMF in the tails within the framework of the Optimum Fluctuation Method. We show that, near the centres of Landau bands, the DOS is a Gaussian function of the energy, whereas the energy dependence of the DOS is non-analytic near the band edge.

Chapter 1

Localization in Disordered Systems

In this chapter we address the quantum-mechanical motion of a particle in a random, static potential. Due to quantum interference processes, disorder localizes all the electronic wavefunctions in one-dimensional and two-dimensional systems. In three dimensions, a transition from metallic to insulating behaviour occurs by changing the strength of disorder.

We start this chapter by discussing the first quantum corrections to the classical behaviour of disordered systems, the weak localization corrections. Then the suppression of this effect due to a magnetic field is discussed, as well as the effect of spin-orbit scattering and spin-flip scattering.

Finally, we focus on more sophisticated, non-perturbative theories of quantum localization. After presenting the scaling theory of localization, we briefly discuss the supersymmetric non-linear σ-model, which has led to significant advances in the study of this problem.

1.1 Weak Localization

In this section we will consider a gas of noninteracting electrons which experience a scalar potential $V(\mathbf{r})$ created by a random distribution of static impurities. The Hamiltonian $p^2/2m_e + V(\mathbf{r})$ is time-reversal invariant (TRI). We will assume that the impurities are dilute, i.e. both the Fermi wavelength λ_F and the range a of the impurity potential are much smaller than the mean free path $l = v_F \tau_{tr}$, where v_F is the Fermi velocity and τ_{tr} is the transport time, defined as the characteristic time an electron can travel before the direction of its velocity is randomized (for a δ-correlated random potential τ_{tr} coincides with the momentum relaxation time τ, see subsection 1.1.1).

Semiclassically, the stochastic motion of electrons in a disordered metal at $T = 0$ is described by the Boltzmann equation [1]. In transport theory of mesoscopic

systems, the large-distance and long-time behaviour of the particle (compared to l and $\tau_{\rm tr}$ respectively) is of interest: in this limit the Boltzmann equation simplifies drastically, yielding the diffusion equation

$$\left(\frac{\partial}{\partial t} - D\nabla^2\right) n(\mathbf{r}, t) = 0. \tag{1.1}$$

The classical transport of disordered metals is thereby characterized by the diffusion constant D, which is related to the conductivity σ by the Einstein relation $\sigma = 2e^2\rho D$, where $-e$ is the electron charge and ρ the density of states. In this picture, quantum mechanics only determines the scattering cross section for electron-impurity scattering in the Boltzmann equation.

It was realized in [2, 3] that fundamental quantum interference effects yield corrections to the classical conductivity. These effects can be qualitatively understood by considering the return probability of a particle, i.e. the probability p_t for an electron which started at a point $\mathbf{r}$ at time 0 to arrive at the same point at time t. According to Feynman, this quantity is the modulus squared of the integral over all paths which start at $\mathbf{r}$ at 0 and end at $\mathbf{r}$ at t:

$$p_t = |\sum_{\eta} A_\eta|^2 = \sum_{\eta} |A_\eta|^2 + \sum_{\eta \neq \eta'} A_\eta A^*_{\eta'}, \tag{1.2}$$

where A_η, the amplitude for the path η, is:

$$A_\eta = \exp\{\frac{i}{\hbar}\int_0^t d\tau (1/2 m_{\rm e}\dot{\mathbf{r}}^2_\eta(\tau) + V(\mathbf{r}_\eta(\tau)))\} \tag{1.3}$$

When $\lambda_{\rm F} \ll l$, only classical paths have to be included. Hence, the first term in equation 1.2 is the classical return probability and the second represents the interference of various amplitudes. For most paths the interference is not essential since their phases differ strongly and, therefore, the interference terms also differ strongly. Hence, the average value of the interference term will vanish when summing over all paths [2, 4]. However, owing to the TRI of our model, the amplitudes of time-reversed trajectories are equal and, therefore, the interference between them cannot be neglected. As a result, the contribution to p_t of two time-reversed paths is

$$|A_\eta|^2 + |A_{-\eta}|^2 + 2ReA_\eta A^*_{-\eta} = 4|A_\eta|^2, \tag{1.4}$$

i.e. twice its classical value. In correspondence to this enhancement of localization of electrons, there is a decrease in conductivity.

Let's now estimate the magnitude of this correction. Since the quantum mechanical width of an electron path is $\sim \lambda_{\rm F}$, the volume covered by a path in an interval dt is given by $\lambda_{\rm F}^{d-1} v_{\rm F} dt$. On the other hand, an electron spreads over a volume $(Dt)^{d/2}$ after a time interval t. Therefore, the probability P for a ray

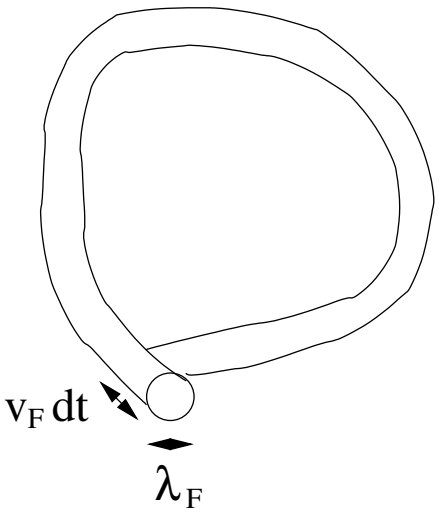

Figure 1.1: Geometry of a self-intersecting path.

tube of width $\sim \lambda_F$ to intersect itself is the ratio of these two volumes integrated over all times (see fig.1.1):

$$P \sim \int_{\tau}^{L^2/D} dt \frac{\lambda_F^{d-1} v_F}{(Dt)^{d/2}}. \tag{1.5}$$

The lower limit of integration is τ since the diffusion equation makes sense only for times $t > \tau$. As regards the upper limit, it's the time it takes for an electron to spread over the whole sample (assuming that L is the linear dimension of the sample). Hence, the weak localization corrections to σ are [4]

$$\delta\sigma \sim -\sigma P = -\frac{2e^2}{\hbar} \begin{cases} (L-l)/\pi & d=1 \\ \ln(L/l)/\pi^2 & d=2 \\ (l^{-1}-L^{-1})/\pi^3 & d=3 \end{cases} \tag{1.6}$$

At $T > 0$, inelastic scattering processes ($e^- - e^-$ and e^-−phonon interactions) tend to destroy the coherence of time-reversed paths. If we introduce a phenomenological, T-dependent phase coherence time $\tau_\phi(T)$ which accounts for all the phase breaking processes, a phase coherence length can be defined as $L_\phi(T) = \sqrt{D\tau_\phi}$. When $L_\phi(T)$ is smaller than the actual dimension of the sample L , L must be replaced by $L_\phi(T)$ in formulas 1.5 and 1.6 (see section 1.1.3).

We want to stress here again that formula 1.6 is valid provided that $\lambda_F \ll l$ or, equivalently, $k_F l \gg 1$ (k_F Fermi wave vector). Moreover, in one and two dimensions, it fails at sufficiently large length scales because the reduction in conductivity grows as L increases. This behaviour strongly supports the scaling theory of localization, which predicts that all the wavefunctions are localized in 1d and 2d systems due to disorder [2, 5] (see section 1.2.1).

1.1.1 Diagrammatic analysis

The quantum corrections to the conductivity and the return probability due to interference can be calculated in a more rigorous way by the use of diagrammatic techniques. We will consider the noninteracting Hamiltonian

$$H = \frac{\mathbf{p}^2}{2m_e} + V(\mathbf{r}), \tag{1.7}$$

where m_e is the electron effective mass and $V(\mathbf{r})$ is the random electrostatic potential. We will assume that $V(\mathbf{r})$ is Gaussian and δ-correlated and that its mean is zero:

$$\langle V(\mathbf{r})\rangle = 0 \qquad \langle V(\mathbf{r})V(\mathbf{r}')\rangle \equiv W(\mathbf{r}-\mathbf{r}') = n_i|V|^2\delta(\mathbf{r}-\mathbf{r}'), \tag{1.8}$$

where n_i is the impurity concentration. The distribution function of the disorder potential is $P(V) \propto \exp[-(n_i|V|^2)^{-1}\int d\mathbf{r}V(\mathbf{r})^2]$ and the disorder average is defined as $\langle ...\rangle_V = \int dV(\mathbf{r})P[V]...$.

In the limit of weak disorder, $\lambda_F \ll l$, the electronic self-energy Σ can be adequately estimated in the self-consistent Born approximation SCBA (see fig.1.2). In the region close to the Fermi energy, $|E - E_F| \ll E_F$, the imaginary part of Σ is given by [6]:

$$\mathrm{Im}\Sigma(E,\mathbf{p}) \equiv \frac{\hbar}{\tau} = 2\pi n_i|V|^2\rho_F, \tag{1.9}$$

where ρ_F is the Density of States at the Fermi energy and τ is the momentum relaxation time at the Fermi energy. For δ-correlated potentials, τ is identical to the transport time τ_{tr}. The real part of Σ, though divergent, can be absorbed into an irrelevant renormalization of the energy.
It can be shown that, if $\lambda_F \ll l$, diagrams where impurity lines cross can be neglected (for the self energy) [6].

Therefore, for large energies $E \sim E_F$, the averaged retarded and advanced Green's functions $G^{R(A)}$ are given by

$$G^{R(A)}(\mathbf{p},E) = \frac{1}{E - E_\mathbf{p} \pm i\hbar/2\tau}, \tag{1.10}$$

where $E_\mathbf{p} = p^2/2m_e$. Fourier tarnsforming Eq. (1.10), we get

$$G^{R(A)}(\mathbf{r}-\mathbf{r}';E) = G_0^{R(A)}(\mathbf{r}-\mathbf{r}';E)e^{-\frac{|\mathbf{r}-\mathbf{r}'|}{2l}}, \tag{1.11}$$

where $G_0^{R(A)}$ is the free electron retarded (resp. advanced) Green's function. G decays on length scales of the order of l due to elastic impurity scattering randomizing the phase of the electronic wavefunction amplitude $\Psi(\mathbf{r},t)$. The Green's function G cannot thus grasp the quantum effects described in section 1.1, which occur at larger length scales. To describe the physics on length scales

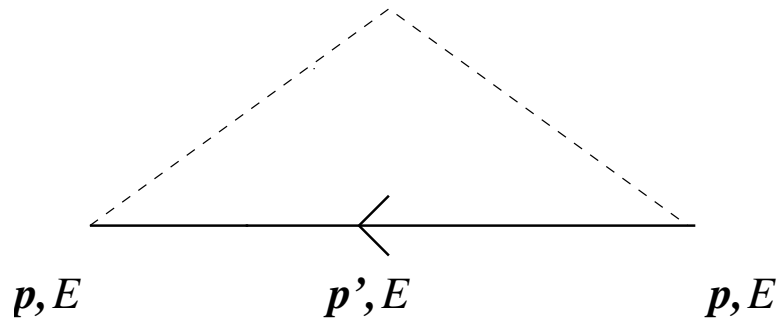

Figure 1.2: The electronic self-energy in the SCBA. The thick internal line represents the exact fermionic Green's function and the dashed line represents the impurity correlator $W(\mathbf{r}-\mathbf{r}')$.

$L > l$ (or, equivalently, on time scales $t > \tau = l/v_{\mathrm{F}}$), one needs to consider quantities containing higher moments of G, such as the disorder average of the electron density $n(\mathbf{r},t) \equiv \langle|\Psi(\mathbf{r},t)|^2\rangle$ or the averaged conductivity σ. In the following, we will consider the averaged electron density.

Since

$$\Psi(\mathbf{r},t) = \int d\mathbf{r}' G^{\mathrm{R}}(\mathbf{r},t;\mathbf{r}',t')\Psi^*(\mathbf{r}',t') \tag{1.12}$$

(where $t > t'$), the averaged density can be written as

$$n(\mathbf{r},t) = \int d\mathbf{r}' d\mathbf{r}'' \Gamma(\mathbf{r},t;\mathbf{r}',\mathbf{r}'',t')\Psi(\mathbf{r}',t')\Psi(\mathbf{r}'',t'), \tag{1.13}$$

where

$$\Gamma(\mathbf{r},t;\mathbf{r}',\mathbf{r}'',t') = \langle G^{\mathrm{R}}(\mathbf{r},t;\mathbf{r}',t)G^{\mathrm{A}}(\mathbf{r}'',t';\mathbf{r},t)\rangle. \tag{1.14}$$

Diagrammatically, this average is given by the sum of two classes of diagrams: a class where the two particle lines are not connected by impurity lines, yielding the product of the impurity-averaged propagators and a class where they are connected. The second class contains the interesting physics.

Classical diffusion (1.14) is "contained" in the quantum correlator (1.14). Since classically the evolution of the amplitude $\Psi(\mathbf{r},t)$ and its conjugate amplitude $\Psi^*(\mathbf{r},t)$ along the diffusion path are not independent, the classical diffusion is described by the ladder diagrams shown in fig 1.3. In these diagrams the impurity lines correlate the evolution of Ψ and Ψ^* at equal positions and equal times. The contribution of the generic ladder diagram with n impurity lines can be written as

$$\zeta^n(\mathbf{q},\omega), \tag{1.15}$$

where

$$\zeta(\mathbf{q},\omega) = n_{\mathrm{i}}|V|^2 \sum_{\mathbf{q}} G^{\mathrm{R}}(\mathbf{p}',E')G^{\mathrm{A}}(\mathbf{p},E)$$

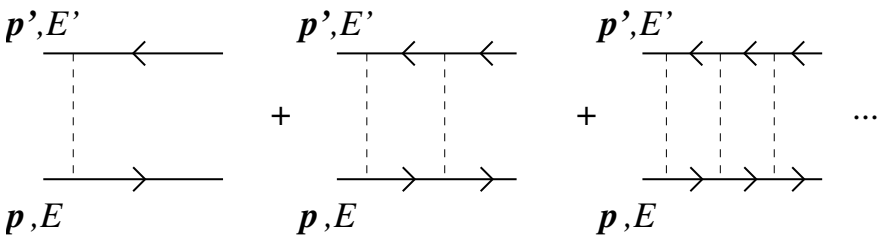

Figure 1.3: The Diffuson ladder diagrams.

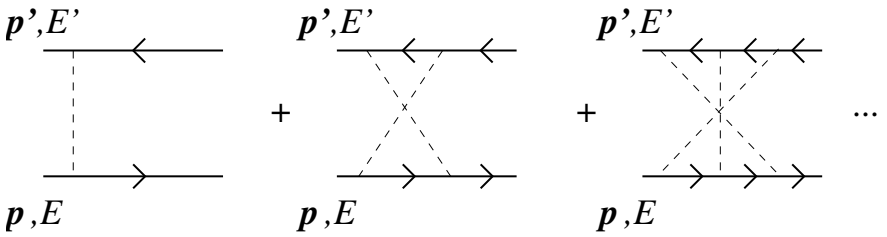

Figure 1.4: The Cooperon crossed diagrams.

$$= 1 + i\tau\omega - \tau D q^2 \tag{1.16}$$

and $\mathbf{p}' = \mathbf{p}+\mathbf{q}$, $E' = E+\omega$. Summing up the geometric series of ladder diagrams (the so called Diffuson), we get

$$D(\mathbf{q},\omega) = \frac{1/\tau}{-i\omega + Dq^2}, \tag{1.17}$$

which is indeed the Fourier transform of the propagator of the diffusion equation (1.1):

$$D(\mathbf{r},t;\mathbf{r}',t') = \frac{\theta(t-t')}{(4\pi D(t-t'))^{d/2}} e^{-\frac{(\mathbf{r}-\mathbf{r}')^2}{4D(t-t')}} \tag{1.18}$$

What about interference effects? If we twist the ladder diagrams of fig.1.3 and then exploit the time-reversal invariance of our system, we get the so called maximally crossed diagrams depicted in fig.1.4 . These diagrams clearly describe the correlation of time reversed paths and are thus responsible for the weak localization corrections to the return probability. The sum of maximally crossed diagrams is called a Cooperon and is given by $C(\mathbf{p},\mathbf{p}',\omega) \equiv D(\mathbf{p}+\mathbf{p}',\omega)$ [4, 6]. We can now take a Gaussian wave packet of width a peaked at the origin at time $t = 0$ and calculate the temporal evolution of the averaged density $n(\mathbf{r},t)$. If we include both ladder diagrams and crossed diagrams in Eq. (1.13), we get

$$n(\mathbf{r},t) = \frac{1}{(4\pi Dt)^{d/2}} (e^{-\frac{r^2}{4Dt}} + e^{-\frac{r^2}{2a^2}})\theta(t), \tag{1.19}$$

where $\theta(t)$ is the step function. It follows from (1.19) that the averaged density at $\mathbf{r} = 0$ is twice as large as expected from the diffusion equation due to the Cooperon, in agreement with the qualitative considerations of section 1.1.

1.1.2 The role of magnetic fields

Classically, the transport properties of electrons in a metal are only weakly affected by a constant magnetic field B, as long as the inequality $\omega_c\tau < 1$ (where $\omega_c = eB/mc$ is the cyclotron frequency) holds [1]. For larger B (such that $\omega_c\tau \geq 1$), the bending of classical trajectories on the scale of the mean free path l is quite dramatic and interesting phenomena occur.

Quantum mechanically, a weak magnetic field can strongly affect the WL-corrections to σ since it breaks the time reversal symmetry [7, 8]. The amplitudes of two time-reversed, self-intersecting paths η and $-\eta$ acquire additional phase factors:

$$A_\eta \to A_\eta \exp\left(i\frac{e}{\hbar c}\oint_\eta \mathbf{A}\cdot d\mathbf{r}\right) = A_\eta \exp\left(i\frac{\pi BS}{\Phi_0}\right)$$
$$A_{-\eta} \to A_\eta \exp\left(-i\frac{\pi BS}{\Phi_0}\right), \tag{1.20}$$

where Φ_0 is the quantum of magnetic flux and Φ is the magnetic flux through the loop η. The phase difference between two time-reversed paths is *definite*, $\Delta\phi = 2\pi\Phi/\Phi_0$, but varies considerably for different loops. Therefore, the weak localization term acquires a random phase depending on the loop size. The randomness of the phase ultimately leads to the suppression of Cooperons and thus to the destruction of the quantum interference effects responsible for WL: the magnetic field acts as an *effective* dephasing source. The weak localization corrections to σ are now:

$$\delta\sigma/\sigma \sim \int_\tau^{L^2/D} dt \frac{\lambda_F^{d-1} v_F}{(Dt)^{d/2}} \langle e^{i\Delta\phi(t)}\rangle, \tag{1.21}$$

where $\langle \ldots \rangle$ indicates an average over all closed, diffusive paths. Upon averaging, we get $\langle \exp(i\Delta\phi(t))\rangle \equiv \exp(-t/\tau_B)$, where τ_B is an effective dephasing time due to B. The latter quantity can be estimated by arguing that interference is destroyed when the magnetic flux through a diffusive loop of size $(D\tau_B)^{1/2}$ is of the order of Φ_0:

$$BD\tau_B \sim \Phi_0 \Rightarrow \tau_B \sim l_B^2/D. \tag{1.22}$$

It is now straightforward to estimate the magnetoconductivity:

$$\sigma(B) - \sigma_{B=0} \sim \frac{e^2}{\hbar}\begin{cases} \ln\frac{eBL^2}{\hbar c} & d=2 \\ \sqrt{\frac{eB}{\hbar c}} & d=3 \end{cases} \tag{1.23}$$

The increase of σ as a function of B (negative magnetoresistance) has been observed for a long time. At $T > 0$, L must be replaced by L_ϕ and the characteristic magnetic fields are determined by the condition $l_B \sim L_\phi$, i.e., $B \sim \hbar c/eL_\phi^2$. This condition is equivalent to $\omega_c \tau \sim \hbar/\tau_\phi \epsilon_F < \hbar/\tau\epsilon_F$. In our model $\hbar/\tau\epsilon_F \ll 1$ and thereby the characteristic fields are so weak that the conventional magnetoresistance is practically zero.

For wires with diffusive width $W \gg l$, the magnetic rate varies quadratically with the magnetic field, $1/\tau_\phi(B) = D\frac{e^2}{\hbar^2}SB^2/K_D$, where S is the cross section of the wire, and the constant K_D depends on the geometry of the wire, the direction of the magnetic field and the scattering mechanisms [9]. For example, for a 2-dimensional wire of diffusive cross section in a perpendicular magnetic field, it yields $K_D = 3$.

For a wire with ballistic cross section, $W \leq l$, and a magnetic field perpendicular to its cross section, the magnetic field dependence of the weak localization correction to the conductivity is weakened by flux cancellation effects due to boundary scattering [10]. If the magnetic field is so small that less than one flux quantum $\phi_0 = hc/e$ is penetrating an area Wl, the effective dephasing rate $1/\tau_\phi(B)$ is quadratically increasing as for diffusive cross sections. However, its slope is smaller by at least a factor W/l, as a consequence of the flux cancellation effect of edge to edge skipping orbits [10, 11].

When $BWl \gg \phi_0$, the effective dephasing rate $1/\tau_\phi(B)$ was found by a semiclassical method to increase only linearly with the magnetic field B [10, 11].

To conclude, a weak magnetic field cancels the leading order WL corrections to the diffusion constant and the conductivity. However, higher order contributions from the *diffusion modes* alone lead to a renormalization of the diffusion constant even in the unitary ensembles. It is difficult to evaluate higher order contributions diagrammatically, since the junctions between diffuson ladder diagrams (so called "Hikami boxes") need to be dressed by a number of impurity lines. The problem is even harder to tackle within semiclassical schemes. In section 1.2.2 we will introduce a field theoretic approach which turns out to be ideal for solving problems which go beyond low order perturbative corrections. Moreover, we will see that higher order, subtle quantum interference effects do lead to localization of all eigenstates in low-dimensional systems, even in the presence of a magnetic field.

1.1.3 Dephasing

At nonzero low temperatures, the interaction of the electron with the environment partially destroys the weak localization effects. Energy exchange between the electron and the environment upsets the constructive interference between time-reversed paths, thus suppressing the Cooperon modes.

At very low temperatures, quasi elastic electron-electron scattering is the dom-

inant dephasing mechanism and τ_ϕ is given by $T^{-\gamma}$, where $\gamma = 2/3$ for a 1-d wire and $\gamma = 1$ for a 2-d film [12, 13].

Due to electron-phonon scattering, the exponent crosses over to $\gamma = 4$ at higher, but not too high, temperatures, fulfilling the inequality $k_{\rm B}T \ll (\hbar^2/\tau\epsilon_{\rm F})\Omega_{\rm D}$, where $\Omega_{\rm D}$ is the optical Debye phonon frequency [14]. This power can be smaller, due to the confinement, in quantum wires. At even higher temperatures, there is a crossover to $\gamma = 3$ (in some amorphous metals, to $\gamma = 2$) which is also due to electron-phonon interactions [14].

Phase coherence is also weakened by impurities with internal degrees of freedom, such as magnetic impurities. We will briefly discuss magnetic impurities in the next section.

In 1D and 2D systems, the phenomenological definition of τ_ϕ given in section 1.1.3 is not applicable at extremely low temperatures, when the phase coherence length L_ϕ becomes comparable to the localization length $L_{\rm c}$ of electronic wavefunctions. If the system size L is also larger than $L_{\rm c}$, the perturbative treatment of disorder outlined in the previous sections breaks down and a non perturbative theory is called for.

1.1.4 Magnetic impurities and spin-orbit scattering

In the presence of magnetic impurities, quantum interference is partially destroyed since the electronic path is partially kept track of, due to the flipped impurity spins revealing the visit of an electron. A phenomenological magnetic scattering rate $\tau_{\rm S}$ can be introduced to account for this new scattering mechanism.

The interaction energy of an electron with a short-range magnetic impurity located at $\mathbf{R}_i$ can be written as $H_{\rm S} = V_{\rm S}\vec{s}\cdot\mathbf{S}_i\delta(\mathbf{r}-\mathbf{R}_i)$, where $\vec{s}$ and $\mathbf{S}_i$ denote the electron and impurity spin, respectively, and $V_{\rm S}$ is the strength of the impurity-electron magnetic interaction. Assuming that the magnetic impurities are dilute (i.e. $\tau \ll \tau_{\rm S}$), the scattering rate $\hbar/\tau_{\rm S}$ takes the form [15]:

$$\frac{\hbar}{\tau_{\rm S}} = 2\pi\rho_{\rm F}(n_{\rm mi}|V_{\rm S}|^2\langle\mathbf{S_i}^2\rangle), \tag{1.24}$$

where $n_{\rm mi}$ is the magnetic impurity concentration and $\langle\ldots\rangle$ denotes an average over the (assumed) random directions of the impurity spins. If $\tau_{\rm S} \gg \tau_\phi(T)$, there is no temperature dependence of the conductivity.

Spin-orbit scattering, in contrast to magnetic-impurity scattering, does not violate time-reversal symmetry. However, its effect on the conductivity is non trivial since it reverses the sign of the quantum correction and reduces the strength by a factor of two [15]. The conductivity is then *larger* than classically expected.

We will now provide a physical picture for the spin-orbit effects following reference [16]. The scattering amplitude for the spin-orbit interaction is (again

assuming a range of the impurity potential $\ll l$):

$$V + iV_{\rm SO}(\mathbf{k} \times \mathbf{k}') \cdot \vec{s} \equiv V(1 + i\mathbf{K} \cdot \vec{s}), \tag{1.25}$$

where $\mathbf{K} = V_{\rm SO}/V(\mathbf{k} \times \mathbf{k}')$, $\mathbf{k}$ and $\mathbf{k}'$ are the electron momenta before and after scattering. This operation yields a rotation of $\vec{s}$ by angles $\mathbf{K}_i$ around the spin axis. When a particle is scattered from state $|\mathbf{k}\rangle|\vec{s}\rangle$ to state $|-\mathbf{k}\rangle|\vec{s}'\rangle$, the accumulative effects on the spin add up to a finite rotation R such that $|\vec{s}\,'\rangle = R|\vec{s}\rangle$. The matrix of the spin rotation is:

$$R = \begin{pmatrix} \cos(\theta/2)e^{i(\Phi+\phi)/2} & i\sin(\theta/2)e^{-i(\Phi-\phi)/2} \\ i\sin(\theta/2)e^{i(\Phi-\phi)/2} & \cos(\theta/2)e^{-i(\Phi+\phi)/2} \end{pmatrix}, \tag{1.26}$$

where Φ,θ and ϕ are Euler angles (see [17]). For the time-reversed scattering process, the final state is $|-\mathbf{k}\rangle|\vec{s}\,''\rangle$, where $|\vec{s}\,''\rangle = R^{-1}|\vec{s}\rangle$. Therefore, the interference term will contain an additional factor $\langle\vec{s}\,''|\vec{s}\,'\rangle = \langle\vec{s}|R^2|\vec{s}\rangle$. Assuming that $|\vec{s}\rangle = |+1/2\rangle$, the latter matrix element becomes

$$\langle\vec{s}\,''|\vec{s}\,'\rangle = -\sin^2(\theta/2) + \cos^2(\theta/2)\exp(i\Phi + i\phi). \tag{1.27}$$

If there is no spin flip, then all angles are zero and the matrix element is 1: we have the regular weak localization correction. If the spin-orbit coupling is strong, the spin state diffuses on the unit sphere and the orientations of the final spin states are statistical. Therefore the average of (1.27) yields the factor $-1/2$ (of course, this result does not depend on the initial state $|\vec{s}\rangle$).

As discussed above, an external magnetic field destroys time reversal invariance and acts as an effective dephasing force. Hence, in the case of systems with strong spin-orbit scattering, the conductivity should decrease when the magnetic field is turned on [13]. This prediction has been confirmed experimentally [16].

1.2 Strong Localization

1.2.1 Single Parameter Scaling

The dimensionless conductance of a d-dimensional macroscopically homogeneous hypercube of linear dimension L is defined as

$$g(L) \equiv \frac{G(L)}{e^2/\hbar}. \tag{1.28}$$

where $G(L) = \sigma L^{d-2}$. According to the one-parameter scaling theory of localization [2, 5], at $T = 0$ the transport properties of a disordered system are determined by $g(L)$ alone. More specifically, if we consider a hypercube of linear dimension NL and divide it into N^d identical hypercubes of length L, then the

conductance of the large cube depends only on N and the conductance of each block:

$$g(NL) = f(N, g(L)) \tag{1.29}$$

For a continuous variation of the linear dimension of the system, we get by differentiating equation (1.29) [2, 5, 6]:

$$\frac{d\ln g}{d\ln L} = \frac{L}{g}\frac{dg(NL)}{dL} = \frac{1}{g}\frac{dg(NL)}{dN} = \frac{1}{g}\frac{df(N,g)}{dN} \equiv \beta(g). \tag{1.30}$$

Therefore, the logarithmic derivative of g is solely a function of g itself. This argument is of course valid only if L is larger than any other microscopic length scale of the system (λ_F,l).

If $\beta(g) > 0$, the conductance increases with the size of the sample, and vice-versa for negative β. Therefore, the scaling function β specifies the transport properties for a system in the thermodynamic limit. The limiting behaviour for the β-function can be easily obtained: in the limit of weak disorder, i.e. for $g \gg 1$, the system should show metallic behaviour and the conductance is described by classical transport theory: $G(L) = \sigma L^{d-2}$. Hence $\beta(g) = d - 2$ depends only on the dimensionality of the system. In the limit of strong disorder ($g \ll 1$), the conductance has the form $g(L) \propto \exp(-L/\xi)$, where ξ is the localization length, and the β-function depends logarithmically on g,

$$\beta(g) = \ln g + c. \tag{1.31}$$

It is thereby negative in any dimension for small g.

It is now reasonable to assume that the scaling function is a continuous, monotonically increasing function of g and to draw it by interpolating from the asymptotic behaviour at large and small g (see fig.1.5). This assumption is corroborated by the theory of weak localization, which predicts negative corrections to the classical conductance in any dimension. For instance, from formula (1.6) we obtain for the asymptotic scaling function in the two-dimensional case:

$$\beta(g) = -\frac{1}{\pi^2 g}. \tag{1.32}$$

The first result of the scaling theory is that in 3D there is a fixed point , defined by $\beta(g_c) = 0$, which corresponds to the metal-insulator transition described by Anderson. If we start with a system with conductance larger than g_c, upon increasing the size of the sample the conductance increases and the system flows to the metallic regime. On the contrary, if the conductance of our sample is smaller than g_c, the system becomes an insulator in the limit $L \to \infty$. In the 1D and 2D case, β is always negative and therefore an insulating regime should always be reached in the thermodynamic limit, no matter how weak the disorder is.

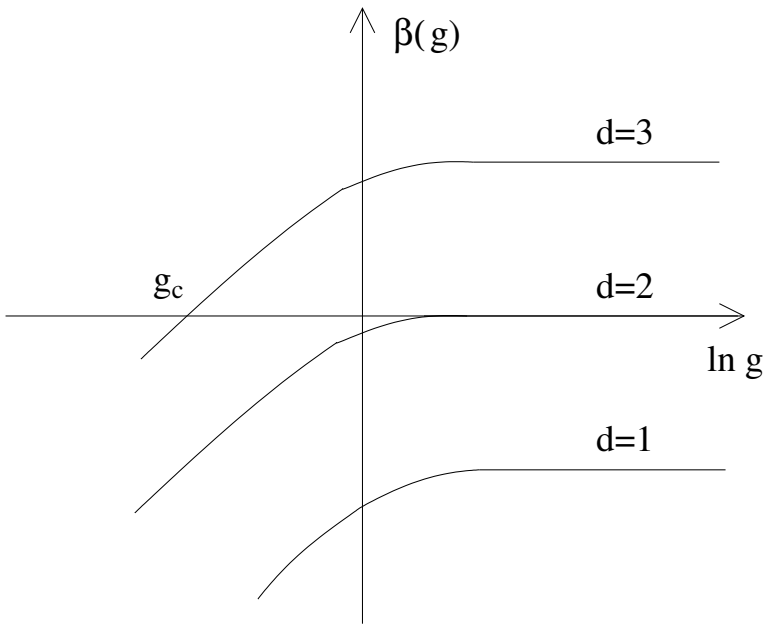

Figure 1.5: The scaling function $\beta(g)$ as a function of $\ln g$.

Shortly after the works on the scaling theory of localization, a field theoretical approach was developed in order to give a formal justification to the assumptions made in [2, 5]. The next section will de devoted to this approach.

1.2.2 The Non-Linear σ-Model

As we discussed in section 1.1.1, the average of the product $G^{\mathrm{R}}(E+\omega)G^{\mathrm{A}}(E)$ contains information on interference effects and thus quantum localization. In the diagrammatic or semiclassical theory of weak localization, that product can be calculated only perturbatively (in the parameter $1/k_{\mathrm{F}}l$). In the Supersymmetric nonlinear σ-model approach, the average $\langle G^{\mathrm{R}}_{E} G^{\mathrm{A}}_{E-\omega}\rangle$ is carried out exactly by expressing it as a functional integral over classical and Grassmannian fields [18].

Let's recall the standard integrals

$$\int \prod_{k=1}^{N} d^2 z_k \exp(-\sum_{ij} z_i^* A_{ij} z_j) = \frac{\pi^N}{\det A}, \tag{1.33}$$

$$\int \prod_{k=1}^{N} d^2 z_k z_l z_m^* \exp(-\sum_{ij} z_i^* A_{ij} z_j) = \frac{\pi^N}{\det A}(A^{-1})_{lm}, \tag{1.34}$$

where $d^2 z_k = d\mathrm{Re}z d\mathrm{Im}z = dz^* dz/2i$ and $\hat{A}$ must have a positive, real part for

convergence. If we take $\hat{A} = i(E + i\eta - \hat{H})$, the second integral yields

$$\int \prod_{k=1}^{N} dz_k^* dz_k z_m z_n^* \exp(i \sum_{ij} z_i^* (E + i\eta - H_{ij}) z_j) = \frac{-i(i\pi)^N G_{mn}}{\det(E + i\eta - H_{ij})}, \quad (1.35)$$

where $\eta > 0$.

Since the impurity potential enters the left-hand side of (1.35) only via the exponential function, it is easy to take the average of the integral for Gaussian disorder. However, performing this average does not yield the average of the electronic Green's function, since the right-hand side of (1.35) also contains the determinant of $\hat{A}$. To get rid of this awkward determinant, Efetov et al. [19, 20] introduced anticommuting Grassmann variables. It can be shown that the Grassmann analogues of the Gaussian "bosonic" integral (1.33,1.34) give

$$\int \prod_{k}^{1\ldots N} d\chi_k^* d\chi_k \exp(-\sum_{ij} \chi_i^\dagger A_{ij} \chi_j) = \det A. \quad (1.36)$$

$$\int \prod_{k}^{1\ldots N} d\chi_k^* d\chi_k \chi_l \chi_m^* \exp(-\sum_{ij} \chi_i^\dagger A_{ij} \chi_j) = (A^{-1})_{lm} \det A. \quad (1.37)$$

Therefore, by introducing a supersymmetric Gaussian integral over a set of symmetric and antisymmetric fields, one can eliminate the unwanted determinant.

Analogously, one can define the average of the product of two Green's function in terms of a more complicated functional integral of two sets (related to the G^{R} and G^{A} respectively) of Grassmann and bosonic fields, composing an eight-component supersymmetric field vector (so called superfield) ψ. After averaging, one obtains an interacting ψ^4-theory, where the interaction strength is proportional to the variance of the random potential ($n_{\mathrm{i}}|V|^2$ for the potential (1.8)). The functional integral defining $\langle G^{\mathrm{R}} G^{\mathrm{A}} \rangle$ is invariant under a group of transformations $\psi \to T\psi$; the matrices T define a symmetric space and consists of two blocks of 4×4 matrices related to the compact and non compact sector of the parameter space respectively. The off-diagonal blocks are parametrized by Grassmann variables.

The interaction term can be decoupled via a Hubbard-Stratonovich transformation by introducing a new Gaussian integral over 8×8 Q matrices. The new field must capture the full symmetry of the functional integral in order to succeed in describing quantum localization effects. Therefore, the field Q must live in the symmetric space defined by the matrices T and is thus composed of both commuting and anticommuting fields.

After integrating out the field ψ, the action of the supermatrices Q becomes

$$S[Q] = \frac{\pi\hbar}{4\Delta\tau} \int d\mathbf{r}\ \mathrm{Str}\ Q^2(\mathbf{r}) + \frac{1}{2} \int d\mathbf{r}\ \langle \mathbf{r} | \mathrm{Str} \ln \mathcal{G}^{-1}(\hat{\mathbf{r}}, \hat{\mathbf{p}}) | \mathbf{r} \rangle, \quad (1.38)$$

where the propagator $\mathcal{G}$ is given by

$$\mathcal{G}(\hat{\mathbf{r}},\hat{\mathbf{p}}) = [-\frac{\hat{p}^2}{2m_{\mathrm{e}}} + \frac{(\omega+i\delta)\Lambda_3}{2} + i\frac{\hbar}{2\tau}Q(\hat{\mathbf{r}})]^{-1} \tag{1.39}$$

and $\Delta = 2\pi\tau n_{\mathrm{i}}|V|^2/\hbar$ is the mean level spacing. Λ_3 is a 8×8 diagonal supermatrix, whose upper and lower 4×4 diagonal blocks are I and $-I$ respectively. A small imaginary part $i\delta$ ($\delta > 0$) is added to ω to assure the convergence of the integrals.

Since in the semiclassical limit $\lambda_{\mathrm{F}} \ll l$ interference effects occur at length scales much larger than l, the physics of localization is governed by long wavelength modes of Q. The effective action of these modes (1.38) can then be obtained by expanding around the homogeneous saddle point solution of (1.38), which satisfies for $\omega = 0$

$$Q = \frac{i}{\pi\rho_{\mathrm{F}}}\langle\mathbf{r}|(E - \frac{\hat{p}^2}{2m_{\mathrm{e}}} + i\frac{\hbar}{2\tau}Q)^{-1}|\mathbf{r}\rangle. \tag{1.40}$$

A solution of this equation is $Q_0 = \Lambda_3$, which corresponds to the SCBA (1.9) for the electronic self-energy. For $\omega = 0$, the rotations U which leave Q in the symmetric space yield the complete manifold of saddle point solutions as $Q = U\Lambda_3 U$. The rotations which leave Λ_3 invariant can be factorized out, leaving the saddle point solutions Q to be elements of a semisimple supersymmetric space.

Moreover, for $\lambda_{\mathrm{F}} \ll l$ there are massive longitudinal modes which only change the short distance physics (at length scales of the order of l) and can thus be integrated out. Therefore, only transverse modes play an important role in the physics of localization. These modes preserve the non-linear constraint $Q^2(\mathbf{r}) = \mathbb{1}$.

If one expands the action $S[Q]$ around the saddle point solution, one gets

$$S[Q] = \frac{\pi\rho_{\mathrm{F}}}{8}\int d\mathbf{r}\mathrm{Str}[D(\nabla Q)^2 + 2i(\omega+i\delta)\Lambda_3 Q]. \tag{1.41}$$

This action describes the slow spatial fluctuations of Q at finite frequency ω. These modes are just the diffusion modes, the Diffusons and the Cooperons, which we discussed in section 1.1.1. Their existence is the consequence of the spontaneous breaking of the supersymmetry. The frequency ω plays the role of an external field. The field theory described by the action (1.41) and the constraint $Q = U\Lambda_3\bar{U}$, $Q^2(\mathbf{r}) = \mathbb{1}$ (where U is an arbitrary unitary supermatrix) belongs to the class of nonlinear σ-models. At $\omega = 0$, $S[Q]$ is invariant with respect to the transformation

$$Q \to UQ\bar{U}. \tag{1.42}$$

A constant magnetic field can be taken into account by making the replacement $\hat{\mathbf{p}} \to \hat{\mathbf{p}} + (e/c)\hat{\tau}_3\mathbf{A}(\hat{\mathbf{r}})$ in formula (1.39). The diagonal Pauli matrix τ_3

has to be introduced since each supervector contains both normal and complex conjugate variables (see [18]). If the field is very weak, $l \ll l_B$, its effect can be considered as a small perturbation and a new effective action for the slow modes of Q can be obtained by making an expansion in both ∇Q and $\mathbf{A}$ around the saddle point solution of the action (1.38). This expansion yields:

$$S[Q] = \frac{\pi\rho_{\mathrm{F}}}{8}\int d\mathbf{r}\ \mathrm{Str}\ [D(\nabla Q + i\frac{e}{c}\mathbf{A}[Q,\tau_3])^2 + 2i(\omega + i\delta)\Lambda_3 Q]. \qquad (1.43)$$

According to this result, the degrees of freedom of Q that commute with τ_3 remain unperturbed by a magnetic field, while those degrees of freedom which do not commute acquire a mass. The former denote the diffusion modes whereas the latter represent the field sensitive Cooperon modes. Therefore, if the field B is strong enough (but still satisfies $l \ll l_B$), the influence of the Cooperons become negligible and can be neglected, in agreement with the discussion presented in section 1.1.2. In this limit the system can be effectively described by 4×4 matrices. The saddle point solutions are then elements of a different symmetric space, since the term containing the vector potential in (1.43) breaks the symmetry (1.42). This effect is ultimately due to the field B breaking the time-reversal symmetry of the Hamiltonian (unitary ensemble).

When l_B becomes comparable to l, the influence of orbital effects becomes significant. In this case we enter the quantum Hall regime, which is not correctly described by the action (1.43). We will discuss this regime in chapter 3.

If one wants to study spin interactions (magnetic impurities and spin-orbit interaction), one has to introduce two eight-components superfields, corresponding to spin-up and spin-down particles. Therefore, the matrices Q must have 16×16 components. In the presence of magnetic impurities, the symmetry of Q is the same as in the presence of a magnetic field (though the dimension of the matrices is higher), whereas a system with spin-orbit interactions (and no magnetic impurities) belongs to a new symmetry class, the symplectic class, in which the time-reversal symmetry of $\hat{H}$ is preserved but the central symmetry is broken.

It is possible to show that, in the limit where the deviations of the matrix Q from the saddle point solution Λ_3 are small, a perturbative expansion of (1.41) yields the quantum corrections to the conductivity discussed in previous sections.

It has been proven that the supersymmetric nonlinear σ-model (NLσ- model) is renormalizable. Moreover, it has been shown that a renormalization group treatment of (1.41) in $(2+\epsilon)$ dimensions yields the scaling function conjectured by Abrahams et al. in [2]. However, it is not clear yet whether the NLσ model and the one parameter scaling theory do correctly describe the metal-insulator transition in disordered metals. Since the statistical distribution of the conductance g does not fulfil the central limit theorem, one could guess that the average conductance alone cannot be representative of the statistical ensemble and higher

moments of the distribution of g should be taken into account. This important issue is currently the subject of intense research.

In the case of quasi-1D systems with diffusive width $W \gg l$, the action (1.41) can be simplified by taking into account only the zero transversal space harmonics of the supermatrix Q:

$$S[Q] = \frac{\pi \rho_{\mathrm{F}} W}{8} \int dx \ \mathrm{Str}\ [D(\frac{dQ}{dx})^2 + 2i(\omega + i\delta)\Lambda_3 Q]. \tag{1.44}$$

The above approximation is valid provided that the number N_{c} of transversal channels of the wire is large. It turns out that the quasi-1D NLσ-model can be solved exactly by using the transfer-matrix method. The basic idea behind this method is to reduce the functional integral over the supermatrices Q to a differential equation. This is completely analogous to deriving a Schrödinger equation from the corresponding quantum-mechanical Feynman path integral. In the present case, the role of the particle coordinate is played by the matrix Q, while the role of the time is played by the coordinate x along the wire. We will discuss this method more extensively in the following chapter.

In [21], the localization length L_{c} of quasi-1D diffusive wires was obtained from the spatial decay of the density correlation function, which was calculated by the above method. The result was:

$$L_{\mathrm{c}} = \beta \pi \hbar \rho S D, \tag{1.45}$$

where S is the wire cross section. In (1.45), $\beta = 1, 2, 4$ corresponds to no magnetic field (orthogonal ensemble), finite magnetic field (unitary ensemble) and strong spin-orbit scattering (symplectic ensemble) or magnetic impurities, respectively. In the next chapter, we will derive formula (1.45) (up to a numerical coefficient) by calculating a spectral correlation function.

Chapter 2

Magnetolocalization in Disordered Quantum Wires

In this chapter we consider the magnetic field dependent localization in a disordered quantum wire in a nonperturbative fashion.

We introduce a correlation function, the autocorrelation function of spectal determinants (ASD), which differs from those introduced in the previous chapter in that it does not necessitate the use of the full supersymmetric method, but still provides information on quantum localization.

We find a continuous increase of the localization length with the magnetic field, saturating at twice its value without magnetic field. The crossover behavior is shown to be governed both in the weak and strong localization regime by the magnetic phase shifting rate τ_B^{-1}. This quantity is derived analytically in closed form as a function of the ratio of the mean free path l, the wire thickness W and the magnetic length l_B. Both parabolic wires and wires with specular boundary conditions are considered. Our results generalize previous derivations of τ_B for disordered wires.

Finally, we discuss the applicability of the analytical formulas to resistance measurements in the strong localization regime and we compare our results with recent experimental work by Gershenson et al. [22]. A comparison with recent numerical work is also made.

The results presented in this chapter have been published in [23].

2.1 The autocorrelation function of spectral determinants

In the previous chapter, we have seen that the study of strong electron localization in a disordered potential necessitates a nonperturbative averaging of products of Green's functions. This can be achieved by means of the super-symmetry method, whereby the product of Green's functions is written as a functional

integral[18]. Thus, the average over the random potential can be done right at the beginning as a Gaussian integral, exactly.

Here we present the derivation of a simpler correlation function, which can be expressed as a functional integral over Grassmann variables only and does contain some information on the localization length of wavefunctions, as shown recently [24, 25].

The statistics of discrete energy levels of a finite coherent, disordered metal particle is an efficient way to characterize its properties [18]. It is well known that the Poisson statistics is related to a spectrum of uncorrelated, localized states [26, 27, 28, 29, 30], whereas the Wigner-Dyson statistics corresponds to a spectrum of extended states [31]. The spectral properties of a mesoscopic system can be studied by calculating a disorder averaged autocorrelation function between two energies at a distance ω in the energy level spectrum.

The autocorrelation function of spectral determinants (ASD) is the simplest such spectral correlation function. It is defined by $C(\omega) = \bar{C}(\omega)/\bar{C}(0)$, where

$$\bar{C}(\omega) = \langle \det(E + \omega/2 - H) \det(E - \omega/2 - H) \rangle, \tag{2.1}$$

and E is a central energy. The behaviour of $\bar{C}(\omega)$ can be easily figured out in two extreme cases: the ASD of an equally spaced spectrum is a periodic function of ω, $C(\omega) = \cos \pi\omega$, whereas a Poissonian spectrum of N_s localized states decays to zero on a scale proportional to $\sqrt{N_s}$. In general, $\bar{C}(\omega)$ is an oscillatory function whose amplitude decays with a power law, when the energy levels in the vicinity of the central energy E are extended, while a Gaussian decay is a strong indication that all states are localized.

The ASD is a product of two spectral determinants: since we know from section 1.2.2 that a spectral determinant can be written as a Gaussian functional integral over Grassmann variables ψ, ψ^* (see formula 1.36), one does need at least a 2-component Grassman field, one for each spectral determinant.

To get the functional integral representation of the ASD, Grassmann fields with one-half the number of components of the corresponding superfields introduced in chapter 1 are in general needed. Hence, 4-components fields must be introduced when the Hamiltonian is independent of the spin of the electrons and each level is doubly spin degenerate. There is one pair of Grassman fields for each determinant in the ASD and each pair is composed of a Grassman field and its time reversed one, as obtained by complex conjugation. Eight-components fields have to be considered when the Hamiltonian does depend on spin, as for the case with moderately strong magnetic impurity or spin- orbit scattering. This necessitates the use of a vector of a spinor and the corresponding time reversed one.

In the following, we will consider the Hamiltonian of disordered noninteracting

electrons is

$$H = \frac{1}{2m_e}(\mathbf{p} + e\mathbf{A}) + V(\mathbf{r}) + \sigma \mathbf{b}_S(\mathbf{x}) + \sigma \mathbf{u}_{SO} \times \mathbf{p}, \tag{2.2}$$

where $-e$ is the electron charge (in this chapter we choose units in which $c = 1$). In (2.2), we have approximated the true electronic dispersion $\epsilon(\mathbf{p} + e\mathbf{A})$ by $(\mathbf{p} + e\mathbf{A})^2/(2m_e)$, but higher moments are sometimes needed to regularize the correlation functions calculated below. $V(\mathbf{x})$ is taken to be a Gaussian distributed random function described by (1.8).

The vector potential is used in the Landau gauge $\mathbf{A} = (-By, 0, 0)$, where x is the coordinate along the wire of length L, y the one in the direction perpendicular both to the wire and the magnetic field $\mathbf{B}$, which is directed perpendicular to the wire. σ is the electronic spin operator, and $\mathbf{b}_S(\mathbf{x})$ is a random magnetic impurity field. $\mathbf{u}_{SO}$ is the local electrostatic field of impurities with large atomic number Z, which do give a stronger spin orbit coupling to the conduction electrons.

The starting point is the representation of the ASD as a Gaussian functional integral over Grassmann variables. It can be easily derived from (1.36). In the spinless case, it is given by

$$\bar{C}(\omega) = \int d\psi(\mathbf{r}) \exp\left\{-\frac{1}{2}\int d\mathbf{r}\bar{\psi}(\mathbf{r})\left[E + \frac{1}{2}\omega\Lambda_3 - \hat{H} - V(\mathbf{r})\right]\psi(\mathbf{r})\right\}, \tag{2.3}$$

where $\psi, \bar{\psi}$ are vectors of anticommuting variables

$$\psi(\mathbf{x}) = \begin{pmatrix} \xi(\mathbf{x}) \\ \xi^*(\mathbf{x}) \\ \eta(\mathbf{x}) \\ \eta^*(\mathbf{x}) \end{pmatrix}, \bar{\psi}(\mathbf{x}) = (\xi^*(\mathbf{x}), -\xi(\mathbf{x}), \eta^*(\mathbf{x}), -\eta(\mathbf{x})), \tag{2.4}$$

and

$$\hat{H}_0 = (\mathbf{p} + e\tau_3\mathbf{A})^2/2m_e \tag{2.5}$$

(see section 1.2.2). To summarize the notation, here and in the following Λ_i are the Pauli matrices in the subbasis of the left and right spectral determinant (Λ_3 is therefore a 4×4 matrix, whereas in the supersymmetric NLσ-model of section 1.2.2 it was an 8×8 matrix), τ_i the ones in the subbasis spanned by time reversal and σ_i the ones in the subbasis spanned by the spinor, for $i = 1, 2, 3$.

Note that $\bar{\psi} = (C\psi)^T$, where the matrix C, which interchanges the Grassmann fields with their conjugate one, has the form

$$C = \begin{pmatrix} 0 & -1 & 0 & 0 \\ 1 & 0 & 0 & 0 \\ 0 & 0 & 0 & -1 \\ 0 & 0 & 1 & 0 \end{pmatrix}. \tag{2.6}$$

A global transformation of the Grassmann vectors $\psi \Rightarrow \tilde{\psi} = A\psi$ leaves the functional integral for $\omega = 0$ invariant, as long as $A^\dagger A = 1$ and $A^{\dagger T} C = CA$.

The derivation of the corresponding matrix field theory is completely analogous to the derivation of the supersymmetric theory outlined in section 1.2.2. The only (albeit very important) difference is that the matrix field Q introduced to decouple the ψ^4 interaction does not have Grassmannian components, since ψ has only anticommuting components. After integrating out the Grassmann field, the action of the matrices Q is given by (1.38), providing that the supertrace Str is replaced by the conventional trace.

The matrix Q is an element of the full symmetric space, including rotations between the subspace corresponding to the left and the right spectral determinant. Therefore, the long wavelength modes of Q do contain the nonperturbative information on the diffuson and Cooperon modes.

The saddle point solution of the action satisfies for $\omega = 0$,

$$Q = \frac{i}{\pi \rho_{\mathrm{F}}} \langle \mathbf{r} | (E - \hat{H} + i \frac{\hbar}{2\tau} Q)^{-1} | \mathbf{r} \rangle. \tag{2.7}$$

Again, this equation is found to be solved by $Q_0 = \Lambda_3$.

Since Q are conventional matrices, they do not belong to the same spaces as the supersymmetric matrices defined in the previous chapter. For spin-independent Hamiltonians and $B = 0$, at $\omega = 0$, they satisfy $Q^T C = CQ$, thereby belonging to the symplectic symmetric space. The rotations U, which leave Q in that space, yield the complete manifold of saddle point solutions as $Q = \bar{U} \Lambda_3 U$, where $U\bar{U} = 1$. The modes which leave Λ_3 invariant are elements of $Sp(1) \times Sp(1)$ and can be factorized out, leaving the saddle point solutions to be elements of the semisimple symmetric space $Sp(2)/(Sp(1) \times Sp(1))$[32].

For a moderately strong magnetic field and spin degenerate levels, the time reversal symmetry is fully broken and the Q-matrices are in the unitary symmetric space $U(2)/(U(1) \times U(1))$.

For spin-dependent Hamiltonians the matrix C is, due to the time reversal of the spinor, substituted by $i\sigma_2\tau_1$ [19]. Both magnetic impurities and spin-orbit scattering reduce the Q matrix to unity in spin space. Thus, C has effectively the form τ_1. The condition $Q^T C = CQ$ leads therefore to a new symmetry class, when the spin symmetry is broken but the time reversal symmetry remains intact. This is the case for moderately strong spin-orbit scattering. Then, Q are 4×4-matrices on the orthogonal symmetric space $O(4)/(O(2) \times O(2))$ [33], which is the nonperturbative consequence of the sign change of a spinor component under time reversal operation, which leads to the positive quantum correction to the conductivity in perturbation theory discussed in section 1.1.4. Note that the ASD of systems belonging to the orthogonal ensemble is described by a functional integral over compact symplectic matrices Q and vice versa. This is due to the Grassmann variables changing sign under time reversal. With

magnetic impurities both the spin and time reversal symmetry is broken, and the Q- matrices again belong to the space $U(2)/(U(1) \times U(1))$.

One could extend this approach to other compact symmetric spaces with physical realizations, see Ref. [34, 35] for a complete classification. Very recently, the problem of localization in quasi 1D systems belonging to non conventional symmetry classes has been addressed within the supersymmetric approach by Lamacraft et al. [36].

For wires with a large number of transversal channels, $N_c \gg 1$, the massive longitudinal modes with $Q^2 \neq 1$ can be integrated out [18], and the ASD thus reduces to a functional integral over the transverse modes U with $Q^2 = 1$. The action at finite frequencies ω and spatial fluctuations of Q around the saddle point solution can now be found by expanding the action S, Eq.(1.38). Inserting $Q = \bar{U}\Lambda_3 U$ into Eq. (1.38), and performing the cyclic permutation of U under the trace Tr, yields,

$$S = -\frac{1}{2}\int d\mathbf{x}\langle \mathbf{x}|\mathrm{Tr}\ln(G_0^{-1} - U[H_0, \bar{U}] + \omega U\Lambda_3\bar{U})|\mathbf{x}\rangle, \tag{2.8}$$

where

$$G_0^{-1} = E - H_0 + \frac{i\hbar}{2\tau}\Lambda_3. \tag{2.9}$$

Expanding up to first order in the energy difference ω and up to second order in the commutator $U[H_0, \bar{U}]$ yields,

$$\begin{aligned} F[U] = &-\frac{1}{2}\omega\int d\mathbf{x}\langle \mathbf{x}|\mathrm{Tr}\ G_{0E}U\Lambda_3\bar{U}|\mathbf{x}\rangle \\ &+\frac{1}{2}\int d\mathbf{x}\langle \mathbf{x}|\mathrm{Tr}\ G_{0E}U[H_0, \bar{U}]|\mathbf{x}\rangle \\ &+\frac{1}{4}\int d\mathbf{x}\langle \mathbf{x}|\mathrm{Tr}\ (G_{0E}U[H_0, \bar{U}])^2|\mathbf{x}\rangle, \end{aligned} \tag{2.10}$$

where

$$[H_0, \bar{U}] = -\frac{\hbar^2}{2m_e}(\nabla^2\bar{U}) - \frac{\hbar^2}{m_e}(\nabla\bar{U})\nabla + \frac{e\hbar}{im_e c}(\tau_3\mathbf{A}\nabla\bar{U} - \bar{U}\tau_3\mathbf{A}\nabla). \tag{2.11}$$

The first order term in $U[H_0, \bar{U}]$ vanishes for Gaussian white noise isotropic scattering.

In general, in order to account for the ballistic motion of electrons in ballistic wires, or to account for different sources of randomness, a directional dependence of the matric $U = U(\mathbf{x}.\mathbf{n})$, where $\mathbf{n} = \mathbf{p}/|\mathbf{p}|$, has to be considered[37, 38]. However, for the geometries considered in this chapter, we found that the form of the action derived below remains valid for ballistic cross sections, when the vector fields $\mathbf{S}$ as introduced in Refs. [37, 38], are integrated out.

Then, one can keep second order terms in $\nabla\bar{U}$ and $\mathbf{A}$, which turns out to be valid for the regime of weak disorder, $l \gg 1/k_{\rm F}$ and for any magnetic field, $l_B \gg k_{\rm F}$. Thus, one gets, using the saddle point equation, Eq. (2.7),

$$S[U] = -\frac{\pi}{4}\frac{\omega}{\Delta}\int \frac{d\mathbf{x}}{SL}\mathrm{Tr}\ \Lambda_3 Q + \\ + \frac{1}{4}\int d\mathbf{x}\langle\mathbf{x}|\mathrm{Tr}\ (G_{0E}U(\frac{\hbar^2}{2m_{\rm e}}(\nabla\bar{U})(\nabla + \frac{i}{\hbar}e\mathbf{A}\tau_3) + \\ + \frac{e\hbar}{m_{\rm e}}[\tau_3, \bar{U}\mathbf{A}\nabla]))^2|\mathbf{x}\rangle. \tag{2.12}$$

Next, one can separate the physics on different length scales, noting that the physics of diffusion and localization is governed by spatial variations of U on length scales larger than the mean free path l. The smaller length scale physics, is then included in the correlation function of Green's functions, being related to the conductivity by the Kubo-Greenwood formula,

$$\sigma_{\alpha\beta}(\omega) = \frac{\hbar}{\pi SL}\frac{e^2}{m_{\rm e}^2}\sum_{\mathbf{p},\mathbf{p}'}\langle\mathbf{p}|(p_\alpha + eA_\alpha)G^R_{0E}|\mathbf{p}'\rangle \times \\ \times\langle\mathbf{p}'|(p'_\beta + eA_\beta)G^A_{0E+\omega}|\mathbf{p}\rangle, \tag{2.13}$$

where $\mathbf{p} = \frac{\hbar}{i}\nabla$. The remaining averaged correlators, involve products $G^R_{0E}G^R_{0E+\omega}$ and $G^A_{0E}G^A_{0E+\omega}$ and are therefore by a factor $\hbar/(\tau E)$ smaller than the conductivity, and can be disregarded for small disorder $\hbar/\tau \ll E$. Here we are interested in the weak magnetic field limit, where $\omega_{\rm c}\tau \ll 1$, with the cyclotron frequency $\omega_{\rm c} = qB/m_{\rm e}$. In this limit the nondiagonal Hall conductivity and the explicit magnetic field dependence of the longitudinal conductivity can be disregarded.

In order to insert the Kubo-Greenwood formula in the saddle point expansion of the nonlinear sigma model, it is convenient to rewrite the propagator in the free energy as $G_{0E} = \frac{1}{2}G^R_{0E}(1+\Lambda_3) + \frac{1}{2}G^A_{0E}(1-\Lambda_3)$. Then, we can use that

$$\mathrm{Tr}\,[\sum_{\alpha=1}^{d}\sum_{s=\pm}(1+s\Lambda_3)U(\nabla_\alpha\bar{U})(1-s\Lambda_3)U(\nabla_\alpha\bar{U})] = -\mathrm{Tr}[(\nabla Q)^2], \tag{2.14}$$

and

$$\mathrm{Tr}\,[\sum_{s=\pm}(1+s\Lambda_3)U[\tau_3,\bar{U}]](1-s\Lambda_3)U[\tau_3,\bar{U}] = -\mathrm{Tr}\,[[\tau_3,Q]^2]. \tag{2.15}$$

Thereby we can rewrite Eq. (2.12) as

$$F[Q] = -\frac{\pi}{4}\frac{\omega}{\Delta}\int\frac{d\mathbf{x}}{SL}\mathrm{Tr}\Lambda_3 Q - \frac{1}{4}\int d\mathbf{x}\mathrm{Tr}\,[(\nabla Q(\mathbf{x}))^2] \times$$

$$\times\langle\mathbf{x}|G^R_{0E}\frac{\hbar^2}{2m_{\rm e}}(\nabla+\frac{i}{\hbar}e\mathbf{A})G^A_{0E}\frac{\hbar^2}{2m_{\rm e}}(\nabla+\frac{i}{\hbar}e\mathbf{A})|\mathbf{x}\rangle+$$
$$-\frac{1}{4}\left(\frac{e\hbar}{m_{\rm e}}\right)^2\int d\mathbf{x}\mathrm{Tr}\,[[\tau_3,Q(\mathbf{x})]^2]\langle\mathbf{x}|G^R_{0E}\mathbf{A}\nabla G^A_{0E}\mathbf{A}\nabla|\mathbf{x}\rangle+c.c. \quad (2.16)$$

For wires of thickness W not exceeding the length scale $L_{CU}=L_{\rm c}(\beta=2)=2\pi\hbar\rho SD_0$, the variations of the field Q can be neglected in the transverse direction, and the action reduces to the one of a one- dimensional nonlinear sigma model. Using the Kubo formula, Eq. (2.13), this functional of Q thus simplifies, for $\omega_{\rm c}\tau\ll 1$, to,

$$F=\frac{\pi\hbar}{16e^2}\sigma(\omega=0)W\int_0^L dx\left[\mathrm{Tr}\,(\nabla_xQ(x))^2-\langle A_x\bullet A_x\rangle\frac{e^2}{\hbar^2}\mathrm{Tr}\,[\tau_3,Q(x)]^2\right]+$$
$$-\frac{\pi}{4}\frac{\omega}{\Delta}\int_0^L\frac{dx}{L}\mathrm{Tr}\Lambda_3Q, \quad (2.17)$$

where the prefactor of the time reversal symmetry breaking term, the correlation function

$$\langle A_x\bullet A_x\rangle\equiv\frac{(\langle\mathbf{x}|G^R_{0E}\mathbf{A}\nabla G^A_{0E}\mathbf{A}\nabla|\mathbf{x}\rangle+c.c.)}{\langle\mathbf{x}|G^R_{0E}(\nabla+\frac{i}{\hbar}e\mathbf{A})G^A_{0E}(\nabla+\frac{i}{\hbar}e\mathbf{A})|\mathbf{x}\rangle}$$
$$=B^2\langle y\bullet y\rangle, \quad (2.18)$$

increases with the magnetic field B, suppressing modes with $[Q,\tau_3]\neq 0$, the Cooperon modes, arising from the self interference of closed diffusion paths (see sections 1.1.1 and 1.2.2). Accordingly, the symmetry of the Q- fields is broken from $Sp(2)/(Sp(1)\times Sp(1))$ to $U(2)/(U(1)\times U(1))$.

In the next section it is shown that this prefactor is related to the magnetic phase shifting rate and is evaluated for a disordered quantum wire.

2.2 The magnetic phase shifting rate

It can be seen that the prefactor of the symmetry breaking term in Eq. (2.17) is proportional to the effective phase shifting rate $1/\tau_B$, governing the weak localization suppression by a magnetic field. To this end, one can use the supersymmetric version of the above nonlinear sigma model introduced in chapter 1, and calculate the weak localization corrections to the conductivity as outlined in [18], by an expansion of Q around the classical saddle point $Q_{\rm c}=\Lambda_3$. Thus, the magnetic phase shifting rate $1/\tau_B$ can be identified as

$$1/\tau_B=4D\frac{e^2}{\hbar^2}\langle A_x\bullet A_x\rangle, \quad (2.19)$$

where the Einstein relation $\sigma = 2e^2\rho D$ has been used. In the following we evaluate τ_B^{-1} for a wire with specular boundary conditions and for a parabolic wire.

2.2.1 Wires with specular boundary conditions

The general expression for the correlation function $\langle y \bullet y\rangle$ is found by inserting the momentum eigenstates of the wire and summing the correlation functions of Green's functions for $l_B \gg W$ in Eq. (2.18). For a two dimensional wire of width W in momentum representation, it is given by,

$$\langle y \bullet y\rangle = \sum_{k_x,k_y,k_y'} k_x^2 (G^R_{0E}(k_x,k_y)G^A_{0E}(k_x,k_y') + c.c.)|\langle k_y|y|k_y'\rangle|^2 / \\ / \sum_{k_x,k_y} (k_x + \frac{e}{\hbar}A_x)^2 G^R_{0E}(k_x,k_y)G^A_{0E}(k_x,k_y). \tag{2.20}$$

Here, $G^{R/A}_{0E}(k_x,k_y) = (E - \hbar^2(k_x^2+k_y^2)/(2m_{\rm e}) \pm i/(2\tau)$.

For a clean wire with hard wall boundaries, the transversal eigenmodes are for $-W/2 < y < W/2$, $\langle k_y|y\rangle = \cos k_y y$ for $k_y = \pi s/W$, s being an odd integer, and $\langle k_y|y\rangle = \sin k_y y$ for $k_y = \pi s/W$, s being an even integer. Hence one obtains

$$|\langle k_y|y|k_y'\rangle|^2 = \frac{1}{W^2}\left[\frac{1}{(k_y-k_y')^2} - \frac{1}{(k_y+k_y')^2}\right]^2, \tag{2.21}$$

when $k_y = \pi s/W$, and $k_y' = \pi s'/W$, s being even, and s' odd, or vice versa. The sum over k_y' in Eq. (2.20) can be performed by use of the Matsubara trick, for s even and odd integers, separately. The remaining sum over k_x, k_y can be transformed as $1/(WL)\sum_{k_x,k_y} = \int d\epsilon\rho(\epsilon)\int d\hat{e}_k/\Omega_k$, noting that the unit vector $\hat{e}_k$ can point only in discrete directions. Thus, while in 2 dimensions

$$\int \frac{d\hat{e}_k}{\Omega_k} = \int_0^{2\pi}\frac{d\theta}{2\pi} = \frac{4}{2\pi}\int_0^1 dy 1/(1-y^2)^{1/2}, \tag{2.22}$$

for a finite number of transverse channels $N = k_{\rm F}W/\pi \gg 1$ the sum

$$\int \frac{d\hat{e}_k}{\Omega_k} = \frac{2}{\pi N}\sum_{s>0} 1/(1-s^2/N^2)^{1/2} \tag{2.23}$$

holds. Thus, $k_y = \pi s/W = k_{\rm F}s/N$ and $k_x = k_{\rm F}(1-s^2/N^2)^{1/2}$. Performing finally for $E \gg \hbar/\tau$ the integral over ϵ, one arrives at

$$\langle y \bullet y\rangle = \frac{W^2}{K_0}\left\{\frac{1}{12}K_1 - \frac{1}{2\pi^2}K_2 - \frac{\lambda^2}{\pi^2N^2}K_3 + \frac{4}{\pi^4}\frac{\lambda^3}{N^4}\sum_{s=1}^{N}\frac{s^2}{N^2}\sqrt{1-\frac{s^2}{N^2}}\times\right. \\ \left.\times{\rm Im}\sqrt{\frac{s^2}{N^2}+i\frac{2}{\lambda}}\tan\left[\frac{\pi N}{2}\left(\sqrt{\frac{s^2}{N^2}+i\frac{2}{\lambda}}-\frac{s}{N}\right)\right]\right\}, \tag{2.24}$$

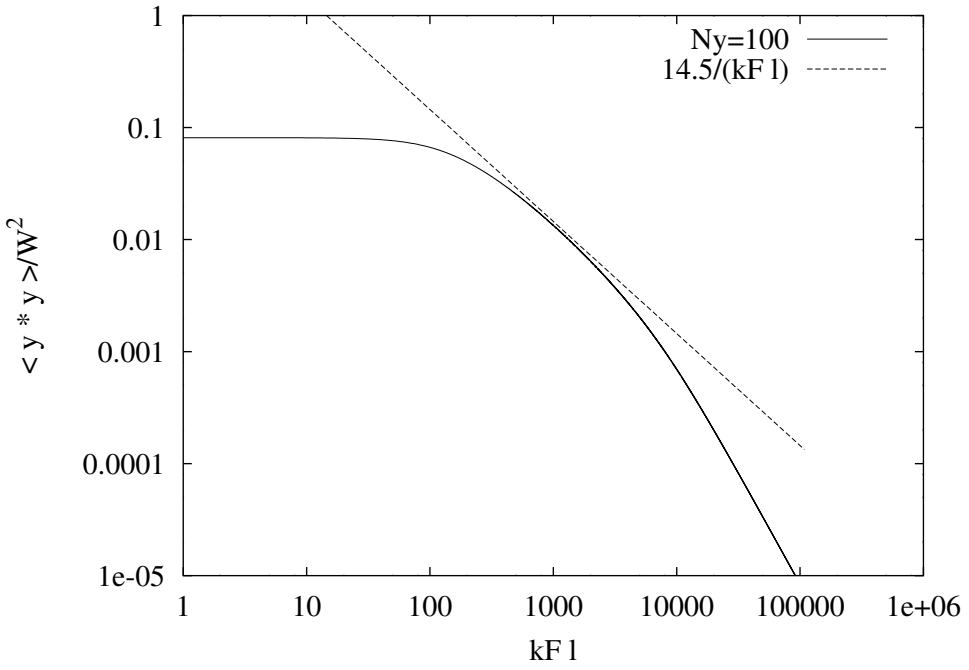

Figure 2.1: The dependence of the correlation function $\langle y \bullet y \rangle / W^2$ on the dimensionless mean free path $\lambda = k_F l$ for $N = 100$ channels. For comparison, the line corresponding to a disorder independent phase shifting rate, approximately valid for $N \ll \lambda \ll N^2$, is shown.

where

$$K_0 = \frac{2}{\pi N} \sum_{s=0}^{N} \sqrt{1 - \frac{s^2}{N^2}}, \quad K_1 = \frac{2}{\pi N} \sum_{s=1}^{N} \sqrt{1 - \frac{s^2}{N^2}},$$

$$K_2 = \frac{2}{\pi N} \sum_{s=1}^{N} \frac{1}{s^2} \sqrt{1 - \frac{s^2}{N^2}}, \quad K_3 = \frac{2}{\pi N} \sum_{s=1}^{N} \frac{s^2}{N^2} \sqrt{1 - \frac{s^2}{N^2}}.$$

The dependence of (2.24) on the mean free path parameter $\lambda = k_F l$ is shown in Fig. 2.1.

Note that, although $N \gg 1$ and $l_B > l, W$ are required for the validity of the NLσ-model (2.17), the equation (2.24) is valid for arbitrary ratios of the width of the wire W and the mean free path l, since the motion remains diffusive along the wire axis on large length scales, even if $l \gg W$. The above derivation is therefore more general than previous works on the magnetic phase shifting rate [10, 11, 13].

For diffusive wire cross sections, $l < W$, $\langle y \bullet y \rangle \to \overline{y^2} = W^2/12$ which re-

sults exactly in the known result for the magnetic phase shifting rate $1/\tau_B = 4D\frac{e^2}{\hbar^2}\overline{y^2}B^2$ [11, 13].

For ballistic wire cross sections, $l > W$, Eq. (2.24) shows that the effect of the magnetic field becomes weaker, as W/l decreases. This is a result of the flux cancellation effect, discussed in the limit of weak localization in section 1.1.2: the matrix element of the vector potential $\langle \mathbf{k}|\mathbf{A}|\mathbf{k}'\rangle$ vanishes for $\mathbf{k} = \mathbf{k}'$, since $\mathbf{A} = (-By, 0, 0)$ is antisymmetric in the coordinate perpendicular to the wire, y. Thus, elastic impurity scattering is needed to mix different momentum states and contribute finite matrix elements of the magnetic vector potential.

One can check that Eq. (2.24) is valid also in the weak disorder limit, by Taylor expanding the correlation function in $1/(k_\mathrm{F}l)$, giving $\langle y \bullet y\rangle = \frac{W^2}{10}(N^3/\lambda^2)$, showing that it vanishes for $\lambda \gg N^2$, corresponding to $\hbar/\tau \ll \pi^2\hbar^2/(2m_\mathrm{e}W^2)$, when the disorder does not mix transversal modes, like $1/\lambda^2$, as seen in Fig. 2.1.

In the intermediate regime, $N < \lambda$, it had been argued in Ref. [10, 11], that $1/\tau_B$ should be reduced by a factor linear in N/λ resulting for a 2 dimensional wire with perpendicular magnetic field in a disorder independent expression

$$\frac{1}{\tau_B} = \frac{1}{C}\frac{W^3 v_\mathrm{F}}{l_B^4}, \tag{2.25}$$

where $l_B = (\hbar/eB)^{1/2}$ is the magnetic length. For specular boundary condition, as considered in this chapter, it was found numerically that $C = 9.5$[11]. Correspondingly, the function $\langle y \bullet y\rangle/W^2$ should approach $\langle y \bullet y\rangle/W^2 \to (\pi/2C)N/\lambda$ or for $N = 100$, $\langle y \bullet y\rangle/W^2 \to 16.5/\lambda$. The result Eq. (2.19) agrees indeed with this behaviour, in a regime $N \ll \lambda \ll N^2$, although the best fit gives a different prefactor 14.5, corresponding to $C = 10.8$. The analytical result shows, furthermore, that this behaviour is only an approximation and that there is a crossover to the perturbative regime, discussed above, where $\langle y \bullet y\rangle/W^2$ decays like $\sim 1/\lambda^2$, see Fig. 2.1. Note that this result is accurate up to corrections of order $1/N$.

2.2.2 Parabolic Wire

As long as the elastic scattering rate exceeds the cyclotron frequency, $1/\tau \gg \omega_\mathrm{c}$, or correspondingly, $l \ll l_{Cyc}$, where $l_{Cyc} = k_\mathrm{F}l_B^2$ is the cyclotron path determining the length scale on which ballistic paths start to bend due to the Lorentz force, the magnetic field dependence of the classical diffusion constant and the density of states can be neglected, being for a 2- dimensional wire $D = \tau v_\mathrm{F}^2/2$ and $\rho(E) = m_\mathrm{e}/(2\pi\hbar^2)$, respectively.

However, the cyclotron length can be small compared to the width of the wire, $l_{Cyc} < W$, while exceeding the elastic mean free path $l_{Cyc} > l$, when the cross section of the wire is diffusive, $l < W$. Thus, the localization length can depend sensitively on the ratio of these length scales, even in the weak magnetic field

limit, where the density of states and classical conductivity are insensitive to the magnetic field. In order to study the crossover as a function of the magnetic field, the dependence of the eigenfunctions on the magnetic field have to be taken into account, therefore. This regime is most conveniently studied for a parabolic wire, having a harmonic confinement,

$$H_0 = \frac{1}{2m_\mathrm{e}}(\mathbf{p} + e\mathbf{A})^2 + \frac{1}{2}m_\mathrm{e}\omega_0^2 y^2. \tag{2.26}$$

The spectrum of the above Hamiltonian is

$$E_{n,k} = (n + \frac{1}{2})\hbar\omega_\mathrm{eff} + \frac{\hbar^2 k^2}{2m_\mathrm{eff}}, \tag{2.27}$$

where the effective mass is $m_\mathrm{eff} = m_\mathrm{e}\omega_\mathrm{eff}^2/\omega_0^2$, and the effective frequency is $\omega_\mathrm{eff} = (\omega_\mathrm{c}^2 + \omega_0^2)^{1/2}$. The corresponding wavefunctions are

$$\psi_{n,k}(\mathbf{r}) = \frac{1}{\sqrt{L}}e^{iky}\chi_n\left(y - \hbar k\frac{\omega_\mathrm{c}}{\omega_\mathrm{eff}}l_\mathrm{eff}^2\right), \tag{2.28}$$

where $l_\mathrm{eff} = \sqrt{\hbar/(m_\mathrm{e}\omega_\mathrm{eff})}$ is the renormalized magnetic length and χ_n are the solutions of the one-dimensional oscillator. Hence, the spatial center of the electron eigenstates are shifted by the guiding center $y_k \equiv \hbar k(\omega_\mathrm{c}/\omega_\mathrm{eff})l_\mathrm{eff}^2$. Thus, at constant Fermi energy E_F the width of the wire is dependent on the magnetic field B. Defining the width of the wire W at fixed Fermi energy as $W^2 = \max(\langle n,k|y^2|n,k\rangle)$ with $E_{n,k} = E_\mathrm{F}$, one finds for the parabolic wire:

$$W^2(B) = l_\mathrm{eff}^2\max\left[2\frac{E_\mathrm{F}}{\hbar\omega_\mathrm{eff}}\frac{\omega_\mathrm{c}^2}{\omega_0^2} + (n+1/2)(1 - \frac{\omega_\mathrm{c}^2}{\omega_0^2})\right]. \tag{2.29}$$

For large magnetic field, $\omega_\mathrm{c} \gg \omega_0$, this approaches exactly twice the value at zero magnetic field, and thus,

$$W(\omega_\mathrm{c} \gg \omega_0) = \sqrt{2}W(0) = l_0(2E_\mathrm{F}/(\hbar\omega_0))^{1/2}. \tag{2.30}$$

Thus, the wire width is a slowly vaying function of the parameter $\omega_\mathrm{c}/\omega_0 = W(B=0)/l_{cyc}$.

The presence of impurities smoothens this function further, and we can thus assume the width to be practically magnetic field independent:

$$W = \frac{1}{\omega_0}\sqrt{\frac{2E_\mathrm{F}}{m_\mathrm{eff}}}. \tag{2.31}$$

This allows us to study the various regimes of interest as a function of the wire width W, the magnetic length l_B and the average mean free path $l = (2E/m_\mathrm{e})^{1/2}\tau$.

Naturally, the classical conductivity in such a wire is anisotropic. We find that

$$\sigma_{xx} = \frac{1+\omega_0^2\tau^2}{1+\omega_{\rm eff}^2\tau^2}\frac{n_e e^2\tau}{m_{\rm e}}, \tag{2.32}$$

and

$$\sigma_{yy} = \frac{1}{1+\omega_{\rm eff}^2\tau^2}\frac{n_e e^2\tau}{m_{\rm e}}, \tag{2.33}$$

where $n_e = (2/3\pi)(m_{\rm eff}E/\hbar^2\omega_0)$ is the average electron density in the wire, which is taken to be approximately independent of the magnetic field. Since we consider magnetic fields where $\omega_{\rm c}\tau \ll 1$, the classical conductivity is magnetic field independent, $\sigma_{xx} = e^2\tau n_e/m_{\rm e}$, and $\sigma_{yy} = \sigma_{xx}/(1+\omega_0^2\tau^2)$.

Thus, the condition that the localization is governed by the one-dimensional nonlinear sigma model is changed to $L_{CU}/(1+\omega_0^2\tau^2) > W$. With $\omega_0\tau = l/W$ follows that the one dimensional localization condition requires, $l < 2NW$, in the weak disorder regime, $k_{\rm F}l \gg 1$.

Rederiving the nonlinear sigm model in the representation of a clean parabolic wire, using the definition of the correlation fucntion, Eq. (2.20), where the sum over transverse momenta is substituted by the sum over the band index, n, $k_y \to n$, we find the result,

$$\langle y \bullet y\rangle = \frac{2}{5}\,W^2\left(\frac{1}{1+\omega_0^2\tau^2} + 3\frac{\omega_{\rm c}^2}{\omega_0^2}\right) = \frac{2}{5}\,W^2\left(\frac{1}{1+l^2/W^2} + 3\frac{W^2}{l_{\rm cyc}^2}\right). \tag{2.34}$$

Note that, since $\omega_0^2\tau^2 = l^2/(W^2)$, the ballistic cross section limit $l > W$, coincides for the parabolic wire with the clean wire limit, where transversal modes are not mixed by the disorder $\hbar/\tau < \hbar\omega_0$. Thus the flux cancellation effect leads in the parabolic wire to a supppression of the phase shifting rate by a factor W^2/l^2 as found for the wire with specular boundaries in the previous subsection.

Thus, it is not surprising that the behaviour of the magnetic phase shifting rate, as known from weak localization corrections for a wire with ballistic cross section, $W > l$, and hard wall boundary conditions, is not reproduced when considering a parabolic wire. In the former case, there is a regime, $W^2 < l_B^2 < Wl$, implying $l_B < l$, where the magnetic phase shifting rate is given by

$$\frac{1}{\tau_B} = \frac{W^2}{C_2\tau l_B^2} < \frac{W^3 v_{\rm F}}{C l_B^4}, \tag{2.35}$$

where $C_2 = 24/5$. This is smaller than expected from Eq. (2.25), and is not obtained for the parabolic wire.

Instead, we find that there is a regime, where the magnetic field sensitivity of localization becomes stronger, when the cyclotron length $l_{\rm cyc}$, becomes comparable to the width of the wire W. When $l < l_{\rm cyc} < W$ the magnetic phase shifting

rate is found to increase with the magnetic field like B^4,

$$\frac{1}{\tau_B} = \frac{24}{5} D \frac{e^2}{\hbar^2} B^2 \frac{W^4}{l_{\rm cyc}^2}. \tag{2.36}$$

When the magnetic field becomes so strong that the cyclotron length $l_{\rm cyc}$, becomes comparable or smaller than the mean free path l, or $\omega_{\rm c}\tau > 1$, the diffusion constant and the density of states become functions of the magnetic field. Then, the spatial modes of the nonlinear sigma model perpendicular to the wire can become soft and contribute to the functional integral, and thus, the nonlinear sigma model becomes effectively two dimensional.

In this limit, the approach used in this chapter does yield qualitative information on the location and size of localized states in a quantum Hall system [39].

2.3 Magnetolocalization

As mentioned in chapter 1, the localization length of a diffusive wire depends on the global symmetry of the system [21]: $L_{\rm c} = \beta\pi\hbar\phi SD$, where $\beta = 1, 2, 4$, correspond to no magnetic field, finite magnetic field, and strong spin-orbit scattering or magnetic impurities, respectively.

Here, we will obtain the localization length as a function of the magnetic field by exploiting the properties of the ASD discussed briefly in section 2.1. Since the ASD shows a crossover from an oscillating behaviour decaying with a power law[40, 41], typical for Wigner- Dyson energy level statistics[42], to a gaussian decaying function, when the length of the wire is increased beyond the localization length[24], the crossover length can be identified as the average localization length of electrons. A similar behaviour has been seen in other measures of correlations in the discrete energy level spectrum of a phase coherent disordered electron system[18, 27, 28, 29, 30].

We take the representation of the ASD derived in the first section,

$$\bar{C}(\omega) = \int \prod dQ(\mathbf{x}) \exp(-F[Q]), \tag{2.37}$$

where the action Eq. (2.17) can be rewritten conveniently as

$$F[Q] = \alpha \frac{1}{16} L_{CU} \int_0^L {\rm d}x {\rm Tr} \left[(\nabla_x Q(x))^2 - \frac{1}{4L_B^2} [Q, \tau_3]^2 \right] + \\ + i\alpha \frac{\pi}{4} \frac{\omega}{\Delta} \int_0^L \frac{{\rm d}x}{L} {\rm Tr} \Lambda_3 Q(x). \tag{2.38}$$

In the above equation $L_B \equiv \sqrt{D\tau_B}$ is the typical diffusion length of an electron in time τ_B and $L_{CU} = L_{\rm c}(\beta = 2) = 2\pi\hbar\rho SD_0$ is the localization length in the wire in a moderately strong magnetic field [21].

In the limit when $L_B < L_c$, a moderately strong magnetic field, Q is reduced to a 2×2- matrix by the broken time reversal symmetry. In this limit Q belongs to the symmetric space $U(2)/(U(1) \times U(1))$.

For $\omega/\Delta < L_{CU}/L$, corresponding to $\omega < E_c$, where $E_c = 2\pi D/L^2$ is the Thouless energy scale of classically free diffusion through the wire of length L, the spatial variation of Q can be neglected and one retains the same ASD as for random matrices of orthogonal or unitary symmetry, respectively [40, 41].

Increasing the length of the wire L, a crossover in the autocorrelation function can be seen as the wire exceeds the length scale L_c [24].

In order to study quantum localization along the wire, the function $C(\omega)$ should be thus considered as a function of the finite length L of the wire and spatial variations of Q along the wire have to be considered, as described by the one dimensional nonlinear sigma model derived above.

The impurity averaged ASD can to this end be written as a partition function [25]

$$\bar{C}(\omega) = \mathrm{Tr} \exp(-L\bar{H}\,[Q]), \tag{2.39}$$

where $\bar{H}$ is an effective Hamiltonian of matrices Q on a compact manifold, determined by the symmetries of the Hamiltonian H of disordered electrons. Thus, the problem reduces to the one of finding the spectrum of the effective Hamiltonian $\bar{H}$.

We can derive the corresponding Hamiltonian $\bar{H}$ by means of the transfer matrix method, reducing the one-dimensional integral over matrix field Q, Eq. (2.38), to a single functional integral. Thus, the ASD is obtained in the simple form of Eq. (2.39), with the effective Hamiltonian

$$\bar{H}(\omega = 0) = \frac{1}{\alpha L_{CU}}(-4\Delta_Q^R - \frac{1}{16}X^2 \mathrm{Tr}_Q[Q, \tau_3]^2). \tag{2.40}$$

Δ_Q^R is that part of the Laplacian on the symmetric space, which does not commute with $\mathrm{Tr}[\Lambda_3 Q]$. The time reversal symmetry breaking due to the external magnetic field is governed by the parameter $X = \alpha L_{CU}/(2L_B)$.

The problem is now equivalent to a particle with "mass" $(\alpha/8)L_{CU}(E)$ moving on the symmetric space of Q in a harmonic potential with "frequency" $1/(2L_B)$, and in an external field $i\alpha(\pi/4)\omega/(L\Delta)$, in "time" x, the coordinate along the wire. To find the ASD as a function of ω and the length of the wire L, one can do a Fourier analysis in terms of the spectrum and eigenfunctions of the effective Hamiltonian at zero frequency, $\bar{H}(\omega = 0)$ [43].

There is a finite gap E_G between the ground state energy and the energy of the next excited state of $\bar{H}(\omega = 0)$. For a long wire, $LE_G \gg 1$, the ASD becomes, $C(\omega) = \exp(-const.L\omega^2/E_G)$, where both $const.\omega^2 = |< 0\,|\bar{H}(\omega) - \bar{H}(0)|\,1\,>|^2$, and the gap between the ground state and the first excited state, $E_G = E_1 - E_0$, do depend on the symmetry of the Hamiltonian $\bar{H}$. This exponential decay with $L\omega^2$ is typical for a a spectrum of localized states [25]. In the other limit

$LE_G \ll 1$, all modes of $\bar{H}$ do contribute to the trace in the partition function Eq. (2.39) with equal weight, yielding the correlation function of a spectrum of extended states [24]. Thus, the crossover length is entirely determined by the gap E_G, through $\xi_c = 1/E_G$, and can be identified with an averaged localization length.

In order to derive the eigenvalues of the effective Hamiltonian at zero frequency, $\bar{H}(\omega = 0)$, we need to introduce a representation of the matrix Q and evaluate the Laplacian in its parameters. This is done in Appendix A.

Without magnetic field, $B = 0$, the Laplacian is obtained to be

$$\Delta_Q^R = \partial_{\lambda_C}(1-\lambda_C^2)\partial_{\lambda_C} + 2\frac{1-\lambda_C^2}{\lambda_C}\partial_{\lambda_C} + \frac{1}{\lambda_C^2}\partial_{\lambda_D}(1-\lambda_D^2)\partial_{\lambda_D}, \tag{2.41}$$

where $\lambda_{C,D} \in [-1,1]$. Its ground state is 1 and the first excited state is $\lambda_C\lambda_D$. Thus, the gap is

$$E_G(B=0) = 16/L_{CU}. \tag{2.42}$$

For moderate magnetic field, with the condition $L_{CU}(\langle y \bullet y\rangle)^{1/2}B \gg \phi_0 = h/q$, all degrees of freedom arising from time reversal invariance are frozen out, due to the term $\mathrm{Tr}_Q[Q,\tau_3]^2 = 16(\lambda_C^2 - 1)$ which fixes $\lambda_C^2 = 1$. Then, the Laplacian reduces to

$$\Delta_Q^R = \partial_{\lambda_D}(1-\lambda_D^2)\partial_{\lambda_D}. \tag{2.43}$$

Its eigenfunctions are the Legendre polynomials. There is a gap above the isotropic ground state of magnitude

$$E_G(X \gg 1) = 8/L_{CU}. \tag{2.44}$$

For moderate magnetic impurity scattering, exceeding the local level spacing, $1/\tau_S > \Delta_c$, $\alpha = 2$, and the Laplacian is given by Eq. (2.43).

Thus, due to $\alpha = 2$, the gap is reduced to $E_G(1/\tau_S > \Delta_c) = 4/L_{CU}$. For moderately strong spin- orbit scattering $1/\tau_{SO} > \Delta_c$, the Laplace operator is

$$\Delta_Q^R = \sum_{l=1,2} \partial_{\lambda_l}(1-\lambda_l^2)\partial_{\lambda_l}, \tag{2.45}$$

where $\lambda_{1,2} \in [-1,1]$. The ground state is $\psi_0 = 1$, the first excited state is doubly degenerate, $\psi_{11} = \lambda_1$, $\psi_{12} = \lambda_2$. Thus, the gap is the same as for magnetic impurities,

$$E_G(1/\tau_{SO} > \Delta_c) = 4/L_{CU}. \tag{2.46}$$

An external magnetic field lifts this degeneracy but does not change the gap.

Thus, using the crossover in energy level statistics as the definition of a localization length as above, we get in a quasi- 1 -dim. wire,

$$\xi_c = 1/E_G(\beta) = (1/16)\beta L_{CU}, \tag{2.47}$$

where $\beta = 1, 2, 4$ corresponding to no magnetic field, finite magnetic field, and strong spin- orbit scattering or magnetic impurities, respectively. The results are summarized in Table 2.1.

Comparing with the known equation for the localization length, L_c, we find that the dependence of the ratios β on the symmetry is in perfect agreement with the results obtained from the spatial decay of the density- density- correlation function [21], while it differs by the overall constant 1/8.

This relation can be proven directly. The ASD at zero frequency $\bar{C}(0)_L$ of the wire of length L, becomes, when the wire is divided into two parts, $\bar{C}(0)^2_{L/2}$. For $L \to \infty$, we find that the relative difference is:

$$f(L) = \frac{\bar{C}(0)^2_{L/2}}{\bar{C}(0)_L} - 1 = 2p \exp(-LE_G/2), \tag{2.48}$$

exponentially decaying with the length L. Here p is the degeneracy of the first excited state of $\bar{H}(\omega = 0)$. $f(L)$ can be estimated, following an argument by Mott [44]: When the two halves of the wire get connected, see Fig. 2.2, the eigenstates of the two separate halves become hybridized and the eigenenergy of a state ψ_n is changed by $\pm\Delta_c \exp(-2x_n/L_c)$. x_n is random, depending on the position of an eigenstate with closest energy in the other half of the wire. Thus, averaging over x_n gives:

$$f(L) \sim + \exp(-4L/L_c). \tag{2.49}$$

Comparison with Eq. (2.48) yields indeed $1/L_c = 8E_G$.

It is thus a remarkable fact that this length scale, defined as the crossover length of the spectral autocorrelation function, and related to the excitation gap of the compact nonlinear sigma model, has exactly the same symmetry dependence as the localization length, defined through the exponential decay of the spatial density correlation function, found in Ref. [21]. This is especially surprising, since the nonperturbative derivation of the disorder average of the density-density correlation function, $\langle \rho(\mathbf{r}, t)\rho(\mathbf{r}', t')\rangle - \langle \rho(\mathbf{r})^2\rangle$, necessitates the use of the supersymmetry method, resulting in a nonlinear sigma model of supermatrices, having in addition to a compact sector, the one considered here, a

Symmetry		Symmetric Space	Cartan class	Gap E_G
T R	S R	$\mathrm{Sp}(2)/(\mathrm{Sp}(1) \times \mathrm{Sp}(1))$	CII	$16/L_{CU}$
no T R	S R	$U(2)/(U(1) \times U(1))$ (Sphere)	AIII	$8/L_{CU}$
T R	no S R	$O(4)/(O(2) \times O(2))$	BDI	$4/L_{CU}$
no T R	no S R	$U(2)/(U(1) \times U(1))$	AIII	$4/L_{CU}$

Table 2.1: Relation between the symmetry of the Hamiltonian and the gap of the quasi-1D NLσM (TR="time reversal", SR="spin reversal"). The third column refers to the classification of symmetric spaces carried out by Cartan in 1926-1927.

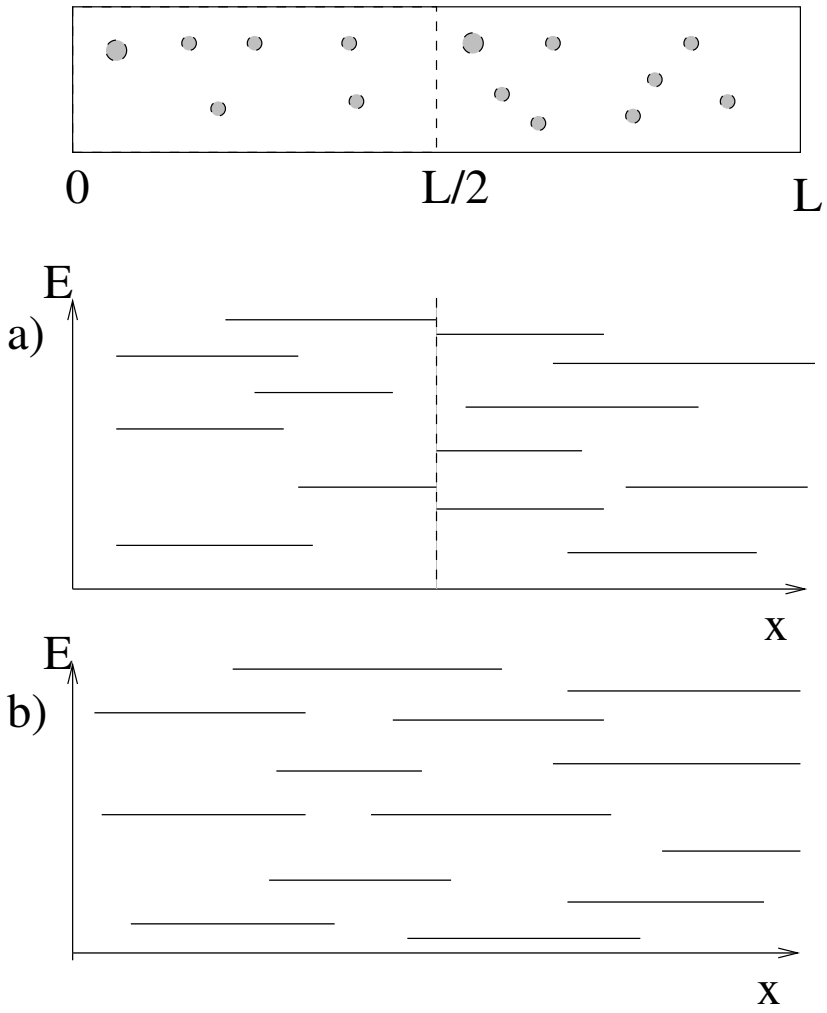

Figure 2.2: Schematic visualization of the energy level spectrum of localized states in a) a disordered quantum wire of length L, when divided into two parts, b) for the same wire when both parts are connected and the eigenstates are hybridized.

non compact sector, where the matrix is parametrized on a semi infinite interval. The full supersymmetry allows furthermore rotations between this compact and noncompact sector which are parametrized by Grassmann numbers ξ, having the property $\xi^2 = 0$. Apart from this increase of the manifold of the matrix fields Q to the supersymmetric space, the structure of the theory is equivalent. Especially, the free energy of the supersymmetric nonlinear sigma model has exactly the same form as Eq. (2.38), replacing Q by supermatrices and the Trace over Q by the supertrace STr [18].

Studying localization in a wire with this supersymmetric nonlinear sigma model, the transfer matrix method yields an effective Hamiltonian of supermatrices Q, of the same form as Eq. (2.40), where the Laplacian is now defined on the respective supersymmetric manifold. In full analogy, the spectrum of $\bar{H}$ determines accordingly the properties of a disordered quantum wire, and has been derived in Ref. [43] for the pure ensembles. The partition function $Z = \mathrm{STr}\exp(-L\bar{H})$ is a generating function of spectral correlation functions[29, 45]. In order to derive spatial correlation functions like the density correlation function, in addition, the eigenfunctions of the respective diffusion equation on the supersymmetric manifold,

$$(-\partial_x + \bar{H}(Q))\psi(x;Q) = 0, \tag{2.50}$$

have to be found [21]. In that way, a formula for the conductance of a finite disordered wire attached to two leads at a distance L, has been derived [43], see also Ref [18]. In the limit of a wire which is perfectly coupled to the leads, that formula for the average conductance simplifies to

$$\langle g\rangle = \frac{1}{2\alpha}\int d\mu(l_i)E(l_i)\exp\left[-\frac{L}{16}E(l_i)\right], \tag{2.51}$$

where $E(l_i)$ are the eigenvalues of the supersymmetric Hamiltonian $\bar{H}(\omega = 0)$ and $d\mu(l_i)$ the corresponding integration measures of the discrete and continous eigenvalues of the angular momentum operator on the compact and noncompact sector, respectively. They were found to be given for $B = 0$ by [43]

$$E(l_i) = 0,\ 4/L_{CU}2(\epsilon^2+1),\ 4/L_{CU}(l^2+\epsilon_1^2+\epsilon_2^2+1), \tag{2.52}$$

where $l = 3, 5, ...$, and $\epsilon > 0, \epsilon_1 > 0, \epsilon_2 > 0$.

For time reversal symmetry broken wires $X > 1$ the eigenvalues were found to be,

$$E(l_i) = 0,\ \frac{4}{\alpha L_{CU})}(l^2+\epsilon^2), \tag{2.53}$$

where $l = 1, 3, 5, ...$, and $\epsilon > 0$.

If spin symmetry is broken, but time reversal symmetry conserved, in the presence of spin orbit scattering, the eigenvalues were found to be,

$$E(l_i) = 0,\ \frac{4}{2L_{CU}}(2(l-1)^2,\ \frac{4}{2L_{CU}}(l_1^2+l_2^2+\epsilon^2-1), \tag{2.54}$$

where $l = 3, 5, ...,$ $l_i = 1, 3, 5, .., i = 1, 2$ and $\epsilon > 0$.

In that case it can be seen that for a distance between the leads much exceeding the localizaion length, $L \gg L_{CU}$, the conductance decays exponentiallly, and that this is entirely determined by the compact gap $\tilde{E}_{\rm G}$ between the lowest angular momentum eigenstates of the compact sector. The integration over the continous eigenvalues of the noncompact sector leads only to a prefactor which decays as a power of the length, $\sim 1/L^{3/2}$. Indeed, the gap between the ground state value $E = 0$ and the first excited state is seen from Eqs. (2.52, 2.53, 2.54) to be $\tilde{E}_G = 8/L_{CU}$ for $B = 0$, $\tilde{E}_G = 4/L_{CU}$ for $X > 1$, $\tilde{E}_G = 2/L_{CU}$ for magnetic impurity scattering, $\alpha = 2$, and $\tilde{E}_G = 2/L_{CU}$ for moderate spin- orbit scattering, coinciding with the symmetry dependence of the compact gap derived above. However, that coincidence might appear as mere chance, since in fact, the Laplacian of the supersymmetric matrix Q cannot be written as a sum of the one of the respective compact nonlinear σ-model, Eqs. (2.41, 2.43, 2.45), because the metric tensor $\hat{g}$ on the supersymmetric space contains mixed factors of compact and noncompact parameters. Therefore, the discrete eigenvalues of $-\Delta_Q$, are not the eigenvalues of the square of the angular momentum on a compact sphere [43]. Only in the limit of infinite, noncompact parameters does one recover the respective Laplacian on the compact symmetric space, Eqs. (2.41, 2.43, 2.45).

Thus, having shown that the ASD yields the correct symmetry dependence of the localization length, we can now use this approach to get an analytical solution for the crossover behaviour of the localization length and the local level spacing as a magnetic field is turned on and there is no spin-orbit scattering.

A self consistent approach [46], a semiclassical analysis [47] and numerical studies [48, 49] all showed a continous increase of the localization length.

The effective Hamiltonian for moderate magnetic fields is found, without spin dependent scattering, $\alpha = 1$, using $\mathrm{Tr}[Q, \tau_3]^2 = 16(1 - \lambda_C^2)$, to be given by:

$$\bar{H} = \frac{1}{L_{CU}}(-4\Delta_Q^R + X^2(1 - \lambda_C^2)), \tag{2.55}$$

where the Laplacian is given by Eq. (2.41) and $X = L_{CU}/(2L_B)$.

In the limit $X \to 0$ the lowest level and the first excited level approach 1 and $\lambda_C\lambda_D$, respectively. In the limit $X \gg 1$, λ_C^2 becomes fixed to 1. Thus, the Ansatz $\psi_0(\lambda_C) \sim \exp(A_0X^2(1-\lambda_C^2))$ and $\psi_1(\lambda_C, \lambda_D) \sim \lambda_C\lambda_D \exp(A_1X^2(1-\lambda_C^2))$, where $A_0 < 0, A_1 < 0$ are negative constants, solves $\bar{H}\psi = \bar{E}\psi$ to first order in $z = X^2(1 - \lambda_C^2)$. One finds that the two lowest magnetic field dependent eigenvalues are $E_0 = 4/L_{CU}(-5+\sqrt{25 + X^2})$, and $E_1 = 4/L_{CU}(-3+\sqrt{49 + X^2})$, and the eigenfunctions are given as above with $A_0 = -L_{CU}E_0/(16X^2)$, and $A_1 = (1 - L_{CU}E_1/16)/X^2$, yielding the right limits for $X \to 0$ and $X \gg 1$, respectively. Thus, there is a magnetic field dependent gap $E_G = E_1 - E_0$ of magnitude:

$$E_G(X) = 4(2 + \sqrt{49 + X^2} - \sqrt{25 + X^2})/L_{CU}. \tag{2.56}$$

This solution is valid in both the limits $X \ll 1$ and $X \gg 1$, interpolating the region $X \approx 1$.

With the magnetic diffusion length $L_B = (D\tau_B)^{1/2}$, and the magnetic phase shifting rate, as given by Eq. (2.19), we obtain:

$$X = L_{CU}/(2L_B) = L_{CU}\frac{e}{\hbar}\sqrt{\langle y \bullet y\rangle}B, \tag{2.57}$$

which is $\sqrt{\langle y \bullet y\rangle}/W$ times the number of flux quanta penetrating a localization area $L_{CU}W$. From Eq. (2.56) follows that the magnetic change of the localization length is $\delta L_{\rm c}(B) \sim B^2$ for small and $\sim 1/B$ at large magnetic fields, which agrees with the result of the self-consistent method as obtained by Bouchaud[46].

2.4 Resistance of quasi-1D wires

In the limit of zero temperature, $T = 0$, the resistivity of a disordered quantum wire, having only localized states at the Fermi energy, is infinite. For finite temperature, $T > 0$, in the strong localization regime $k_{\rm B}T < \Delta_{\rm c}$, the mechanism of conduction is hopping of electrons between localized states. Then, the resistivity increases exponentially with temperature. According to the resistor network model [50, 51], each pair of localized states i and j is linked by a resistance R_{ij}:

$$R_{ij} = \exp\left(\frac{2r_{ij}}{L_{\rm c}} + \frac{\epsilon_{ij}}{k_BT}\right) \tag{2.58}$$

where $r_{ij} = |r_i - r_j|$ and $\epsilon_{ij} = (|\epsilon_i - \mu| + |\epsilon_j - \mu| + |\epsilon_i - \epsilon_j|)/2k_BT$ (r_i and ϵ_i are the position and energy of the state i, μ being the Fermi energy). Because of the exponential dependence of R on r_{ij} and ϵ_{ij}, percolation theory methods can be applied [52, 53, 54]. In 2-D and 3-D systems, the dependence of R on temperature T shows a crossover from an activated behaviour to the variable range hopping (VRH) regime. In this regime the temperature is so low that the typical resistances between neighbouring states are large because of the second term in Eq. (2.58). Therefore electrons tunnel to distant states whose energies are close to the Fermi level. If we neglect electron-electron interactions the resistivity is described by Mott's law [52, 55]:

$$R(T) = R_0 \exp[(\gamma T_0/T)^{1/(d+1)}] \tag{2.59}$$

where d is the dimensionality of the system, γ a numerical coefficient which depends on d, $T_0 = 1/\rho L_{\rm c}^d$ and ρ_d is the dimension dependent density of states. However, in the quasi-1-D case and for sufficiently long wires the variable range hopping result, Eq. (2.59), cannot used due to the presence of exponentially rare segments inside which all the localized states have energies far from the Fermi level [56, 57, 58]. These large resistance segments (LRS) do not affect

the resistivity of 2-D and 3-D systems because they can be circumvented by the current lines. In 1-D this is not possible and the total resistance of a wire is given by the sum of the resistances of all the LRS's. This sum yields an activated type dependence of R on T [57] for infinite wires:

$$R = R_0 \frac{L}{L_c} \left(\frac{T_0}{T}\right)^{\frac{1}{2}} \exp\left(\frac{T_0}{2T}\right), \tag{2.60}$$

where $k_B T_0 = 1/\rho L_c = \Delta_c$ coincides with the local level spacing, and L is the length of the wire. Eq. (2.60) is valid provided that the number of optimal LRS's (i.e. those LRS's which give the largest contribution to R [57]) in the system is large. For a finite wire length this condition fails to be fulfilled at very low temperature T, and the resistance of the chain is determined by smaller LRS's; in this regime Eq. (2.60) is replaced by [56, 57]:

$$R \approx R_0 \exp\left\{\sqrt{2\frac{T_0}{T}\log\left[\frac{L}{L_c}\left(\frac{T}{T_0}\right)^{\frac{1}{2}}\log^{\frac{1}{2}}\left(\frac{L}{L_c}\right)\right]}\right\}, \tag{2.61}$$

which is valid at temperatures below

$$T_1 = \frac{T_0}{2\ln(L/L_c)}. \tag{2.62}$$

So far, electron-electron interactions have not been taken into account. This approximation is valid if the Coulomb interaction is screened over distances of the order of the hopping length, as by a metal gate electrode deposited on top of the wires at a distance smaller than the typical hopping lengths. When this is not the case, long range electron-electron interactions affect both the density of states and the resistance of the samples [59, 60].

2.5 Symmetry dependence of Localization in Disordered Wires: Experimental Analysis

The magnetic field dependent activation energy was measured recently in transport experiments of Si δ-doped GaAs quantum wires [22]. As an example, we discuss here the sample 5 of Ref. [22], with a width $W = 0.2\mu m$, a localization length $L_{CO} = 0.61\mu m$, a length $L = 40\mu m$ and $N = 30$ channels.

The activation energy coincides with the local level spacing $k_B T_0 = \Delta_c = 1/(\rho W L_c)$ and is estimated for sample 5 to be $T_0 = 0.34K$.

Thus, according to the theory outlined in the previous section, there is an activated resistance in an order of magnitude temperature range $T_1 = 0.04K < T < T_0 = 0.34K$, allowing in good approximation the direct measurement of the

magnetic field dependent activation energy $\Delta_c(B)$ and thus the magnetic field dependence of the localization length $L_c(B)$.

The ratio of the cyclotron frequency and the elastic scattering rate, $\omega_c\tau = l/(k_F l_B^2) \ll 1$, is small in the whole range of magnetic fields considered there, so that the classical conductance would be magnetic field independent, $\sigma = n_e e^2\tau/m_e(1+\omega_c^2\tau^2)^{-1} \approx n_e e^2\tau/m_e$.

The mean free path $l \sim 2 \cdot 10^{-2}\mu m$ is small compared to the width of the sample $W = 0.2\mu m$. The magnetic length is $l_B = 0.026\mu m(B/T)^{-1/2}$ and thus, while $\omega_c\tau \ll 1$, the magnetic length becomes smaller than the width of the sample at magnetic fields $B > 1.65 \cdot 10^{-2}T$.

The experimental magnetic field dependence of the ratio of activation energies is shown in Fig. 2.3 together with the theoretical curve for the ratio of local energy level spacings $\Delta_c(B)/\Delta_c(0) = E_G(B)/E_G(0)$, as derived above, Eq. (2.56), using for the magnetic phase shifting rate the results for a wire with specular boundary conditions, Eq. (2.24), and, for comparison, the one derived for a parabolic wire, Eq. (2.34).
There is a quantitative discrepancy between the best fit $X = 0.036B/G$, and $X = 2\pi\phi/\phi_0$, $\phi = \mu_0 H L_{CU}(\overline{y^2})^{(1/2)}$, when using the analytical formula Eq. (2.24). With the experimental parameters $\alpha = 1, L_{CO} = 0.61\mu m$, width $W = 0.2\mu m$ of sample 5 in Ref. [22] and $\overline{y^2} = W^2/12$ for a wire with specular boundary conditions, it yields rather $X = 10^{-2}B/G$. We note that smooth confinement can give $\overline{y^2} > W^2/12$. A similar discrepancy was observed between W as obtained from the sample resistance and estimated from the analysis of the weak localization magnetoresistance, which also depends on $\overline{y^2}$ [61].

We note that, when using the experimental parameters, the agreement for the parabolic wire is better. The cyclotron length $l_{cyc} = k_F l_B^2 = 0.32/(B/T)\mu m$, is found to be larger than the mean free path l for $B < 15T$ and larger than the wire width for $B < 1.5T$. We find for the parabolic wire: $X = 2.4 \cdot 10^{-2}(0.99 + 1.33\ 10^{-8}(B/G)^2)^{1/2}B/G$. The enhancement of the magnetic phase shifting rate in a parabolic wire, Eq. (2.34), is thus too weak to be seen at the magnetic fields used in the experiment, $B < 0.2T$, as shown in Fig. 2.3, and seems thus not to be the origin of the increase in the decay of the activation gap at about $0.1T$.

An extension of the derivation given in section 2.2 to include a dependence of the eigenfunctions on the magnetic field also for a 2-dimensional wire with specular boundary conditions has to be done, in order to make the comparison with the experiment more quantitative, and draw conclusions from the magnetolocalization on the form of the confinement potential in these Si-δ-doped Ga As quantum wires. However our results may indicate that the harmonic confinement model of the parabolic wire is a better description of the wires in sample 5.

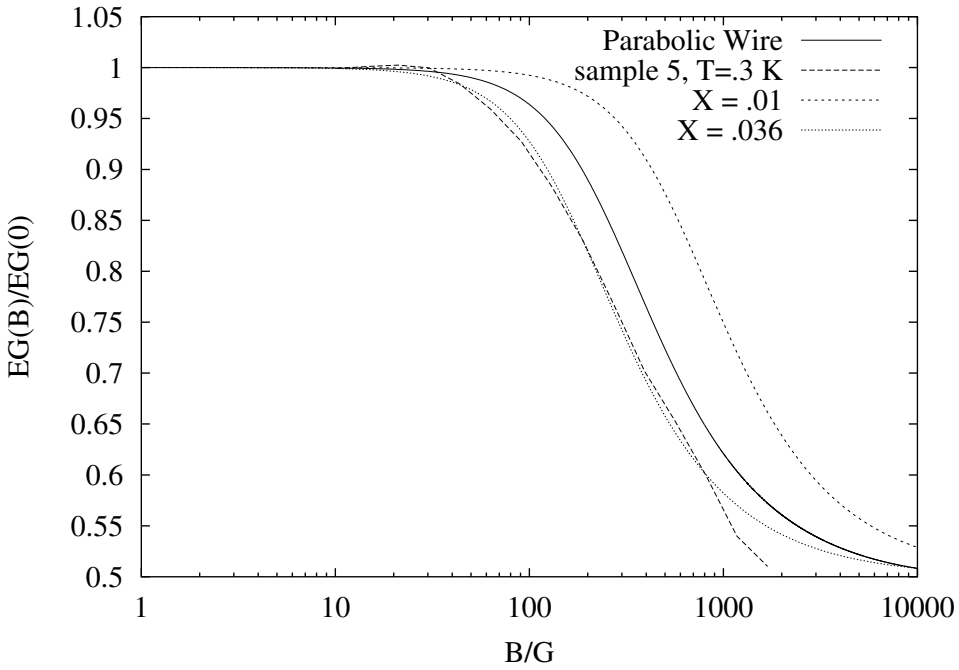

Figure 2.3: The activation gap ratio $T_0(H)/T_0(0)$ as a function of the magnetic field B in G of sample 5 measured at temperature $T = 0.3K$ as reported in Ref. [22], together with the theoretical curves for a parabolic wire, using the parameters of sample 5. and a 2D wire with specular boundary conditions for a best fit value $X = 0.036B/G$, and the value obtained from the experimental parameters, $X = 0.010B/G$.

Chapter 3

The Quantum Hall Effects

"dai diamanti non nasce niente
dal letame nascono i fior"
F. De Andre', *Via del Campo*

In this chapter we present a short introduction to the theory of the Integer and the Fractional Quantum Hall Effect.

We start by considering the integer case. After recalling the basic experimental facts, we present a qualitative description of metal-insulator transitions driven by disorder in a strong magnetic field, which are believed to underlie this effect. Then we study the density of states of electrons subject to a magnetic field and an impurity potential. Finally, we briefly introduce the percolation model, which provides a nice, semiclassical picture of the effect and the field theoretical approach, which aims to explain the transitions by a generalization of the supersymmetric method introduced in Chapter 1.

In the fractional case, Coulomb interactions play a fundamental role. Due to interactions, electrons form a quantum, incompressible liquid state, which is believed to underlie the fractional effect. After discussing the properties of wavefunctions in the lowest Landau level, we introduce the novel wavefunction invented by Laughlin to describe this special condensed state. Finally, we discuss some remarkable properties of the elementary charged excitations of the system.

3.1 The Integer Quantum Hall Effect: basics facts

According to the Drude theory, the longitudinal and transversal resistivities of a two dimensional electron gas subjected to a perpendicular, constant magnetic field B are [1]

$$\rho_{xx} = \frac{m}{n_e e^2 \tau}$$

$$\rho_{xy} = \frac{B}{n_e ec}. \tag{3.1}$$

The magnetic field does not affect the diagonal component of ρ, the magnetoresistivity, whereas the Hall resistance ρ_{xy} is proportional to B. In 1980, K. von Klitzing [62] observed dramatic deviations from the classical picture: at very low temperatures and for large magnetic fields, the Hall resistance showed plateaux around quantized values,

$$\rho_{xy} = \frac{h}{\nu e^2}, \tag{3.2}$$

where ν is an integer. Moreover, the magnetoresistivity was nearly vanishing in the regions where ρ_{xy} is constant. This effect was called Integer Quantum Hall Effect (IQHE). It turned out that the quantization of the Hall resistance is universal and independent on the microscopic details of the sample: in particular, it is not affected by impurities (provided that the the amount of disorder is not too large).

In 1982, Tsui, Stoermer and Gossard [63] observed quantized plateaux at filling factor $\nu = 1/3$ in very clean devices (the Fractional Quantum Hall Effect, FQHE). Subsequently, many more fractions were observed (see Fig. 3.1), most of them belonging to the principal series

$$\nu = p/(2mp \pm 1) \tag{3.3}$$

(p and m nonnegative integers) or to families obtained by adding integers to (3.3). Until recently, the only exceptions were the even denominator fractions $\nu = 5/2$ and $\nu = 7/2$. Last year Pan et al. [64] observed plateaux at $\nu = 4/11$ and $\nu = 5/13$, which do not fit into the standard series (3.3).

The FQHE is also universal but very pure samples are needed in order to observe it (extremely pure in the case of non standard fractions).

It is not difficult to show that the QHE could not occur in a device free from imperfections: as a consequence of Lorentz covariance, the Hall resistance of a translationally invariant system would be given by (3.1), no matter whether the system is classical or quantum (of course, the magnetoresistance would be zero, as in the QHE). Disorder is responsible for the exactness of the quantization of ρ_{xy}!

The 2x2 resistivity tensor of Quantum Hall systems can be easily inverted: the diagonal components of the conductivity matrix are also zero. Hence, QH devices are perfect insulators and yet they are perfect conductors due to the current running perpendicular to the voltage.

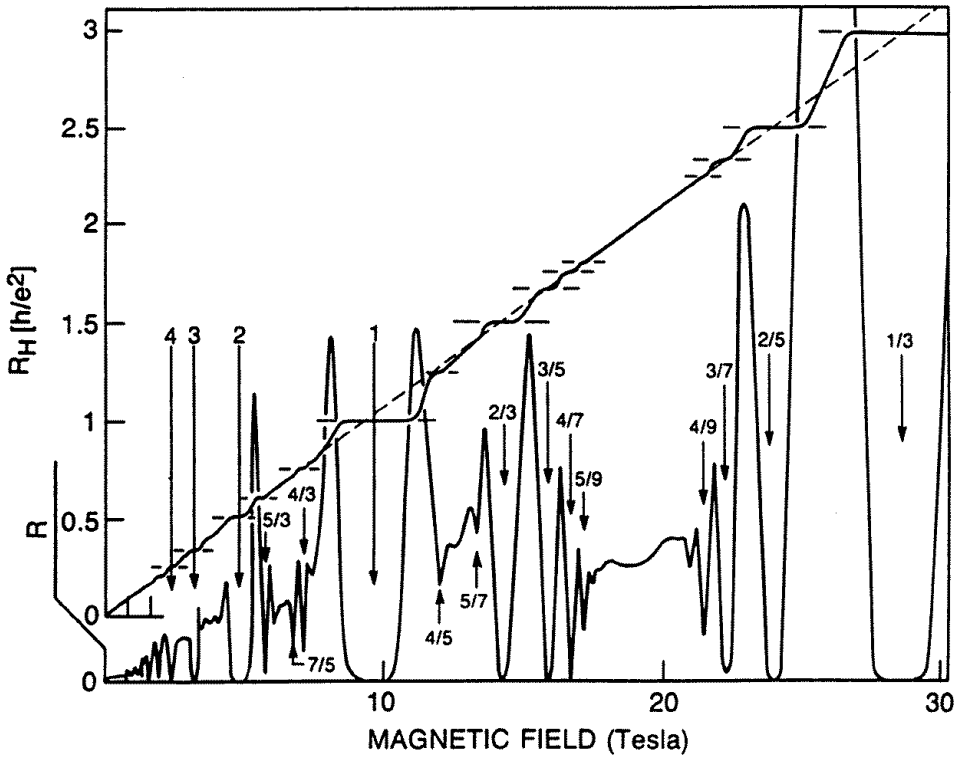

Figure 3.1: The Hall resistance $R_H \equiv \rho_{xy}$ and the diagonal resistance $R \equiv \rho_{xy}$ as functions of the magnetic field. Many plateaux in R_H and associated dips in R are visible, both at Integer and Fractional filling factors ν. The numbers indicate the values of ν at which plateaux occur. After Ref. ([65]).

3.2 The Role of Disorder: Localization-Delocalization Transitions

In this section we will focus on the IQHE at $T = 0$. Since Coulomb interactions seem not to play an important role in this phenomenon, we will neglect them altogether.
Let's consider for a moment the noninteracting Hamiltonian for N electrons without disorder:

$$H = \sum_i^N \frac{1}{2m_e} \left(\mathbf{p}_i + \frac{e}{c} \mathbf{A}(\mathbf{r}_i) \right)^2, \tag{3.4}$$

where m_e is the electron effective mass and $\mathbf{A}(\mathbf{r})$ is the vector potential related to B. It is well known that the spectrum of (3.4) is discrete:

$$E_n = (n + \frac{1}{2})\hbar\omega_c, \tag{3.5}$$

where $\omega_c = eB/m_e c$ is the cyclotron frequency. For a macroscopic 2D sample of area S, the discrete levels, named Landau Levels (LLs), are hugely degenerate: the total number of states in a LL is

$$\frac{S}{2\pi l_B^2} = \frac{\Phi}{\Phi_0} \equiv N_\Phi, \tag{3.6}$$

where $l_B = \sqrt{\hbar c/eB}$ is the magnetic length, $\Phi = SB$ and N_Φ is the number of flux quanta penetrating the sample. Therefore there is one state per Landau level per flux quantum.
The filling factor ν is the ratio between the number of electrons and the LL degeneracy: $\nu = N/N_\Phi = n\Phi_0/B$.
When an integer number of levels are completely filled at $T = 0$, the diagonal conductivity is zero due to the energy gap. Furthermore, the Hall conductivity is correctly quantized, being given by

$$\sigma_{xy} = n_e ec/B = \nu ec/\Phi_0 = \nu e^2/h. \tag{3.7}$$

However, this argument is quite deceptive: actually, it cannot explain the plateaux at all. In experiments, the density or the field B can be varied. When a LL is filled completely, the Fermi energy jumps discontinuously to the next LL and therefore σ_{xy} must be an increasing function of the density. Formula (3.7) simply states that σ_{xy} is a linear function of ν!

Static disorder is expected to broaden Landau levels into bands, thus lifting the LL degeneracy, and to create localized states between LLs, which do not contribute to transport. In the presence of extra localized states in the gap, the Fermi energy has to progress through them when the density (or the magnetic

field) is varied and σ_{xy} does not change in this region, i.e. a plateaux can form. Moreover, σ_{xx} ought to be zero when the Fermi energy pins to localized states.

We have seen in chapter 1 that, for $d = 2$ and in the absence of magnetic fields and spin-orbit scattering, all the states of a disordered system are localized. In the QH case there must be some extended states, since there is a non-vanishing σ_{xy}. It is believed that, in the presence of a strong B, the states close to the center of the LLs are extended (i.e. their localization radius is larger than the system size) and that the localization length diverges exactly at the center. Moreover, there are convincing indications that the critical exponent which govern the disorder-driven localization-delocalization transition is universal.

In order to get the correct quantized values (3.2) of ρ_{xy}, the amount of current which is lost when a localized state is formed must be compensated by the remaining extended states: it was shown by Prange in [66] that this is indeed the case. Later on, Laughlin [67] and Halperin [68] argued that the accuracy of the effect is a consequence of gauge invariance.

The localization problem in the presence of a strong B has not been fully solved yet: a promising and partially successful (but not complete yet) effective field theory has been developed in [69] and subsequent papers. Its derivation follows the steps outlined when introducing the non-linear sigma model (see chapter 1). Moreover, much light can be shed on this problem in the semiclassical limit where l_B is much smaller than the correlation radius of the potential r_c by studying a classical percolation model. We will discuss both approaches in section 3.4 but first we will focus on the Density of States of impure Landau Hamiltonians.

3.3 The Density of States: perturbative and nonperturbative calculations

In this and the following section we will assume that $T = 0$ and thus completely neglect the interaction of electrons with phonons. As we discussed in the previous section, disorder broadens Landau levels by creating localized states in the gap between LLs. The most relevant source of disorder in a real 2DEG is the electrostatic potential created by randomly distributed fixed impurities. Again, we assume that the potential $V(\mathbf{r})$ is a Gaussian, stochastic quantity with zero mean and correlator $W(\mathbf{r} - \mathbf{r}') = n_i|V|^2\delta(\mathbf{r} - \mathbf{r}')$ (n_i is the impurity concentration). The single-particle Hamiltonian is

$$H = \frac{1}{2m_e}\left(\mathbf{p} + \frac{e}{c}\mathbf{A}(\mathbf{r})\right)^2 + V(\mathbf{r}), \tag{3.8}$$

and we choose the Landau gauge $\mathbf{A} = (0, Bx, 0)$. In this gauge, the eigenfunctions of the clean single particle Hamiltonian are:

$$\psi_{n,k}(\mathbf{r}) = \frac{1}{2\pi}\frac{1}{\sqrt{2^n n!\sqrt{\pi}l_B}}e^{ikx}H_n(\frac{y+kl_B^2}{l_B})e^{-\frac{1}{l_B^2}(y+kl_B^2)^2} \equiv \frac{e^{ikx}}{2\pi}\phi_{n,k}(x), \qquad (3.9)$$

where n is the Landau index and the quantum number k is the (canonical) momentum along the $\hat{y}$ direction. The states with the same number n are degenerate.

The exact impurity averaged DOS is given by:

$$\rho(E) = \int DV(\mathbf{r}) \exp\{-S[V(\mathbf{r})]\}\rho(E, [V(\mathbf{r})]), \qquad (3.10)$$

where $\rho(E, [V(\mathbf{r})])$ is the DOS of the given realization of the Hamiltonian $H[V(\mathbf{r})] = (\mathbf{p} + e/c\mathbf{A})^2 + V(\mathbf{r})$ and

$$S[V(\mathbf{r})] = -\frac{1}{2n_i|V|^2}\int V^2(\mathbf{r})d\mathbf{r} \qquad (3.11)$$

is the action of the potential.

In the following, we will calculate the broadening of LLs due to $V(\mathbf{r})$ perturbatively; then, we will briefly discuss more sophisticated, non-perturbative methods.

We exploit the well-known relation between the averaged electronic Green's function and the DOS $\rho(E)$:

$$\rho(E) = \frac{1}{\pi}\mathrm{Im}G(z). \qquad (3.12)$$

Since $V(\mathbf{r})$ is rotationally invariant with respect to the z-axis, $G(z)$ is diagonal in the Landau model and its diagonal elements depend only on n:

$$G_n(z) = \frac{1}{z - E_n - \Sigma_n(z)}. \qquad (3.13)$$

The self-energy can be decomposed into its real and imaginary parts: $\Sigma_n(E) = \Delta_n(E) - i\Gamma_n(E)$.

In the self-consistent Born approximation,

$$\Sigma_n(E) = \sum_{n'} r_{nn'}G_{n'}(E) = \sum_{n'}\frac{r_{nn'}}{E - E_{n'} - \Sigma_{n'}(E)}, \qquad (3.14)$$

where

$$r_{nn'} = \int d\mathbf{q}dpW(q)|\langle n, k|e^{i\mathbf{q}\cdot\mathbf{r}}|n', p\rangle|^2. \qquad (3.15)$$

If the field B is so strong that the inequality $\Gamma_n \ll \hbar\omega_c$ holds, Landau level mixing can be neglected and formula (3.14) reduces to an algebraic equation:

$$\Sigma_n(E) = \frac{r_n}{E - E_n - \Sigma_n(E)}, \qquad (3.16)$$

where $r_n \equiv r_{nn}$. The solution of 3.16 is

$$\Sigma_n(E) = \Delta_n(E) + i\Gamma_n(E), \tag{3.17}$$

where

$$\Delta_n(E) = \frac{1}{2}(E - E_n), \qquad \Gamma_n(E) = \frac{1}{2}\sqrt{4r_n - (E - E_n)^2}). \tag{3.18}$$

The DOS (3.12) is given by:

$$\rho(E) = \frac{1}{2\pi l_B^2}\sum_n \frac{1}{\pi}\frac{\Gamma_n(E)}{(E - E_n - \Delta_n(E))^2 + \Gamma_n^2} = \frac{1}{2\pi l_B^2}\sum_n \frac{\Gamma_n(E)}{\pi r_n}. \tag{3.19}$$

Hence, $\rho(E)$ consists of semiellipses centered around the LLs E_n, with a width $\Gamma_n = 2\sqrt{r_n}$.

We can now calculate r_n for a δ-correlated $V(\mathbf{r})$:

$$\begin{aligned} r_n =& n_i|V|^2 \int d\mathbf{q}dp|\langle n,k|e^{i\mathbf{q}\cdot\mathbf{r}}|n,p\rangle|^2 \\ =& n_i|V|^2 \int d\mathbf{q}dp\delta(p - q + q_y)| \int dx\phi_{n,k}(x)e^{iq_x x}\phi_{n,p}(x)|^2 \\ =& n_i|V|^2 \int d\mathbf{q}|L_n^0(\frac{l_B^2q^2}{2})e^{-\frac{l_B^2q^2}{4}}e^{-\frac{i}{2}(k+p)l_B^2}|^2 \\ =& \frac{n_i|V|^2}{2\pi l_B^2}\int_0^\infty d\xi[L_n^0(\xi)]^2e^{-\xi} = \frac{n_i|V|^2}{2\pi l_B^2}. \end{aligned} \tag{3.20}$$

Since

$$2\pi n_i|V|^2\rho_{B=0} = \frac{\hbar}{\tau}, \tag{3.21}$$

where τ is the electronic relaxation time due to $V(\mathbf{r})$ at $B = 0$ in the Born approximation and $\rho_{B=0} = m/(2\pi\hbar^2)$ is the density of states of free electrons, Γ_n can be written as [71, 72]

$$\Gamma_n = \sqrt{\frac{2\hbar\omega_c}{\pi}\frac{\hbar}{\tau}}. \tag{3.22}$$

Γ_n does not depend on n and scales as $\sqrt{B}$. In general, in the case of non δ-correlated potentials, Γ_n will show a dependence on n.

The cusps of $\rho(E)$ are due to the approximations involved in our derivation and more sophisticated approaches are needed in order to get rid of them. Actually, for the case of $B \to \infty$ (i.e., no LL mixing) and a δ-correlated V, the DOS for the lowest LL has been calculated exactly by Wegner in [73]. In this remarkable paper, Wegner succeeded in summing up all the diagrams contributing to $\rho_{n=0}(E)$

by mapping the system onto a zero-dimensional, ϕ^4 field theory. The exact DOS for the lowest LL is

$$\rho_{n=0}(E) = \frac{1}{2\pi l_B^2}\frac{d}{dE}\tan^{-1}\left(\frac{2}{\sqrt{\pi}}\int_0^{(2\pi l_B^2\Delta E^2/n_i|V|^2)^{1/2}} e^{\eta^2}d\eta\right), \tag{3.23}$$

where $\Delta E = E - E_0 = E - 1/2\hbar\omega_c$. Near the band centre of the lowest LL, the approximate, self-consistent DOS (3.19) is surprisingly good: in the very centre $E = E_0$, (3.19) differs only 0.3 per cent from the exact value (3.23). However, far from the band centre, the Landau band shows tails which are beyond a perturbative treatment.

The non perturbative tails of an arbitrary Landau band attracted considerable interest both prior to and after the publication of [73] and different approaches were employed to study them. For instance, the Lifshitz's Optimum Fluctuation Method (OFM) [74] and the supersymmetric method [75] were successfully applied to the study of the tails near the band centre

$$\Gamma_n \ll |E - E_n| \ll \hbar\omega_c \tag{3.24}$$

to yield a Gaussian DOS. This result agrees with Wegner's result: in the limit (3.24) for $n = 0$, Eq. (3.23) becomes

$$\begin{aligned}\rho(E) &\to \frac{1}{2\pi l_B^2}\frac{d}{dE}\tan^{-1}\left(\frac{n_i^{1/2}|V|}{\sqrt{2\pi}l_B\Delta E}e^{\frac{2\pi l_B^2\Delta E^2}{n_i|V|^2}}\right)\\ &\to \frac{2\sqrt{2}\pi l_B\Delta E^2}{n_i^{3/2}|V|^3}e^{-\frac{2\pi l_B^2\Delta E^2}{n_i|V|^2}}.\end{aligned} \tag{3.25}$$

The OFM employed by Larkin et al. [74] relies on the following idea, which is due to Lishitz: in the tails of the DOS, states are localized around strong fluctuations of the random potential $V(\mathbf{r})$, the probability of which is exponentially small. Therefore, the average (3.10) over all configurations yielding states of energy E, is dominated by the most probable realization of $V(\mathbf{r})$ and the functional integral (3.10) can be evaluated in the saddle point approximation. We will dwell on this method more thoroughly in chapter 6, where we will apply it to systems subject to Random Magnetic Fields.

As expected (see chapter 1), the exact DOS (3.23) does not provide information on localization; again, more complicated objects (i.e. products of Green's functions) are needed to obtain informations about localization-delocalization transitions in the Landau problem.

3.4 Localization in a strong magnetic field

3.4.1 Field theoretic approach

The conventional σ-model (1.43) leads to the localization of all states in two dimensions; it cannot thus predict the Hall quantization. It was realized by Levine et al. [69] that something was missing in (1.43) and that a more careful expansion of the logarithm in (1.38) yielded a new topological term in the action, which turned out to be responsible for the QHE. In [69] a δ-correlated potential was considered but it should be possible to generalize their method to random potentials with arbitrary correlation length (see [37]).

The new action can be written as [69, 70]

$$S_B[Q] = \frac{1}{16}\int d\mathbf{r}\mathrm{Str}\{\sigma^0_{xx}(\nabla Q)^2 - \sigma^0_{xy}Q[\nabla_x Q, \nabla_y Q] + 4\pi i\nu\omega\Lambda Q\}, \tag{3.26}$$

where the parameters σ^0_{xx} and σ^0_{xy} are the longitudinal and Hall conductivities in SCBA expressed in units of e^2/h. The second term in (3.26) is topological in nature and cannot be obtained in any order of perturbation theory in the Diffusons and the Cooperons. It can be rewritten in this form (using the constraint $Q^2 = \mathbb{1}$):

$$S_{top} = -\frac{\sigma^0_{xy}}{8}\int d\mathbf{r}\ \mathrm{Str}(Q\nabla_x Q\nabla_y Q). \tag{3.27}$$

To see the topological origin of S_{top}, one can substitute the representation $Q = U\Lambda\bar{U}$ (see section 1.2.2) into 3.27; then, one gets

$$\begin{aligned} S_{top} &= -\frac{\sigma^0_{xy}}{4}\int d\mathbf{r}\ \nabla \times \mathrm{Str}(\Lambda\bar{U}\nabla U) \\ &= -\frac{\sigma^0_{xy}}{4}\oint_{\mathcal{C}} \mathrm{Str}(\Lambda\bar{U}\nabla U)\cdot d\mathbf{l}, \end{aligned} \tag{3.28}$$

where $\mathcal{C}$ is a contour encircling the sample. It can be shown that, for a homogeneous Hall conductance, S_{top} can take only purely imaginary discrete values,

$$S_{top} = 2\pi i\sigma^0_{xy}s, \tag{3.29}$$

where s is an integer.

In order to establish a renormalization group approach to this complicated field theory, both σ^0_{xx} and σ^0_{xy} must be taken as scaling parameters (unlike the one parameter scaling theory valid at $B = 0$). There is an infinite number of topologically distinct solutions (with different quantum numbers n) of the saddle point equation $\delta S = 0$. By summing over all these instanton solutions and integrating out slow spatial fluctuations around them, one finds that σ^0_{xx} is renormalized to smaller values and thus flows towards localization. However,

at half-integer values of the non diagonal conductance, $\sigma_{xy}^0 = (n + 1/2)$, the renormalization flow is slowed down. Indeed, it has been proven that the theory is critical at these values of σ_{xy} and a two-parameter scaling theory has finally been established.

So far, it has not been possible to calculate the critical exponents of the metal-insulator transitions, since the critical points are located in the strong-coupling limit of the theory. Recently, however, the non linear σ-model for short-ranged disorder at $\sigma_{xy}^0 = (n+1/2)$ has been mapped onto the Hamiltonian of a quantum superspin chain [76]. Since the latter problem is closely related to the Chalker-Coddington model (which mimicks a QH system with long-range disorder in the high-field limit), the mapping of [76] confirms the notion of universality of the QHE. Moreover, starting from this mapping, supersymmetric conformal field theories have been introduced, which should yield the critical exponents of the transitions [77].

3.4.2 Other approaches

For smooth disorder potentials with large correlation length r_c and strong magnetic fields, the inequality $l_B \ll r_c$ is fulfilled. When this is the case, the electronic wavefunctions live on equipotential lines, since the kinetic energy is quenched. They have a width perpendicular to these lines which is of the order of l_B.

In the limit $B \to \infty$ this confinement to lines of constant potential becomes exact for any disorder potential (provided that r_c is finite) and a good deal of light can be shed on the quantum mechanical problem of localization by investigating a classical percolation problem.

In the percolation model, low-energy states lie along closed contours in deep valleys of the potential landscape, while high-energy states live on lines encircling potential hills. At intermediate energies, the states take more complex shapes and have thus larger localization radii. For an infinite system, it can be proven that there is exactly one percolating path, i.e. one extended state, at a critical energy E_c in the intermediate region.

Within this classical picture, the critical exponents describing the localization-delocalization transition can be computed numerically. In particular, the exponent ν, which determines the singular behaviour of the localization length ξ near the Landau energies $E_n = (n + 1/2)\hbar\omega_c$,

$$\xi = \xi_n |E - E_n|^{-\nu}, \tag{3.30}$$

is given by $\nu_{cl} = 4/3$ [78].

However, tunneling between percolating paths close to each other plays an important role for states with energies close to the percolation threshold, no matter how large B is. Tunneling enhances the localization length of these states, thus affecting the exponent ν. An argument by Mil'nikov and Sokolov [79] which takes into account this effect yields $\nu = 7/3$.

Since a complete theory of the QH transition has not been established yet, a variety of numerical methods have been used to estimate the critical parameters. The results strongly confirm the conjecture of universality of the transitions. According to most numerical estimates, $\nu \sim 2.3 \pm 0.1$, independent on the LL [80, 81]; this value is in good agreement with the estimate of Mil'nikov and Sokolov [79].

3.5 The Fractional Quantum Hall Effect

3.5.1 Properties of wavefunctions in the LL level

In this and the following two sections we will neglect disorder and focus on the theory developed by Laughlin to describe a system of interacting electrons at fractional filling factors [82, 83, 84]. In the Coulomb gauge

$$\mathbf{A} = -\frac{1}{2}\mathbf{r} \times \mathbf{B}, \tag{3.31}$$

the rotational symmetry of Hall systems is preserved and the angular momentum is a good quantum number. For very large B, the cyclotron energy is the largest energy scale and we can thus consider the lowest LL only. Moreover, in this limit the Zeeman splitting is larger than the typical Coulomb energy $e^2/(\varepsilon l_B)$ and we can assume that the electron system is fully spin polarized. The lowest level solutions of the one particle Schrödinger equation with angular momentum $\hbar m$, $m \geq 0$, are given by

$$\phi_m(z) = \frac{1}{\sqrt{2\pi l_B^2 2^m m!}} (\frac{z}{l_B})^m e^{-\frac{|z|^2}{4l_B^2}}, \tag{3.32}$$

where $z = (x+iy)$. All the basis states being degenerate, any linear combination of them is also a solution of the Hamiltonian with energy $\hbar\omega_c/2$. Hence, in the thermodynamic limit, any function of the form

$$\psi(z) = f(z) e^{-\frac{|z|^2}{4l_B^2}}, \tag{3.33}$$

is an eigenstate in the LL level if and only if $f(z)$ is analytic. In particular, arbitrary polynomials of any degree N

$$f(z) = \prod_{i=1}^{N} (z - Z_i) \tag{3.34}$$

are allowed, defined by the locations of their N zeros.
Arbitrary many-body wavefunctions will have the form

$$\Psi(z_1, \ldots, z_N) = F(z_1, \ldots, z_N) e^{-\frac{1}{4l_B^2}\sum_i |z_i|^2}, \tag{3.35}$$

where F is analytic and antisymmetric; hence, if we fix the positions of all the particles except one, z_1 for instance, then F, as a function of z_1 only, has at least one zero at the positions $z_2, \ldots, z_N$.

Due to analiticity, the zeros of F behave like vortices and the phase accumulated by our test particle moving adiabatically around an area S is $\exp(2\pi i N_z)$, where N_z is the number of zeros of F enclosed in the loop. This quantity must be equal to $\exp(2\pi i \Phi/\Phi_0)$ (where $\Phi = BS$), the Aharonov-Bohm phase accumulated by the particle while moving around the loop. Hence, for any lowest Landau level function Ψ, the number of zeros inside an arbitrary area S must be equal to the number of flux quanta crossing S.

We can now write down the wavefunction for a fully filled Landau level: for N particles, F is given by the Slater determinant of the polynomials $1, z, \ldots, z^{N-1}$. It is not difficult to show that this determinant can be rewritten as a Vandermonde polynomial,

$$\prod_{i<j}(z_i - z_j). \tag{3.36}$$

Therefore, the ground state for $\nu = 1$ is:

$$\Psi_{\nu=1}(z_1, \ldots, z_N) = \prod_{i<j}^{N}(\frac{z_i - z_j}{l_B}) \prod_{j=1}^{N} e^{-\frac{1}{4l_B^2}|z_j|^2}. \tag{3.37}$$

3.5.2 The Laughlin state

In his seminal paper [82], Laughlin wrote down a wavefunction for N particles at filling factors $\nu = 1/(2m+1)$ (m integer) which looks similar to the $\nu = 1$ wavefunction:

$$\Psi_{\nu=\frac{1}{2m+1}}(z_1, \ldots, z_N) = \prod_{i<j}^{N}(\frac{z_i - z_j}{l_B})^{2m+1} \prod_{j=1}^{N} e^{-\frac{1}{4l_B^2}|z_j|^2}. \tag{3.38}$$

As we showed in the previous section, the number of zeros of arbitrary wavefunctions at $\nu = 1/(2m+1)$ must be $(2m+1)N$. The Laughlin state (3.38) clearly fulfils this condition because it has a $(2m+1)$-fold zero at the position of each particle. The attachment of the largest possible number of zeros to each particle helps to *reduce* the probability for two or more particles to approach each other and hence to *minimize* the expectation value of the Coulomb energy.

As we saw in the previous sections, an excitation gap is essential to the existence of the QHE (together with disorder). Indeed, it turns out that the Laughlin state is an incompressible fluid, separated from elementary excitations (both neutral and charged) by an energy gap which scales as the Coulomb interaction $e^2/(\varepsilon l_B)$ (where ε is the dielectric constant).

Numerical studies showed that the overlap between the true ground state and the Laughlin state is very good for Coulomb interactions [85]; furthermore, (3.38) is the exact ground state for hard-core interactions [86].

By mapping this problem onto a classical statistical mechanics problem, Laughlin managed to shed much light on the properties of the ground state and its charged elementary excitations. The norm of the wavefunction (3.38)

$$Z \equiv \int d^2 z_1 \cdots \int d^2 z_N |\Psi_{\nu=\frac{1}{2m+1}}(z_1, ..., z_N)|^2 \tag{3.39}$$

can be thought of as the partition function of a statistical mechanics problem with weight $|\Psi|^2 \equiv \exp[-2U/(2m+1)]$, where

$$U(z_1, \ldots, z_N) = (2m+1)^2 \sum_{i<j} (-\ln|z_i - z_j|) + \frac{2m+1}{4l_B^2} \sum_k |z_k|^2. \tag{3.40}$$

The quantity U is the potential energy of N particles of fake charge $(2m+1)$ interacting via Coulomb forces in a negative, jellium background. The first term is the Coulomb energy of interaction among the particles in a two dimensional space (under the assumption that all the field lines are confined to the 2D space) and the second term is the interaction energy between the particles and a constant, negative charge density distribution $n_B \equiv -(2\pi l_B^2)^{-1} = B/\Phi_0$.

Due to the long range Coulomb forces, this system must be everywhere locally neutral in order to minimize the potential energy. Therefore, the density n_f of fake particles of charge $(2m+1)$ must be constant:

$$n_f = -\frac{n_B}{2m+1} = \frac{1}{2m+1}\frac{1}{2\pi l_B^2}. \tag{3.41}$$

This means that the probability distribution $|\Psi|^2$ assumes large values for configurations in which the density of electrons is equal to n_f almost everywhere (again, we get the correct filling factor $\nu = 1/(2m+1)$); configurations with significant deviations from n_f on long length scales have very small probabilities.

The Laughlin state can be rewritten as:

$$\begin{aligned} \Psi_{\nu=\frac{1}{2m+1}}(z_1, \ldots, z_N) \propto \; & \prod_{i<j}^N \left(\tfrac{z_i - z_j}{l_{\Delta B}}\right) \prod_{j=1}^N e^{-\frac{1}{4l_{\Delta B}^2}|z_j|^2} \times \\ & \prod_{i<j}^N \left(\tfrac{z_i - z_j}{l_b}\right)^{2m} \prod_{j=1}^N e^{-\frac{1}{4l_b^2}|z_j|^2}, \end{aligned} \tag{3.42}$$

where $\Delta B = n_e \Phi_0$ and $b = 2mn_e\Phi_0$. The first factor is the wavefunction for a filled Landau level $\nu = 1$ and the second factor is a bosonic Laughlin state (i.e. symmetric under particle interchange) at filling fraction $\nu = 1/(2m)$. We can think of the latter factor as the binding of $2m$ zeros to each electron. Hence, the Laughlin state can be thought of as the $\nu = 1$ wavefunction for a composite object made out of one electron and $2m$ vortices. This idea is due to Jain [87]:

it was developed into a powerful theory, the theory of Composite Fermions, by Jain himself and others. We will dwell extensively on Composite Fermions in the next chapter.

3.5.3 Charged Excitations: Fractional Charges and Fractional Statistics

To create a density fluctuation in the Laughlin state, we can introduce a zero (i.e. a vortex) at position Z:

$$\Psi_Z^{(+)}(z_1,\ldots,z_N)=\prod_{i=1}^{N}(\frac{z_i-Z}{l_B})\Psi_{\nu=\frac{1}{2m+1}}(z_1,\ldots,z_N). \tag{3.43}$$

The vortex suppresses the amplitude of the wavefunction in the vicinity of Z, thus creating a quasi-hole at Z. The corresponding quasi-electron involves $\partial/\partial z_j$, the projection of the operator z_j^* onto the LL level:

$$\Psi_Z^{(-)}(z_1,\ldots,z_N)=\prod_{i=1}^{N}(\frac{2\partial_{z_i}-Z^*}{l_B})\Psi_{\nu=\frac{1}{2m+1}}(z_1,\ldots,z_N). \tag{3.44}$$

By exploiting the plasma analogy, Laughlin showed that these quasiparticles carry a fractional charge. Even more remarkably, it was shown by Halperin [88] that they obey fractional statistics too.

We will now present Laughlin's analysis and prove that the quasihole (3.43) has charge $e/(2m+1)$ (we will skip the proof that quasielectrons have opposite charge due to (3.44) being much harder to work with). The modulus squared of (3.43) can be written as:

$$|\Psi_Z^{(+)}|^2\equiv e^{-\frac{2}{2m+1}(U+V)}, \tag{3.45}$$

where U is given by (3.40) and

$$V=-(2m+1)\sum_{i=1}^{N}\ln|z_i-Z|. \tag{3.46}$$

The potential energy V represents the interaction of the fake particles with an impurity having positive, unit charge located at Z. To maintain charge neutrality, the fake particles will be repelled from Z and the net reduction of particles around Z will be equal to $1/(2m+1)$ (because our fake objects have charge $(2m+1)$). Hence, the quasihole must have fractional charge $q=e/(2m+1)$.

Since Laughlin quasiparticles are charged objects, they can be excited only in pairs, resulting in a charge excitation gap $\Delta=\Delta_++\Delta_-$, where Δ_+ (Δ_-) is the quasielectron (quasihole) excitation energy. The gap Δ was estimated

both analytically and numerically and it was experimentally determined from transport measurements. As expected, it scales as the Coulomb energy but its typical values are only a few percent of $e^2/(\varepsilon l_B)$ [89].

3.5.4 What about Disorder?

As was pointed out in section 3.1, disorder is needed to have a quantized Hall plateau of finite width. In the FQHE, the fractionally charged excitations play the role of charge carriers; therefore, the Hall resistance will not change with the filling factor if the excess Laughlin quasiparticles are localized by disorder, in analogy with the IQHE.

Typically, the excitation gap of the Laughlin state $\Delta \propto e^2/(\epsilon l_B)$ is smaller than the cyclotron energy and the FQHE will not be observable when the disorder induced broadening of the levels is larger than Δ: that's the reason why the FQHE is observed only in very clean samples.

If the density of charged excitations becomes very high, they tend to delocalize and eventually condense into a Laughlin state of their own. This gives rise to the hierarchical family of Hall states at filling $p/(2mp \pm 1)$ (see [88, 90]).

As we shall see in the next chapter, the theory of Composite Fermions can account for the principal sequence in a very easy way. Moreover, it provides an explanation for the new Hall states observed by Pan et al. [64].

Chapter 4

Composite Fermions

In this chapter the Composite Fermion (CF) model of the Fractional Quantum Hall Effect is discussed.

In the first section, we introduce the Chern-Simons transformation and the Hamiltonian of CFs. Then we present the mean-field approximation, which completely neglects Coulomb interaction and gauge field fluctuations, and we show that non trivial results are obtained in this approximation: in particular, the fractional Hall effect of electrons is mapped onto the integer effect of Composite Fermions at the mean field level. Then we calculate the electromagnetic response function of CFs in the more sophisticated random phase approximation (RPA). Finally we consider the role of disorder and we show that a random potential produces static fluctuations of the Chern-Simons magnetic field, which affect the transport properties of CFs. We explicitly calculate the correlator of the random magnetic field experienced by CFs at the RPA level, in the limit when CFs completely fill an integer number of Landau levels.

4.1 The Chern-Simons transformation: a singular Gauge transformation

In this section we will introduce Composite Fermions via the Chern-Simons (CS) transformation [70, 84, 91, 92]. This approach is not completely equivalent to Jain's approach, which was very briefly discussed in the previous chapter. However, they both provide the same answers to many relevant questions concerning the FQHE. For a discussion about the differences in the two approaches see [84].

In the following, we will assume that the magnetic field B is so large that the many-electron ground state is completely *polarized*. The starting point is the Hamiltonian of N interacting electrons in a constant field B:

$$H = \sum_i \frac{1}{2m_e} \left(\mathbf{p}_i + \frac{e}{c} \mathbf{A}(\mathbf{r}_i) \right)^2 + \sum_{i<j} V(\mathbf{r}_i - \mathbf{r}_j), \tag{4.1}$$

where m_e is the effective mass of an electron. Given an eigenstate Ψ_e of (4.1), the Chern-Simons transformation is defined as

$$\Phi(\mathbf{r}_1,\ldots,\mathbf{r}_N)=\left[\prod_{i<j}e^{-i\phi\theta(\mathbf{r}_i-\mathbf{r}_j)}\right]\Psi_e(\mathbf{r}_1,\ldots,\mathbf{r}_N), \tag{4.2}$$

where $\theta(\mathbf{r}_i-\mathbf{r}_j)$ is the angle between $\mathbf{r}_i-\mathbf{r}_j$ and the x axis and $\phi=2m$ (m is an arbitrary integer, not to be confused with the electron mass m_e). It is easy to see that, for this choice of ϕ, Φ obeys fermionic statistics.

The new wavefunction Φ is an eigenstate of

$$H_{CS}=\sum_i\frac{1}{2m_e}\left(\mathbf{p}_i+\frac{e}{c}\mathbf{A}(\mathbf{r}_i)-\frac{e}{c}\mathbf{a}(\mathbf{r}_i)\right)^2+\sum_{i<j}V(\mathbf{r}_i-\mathbf{r}_j), \tag{4.3}$$

where the Chern-Simons vector potential $\mathbf{a}(\mathbf{r})$ related to the transformation (4.2),

$$\mathbf{a}(\mathbf{r})=\frac{\phi\Phi_0}{2\pi}\sum_{j\neq i}\nabla_i\theta(\mathbf{r}-\mathbf{r}_j)=\frac{\phi\Phi_0}{2\pi}\sum_{j=1}^{N}\frac{\hat{z}\times(\mathbf{r}-\mathbf{r}_j)}{|\mathbf{r}-\mathbf{r}_j|^2}, \tag{4.4}$$

has a singularity at the position of each electron due to the non-single-valuedness of θ. Owing to that, the "fictitious" magnetic field related to $\mathbf{a}$ is not everywhere zero (in contrast to ordinary gauge transformations):

$$\mathbf{b}(\mathbf{r})=\hat{z}\phi\Phi_0\sum_i\delta(\mathbf{r}-\mathbf{r}_i)=\hat{z}\phi\Phi_0 n(\mathbf{r}). \tag{4.5}$$

According to the latter formula, the effect of the CS transformation is to attach $2m$ fictitious flux quanta to the position of each electron. These new composite objects, called Composite Fermions (CFs), are different from Jain's quasiparticles (which are formed by attaching some of the already present flux quanta to the particles, see section 3.5.2), though closely related to them. From (4.2) it is obvious that the densities of electrons and CFs coincide.

The fictitious field (4.5) doesn't have any effect on the spectrum and the statistics of the system. If we had chosen odd (non integer, respectively) values of ϕ, the resulting Hamiltonian would have described bosons (resp. anyons, i.e. particles with fractional statistics).

It is clear from (4.5) that the CS potential does not lead to classical forces among the particles. However, if one looks at the Hamiltonian (4.3), one could argue that this cannot be the case: since (4.4) depends on the particle positions, it varies in time and there ought to be electric fields depending on the positions of the particles and thus forces among them.

The reason why there are not classical forces is the nonlocality of $\mathbf{a}(\mathbf{r})$ as a function of the particle positions (see (4.4)): if one derives the equations of motion of (4.3), there will be additional terms due to non locality which do not appear in the usual equations for particles interacting with an external vector potential and which will account for the absence of classical forces.

4.2 The mean field approximation

As we said in the previous chapter, nonperturbative techniques are needed to study the electron Hamiltonian (4.1) at fractional filling factors. Although the CS Hamiltonian looks even more complicated than (4.1), approximate methods can be successfully applied to it.

The simplest approach is the mean field approximation, which consists of assuming a uniform particle density n_e (we neglect disorder in this section) and thus a uniform fictitious field $\bar{b} = 2m\Phi_0 n_e$. The total magnetic field experienced by CFs is then:

$$\Delta B = B - 2m\Phi_0 n_e = B(1 - 2m\nu). \tag{4.6}$$

Moreover, for uniform densities the Coulomb term is just an irrelevant constant. Hence, at the mean field level CFs are free fermions in a constant field ΔB. If we define a CF filling factor as

$$p = \frac{n_e \Phi_0}{\Delta B}, \tag{4.7}$$

we can straightforwardly derive an appealing relation between p and ν:

$$\nu = \frac{p}{2mp + 1}. \tag{4.8}$$

At the mean field level, the FQHE of electrons is mapped onto the IQHE of CFs! If $\nu > 1/(2m)$, the total field ΔB is negative and we get the sequence

$$\nu = \frac{p}{2mp - 1}. \tag{4.9}$$

Though intriguing, the mean field description is inaccurate: in this approximation both the Hall resistivity ρ_{xy} and the energy gap are not correctly obtained. As regards ρ_{xy}, if the FQHE at filling (4.8) were simply an integer state p of CFs, the Hall resistivity would be $\rho_{xy} = h/(pe^2)$ rather than $\rho_{xy} = (2mp + 1)h/(pe^2)$. As far as the energy gap is concerned, this approximation completely neglects Coulomb correlations which are ultimately responsible for the fractional Hall gap. However, since the mean field ground state is nondegenerate, perturbative methods can be applied to it. Indeed, the correct conductivity and energy scale for the gap have been obtained by considering the residual interactions (Coulomb and gauge field mediated interactions) of CFs beyond mean field (see next section).

If fractional filling factors of CFs are considered, new electronic fillings ν are obtained, which do not belong to the sequences 4.8 and 4.9). The recently observed plateaux at $\nu = 4/11$ and $\nu = 5/13$ [64] correspond to CF filling factors $p = 4/3$ and $p = 5/3$ respectively. It is believed that these FQHEs for CFs are due to their residual interactions, which are completely neglected in the mean-field approximation.

From equation (4.6) follows that, when $\nu = 1/(2m)$, the total effective field ΔB is zero. Thus, for those filling factors, the ground state of the system is just a Fermi sea of Composite Fermions (at the mean field level) and the radius of the Fermi sphere is $k_F = \sqrt{4\pi n_e} = 1/(l_B\sqrt{m})$.
Indeed, experimentally the even denominator states have not shown QHE so far (except for the $\nu = 5/2$ and $\nu = 7/2$ states, which are believed to be condensates of CFs in the uppermost, half filled LL); see, for example, fig. 3.1.

When ν is slighty different from $1/(2m)$, CFs experience a weak magnetic field ΔB and they should then move along cyclotron orbits of radius

$$R_c = \frac{\hbar c k_F}{e\Delta B}. \tag{4.10}$$

This new length scale was observed in a beautiful experiment carried out by Smet et al. [93].

Again, the mean field approximation is not very satisfactory: its most spectacular shortcoming is the prediction that the Hall conductivity of the system is zero (since $\Delta B = 0$). Nonetheless, it has proven to be a very good starting point for more sophisticated approaches which take into account the residual interaction among CFs at the Random Phase Approximation (RPA) level and beyond (see, among others, [94]).

4.3 The Random Phase Approximation: conductivity and electromagnetic response function

In this section we will calculate the electromagnetic response function of CFs in the random phase approximation. We will assume that an integer number p of CF LLs are filled. To calculate the response function is useful in many respects: not only it yields information about the linear response of the system to an external perturbation but its poles are also related to the energies of collective excitations and to the energy gap. The RPA response function at $\Delta B = 0$ was first calculated by Halperin, Lee and Read[94]. The case $\Delta B \neq 0$ was addressed in earlier works on anyon superconductivity [95, 96]; later on, their calculations were extended by Lopez and Fradkin [91] and Simon and Halperin [97] to include an external magnetic field and Coulomb interactions, which play a major role in CF physics. Moreover, in [97] a Fermi-liquid theory approach was used to go beyond RPA and take into account the renormalization of the CF mass.

Before embarking on these calculations, we want to show that, at the RPA level, the Hall resistivity of CFs at integer filling factors p is correctly quantized. Since, when moving, a CF carries $2m$ flux quanta, a CF current $\mathbf{j}$ induces a Chern-Simons electric field $\mathbf{e}$ given by

$$\mathbf{e} = \frac{2m}{ec}\Phi_0 \hat{\mathbf{z}} \times \mathbf{j} \equiv -\rho^{CS}\mathbf{j}, \tag{4.11}$$

where

$$\rho_{CS} = \frac{2mh}{e^2}\begin{pmatrix} 0 & 1 \\ -1 & 0 \end{pmatrix}. \tag{4.12}$$

We want to stress here that this electric field is fictitious, i.e. it is not measurable experimentally. It originates from the fact that, in formula (4.11), $\mathbf{j}$ is the *mean* value of the quantum-mechanical current. The Chern-Simons field does not produce classical forces among the particles (remember section 4.1).
CFs respond both to the external field $\mathbf{E}$ and to the self-consistent field $\mathbf{e}$:

$$\mathbf{j} = \sigma_{CF}(\mathbf{E} + \mathbf{e}) \tag{4.13}$$

where $\mathbf{e}$ is related to $\mathbf{j}$ through formula (4.11). Hence, the true resistivity tensor ρ (defined by $\mathbf{E} = \rho\mathbf{j}$) is the sum $\rho = \rho_{CF} + \rho_{CS}$. In the RPA, the CF resistivity is replaced by its mean field value ρ_{mf}. The resistivity is thus:

$$\rho = \rho_{mf} + \rho_{CS} = \frac{h}{e^2}(2m + \frac{1}{p})\begin{pmatrix} 0 & 1 \\ -1 & 0 \end{pmatrix}, \tag{4.14}$$

which is the correct value observed in the FQHE at fillings $\nu == \frac{p}{2mp+1}$.

Let's now focus on the response function. The vector potential related to the effective constant field $\Delta B = B - \phi\Phi_0 n_\mathrm{e}$ will be $\mathbf{a}_{mf} \equiv \Delta B/2\hat{z}\times\mathbf{r}$, in the Coulomb gauge. We will treat the system of free CFs subjected to ΔB as the reference system and regard the rest of the Hamiltonian as an interaction term, which we will treat perturbatively. In second quantized notation, the perturbation is

$$\begin{aligned} H_I \equiv & \int d^2\mathbf{r}\frac{1}{2m_\mathrm{e}}\Psi^\dagger(\mathbf{r})[2\frac{e}{c}(\mathbf{p} + \frac{e}{c}\mathbf{a}_{mf})(\mathbf{a} - \mathbf{a}_{mf}) + \frac{e^2}{c^2}(\mathbf{a} - \mathbf{a}_{mf})^2]\Psi(\mathbf{r}) \\ & + \int d^2\mathbf{r}'\, d^2\mathbf{r}''(n(\mathbf{r}') - n_\mathrm{e})V(\mathbf{r}' - \mathbf{r}'')(n(\mathbf{r}'') - n_\mathrm{e}). \end{aligned} \tag{4.15}$$

More explicitly, the contribution to the interaction from the fluctuations of the CS field (the first term of H_I) can be written as a sum $H_1 + H_2$. H_1 is given by

$$H_1 \equiv -\frac{\phi\Phi_0 e}{2\pi m_\mathrm{e} c}\int d^2\mathbf{r}\, d^2\mathbf{r}'\mathbf{j}(\mathbf{r})\cdot\frac{\hat{z}\times(\mathbf{r} - \mathbf{r}')}{|\mathbf{r} - \mathbf{r}'|^2}[n(\mathbf{r}) - n_\mathrm{e}], \tag{4.16}$$

where

$$\mathbf{j}(\mathbf{r}) = \frac{1}{m_\mathrm{e}}\Psi^\dagger(\mathbf{r})[\mathbf{p} + \frac{e}{c}\mathbf{a}_{mf}]\Psi(\mathbf{r}) \tag{4.17}$$

is the mean field current operator. The second term H_2 can be written as

$$H_2 \equiv \frac{(\phi\Phi_0 e)^2}{(2\pi c)^2 m_\mathrm{e}}\int d^2\mathbf{r}\, d^2\mathbf{r}'\, d^2\mathbf{r}'' n(\mathbf{r})[\frac{\hat{z}\times(\mathbf{r} - \mathbf{r}')}{|\mathbf{r} - \mathbf{r}'|^2}(n(\mathbf{r}') - n_\mathrm{e})]$$

$$\times[\frac{\hat{z}\times(\mathbf{r}-\mathbf{r}'')}{|\mathbf{r}-\mathbf{r}''|^2}(n(\mathbf{r}'')-n_{\rm e})] \tag{4.18}$$
$$\equiv C_2\int d^2\mathbf{r}\; d^2\mathbf{r}'\; d^2\mathbf{r}'' n(\mathbf{r})\frac{(\mathbf{r}-\mathbf{r}')\cdot(\mathbf{r}-\mathbf{r}'')}{|\mathbf{r}-\mathbf{r}'|^2|\mathbf{r}-\mathbf{r}''|^2}(n(\mathbf{r}')-n_{\rm e})(n(\mathbf{r}'')-n_{\rm e}),$$

where $C_2=(\phi\Phi_0 e)^2/(2\pi c)^2 m_{\rm e}$. We will now replace the first density operator in (4.18) by its average and thus neglect the third order fluctuations in the density, which would lead to three particle interactions. In this approximation, (4.18) becomes

$$H_2=-2\pi C_2 n_{\rm e}\int d^2\mathbf{r}'\; d^2\mathbf{r}''(n(\mathbf{r}')-n_{\rm e})\ln|\mathbf{r}'-\mathbf{r}''|(n(\mathbf{r}'')-n_{\rm e}), \tag{4.19}$$

which represents an effective two-dimensional Coulomb interaction.

The electromagnetic response function $K_{\mu\nu}$ determines the linear response of the interacting system to an external perturbing field $\mathbf{A}^{\rm ext}$:

$$\bar{J}_\mu(\mathbf{q},\omega)=\frac{e}{c}K_{\mu\nu}(\mathbf{q},\omega)\mathbf{A}^{\rm ext}_\nu(\mathbf{q},\omega), \tag{4.20}$$

where the greek indices represent both spatial and temporal coordinates and $\bar{J}_\mu$ is the mean value (not to be confused with the mean field current j_μ!) of the true density-current operator of CFs; its spatial components are

$$\mathbf{J}(\mathbf{r})=\frac{1}{m_{\rm e}}\Psi^\dagger(\mathbf{r})[\mathbf{p}+\frac{e}{c}\mathbf{a}(\mathbf{r})]\Psi(\mathbf{r}) \tag{4.21}$$

and its temporal part is $J_0\equiv j_0\equiv\delta n(\mathbf{r})=n(\mathbf{r})-n_{\rm e}$.

$K_{\mu\nu}$ is a 3×3 matrix by definition; however, if we choose the convention that $\mathbf{q}$ is parallel to the x-axis, the current conservation equation yields $qj_x=\omega j_0$ and j_x is determined once we know j_0. If we further choose the Coulomb gauge, $A^{\rm ext}_x q_x+A^{\rm ext}_y q_y=0$, then $A^{\rm ext}_x$ must be zero since $q_y=0$ and we can treat $K_{\mu\nu}$ as a 2×2 matrix with indices taking the values 0 (time components) and 1 (y-components).

Since the interaction W contains long-range terms, we expect that the random phase approximation provides the leading contribution to the response function of the interacting CF gas at long wavelengths.

To calculate $K_{\mu\nu}$ in the RPA we need first to evaluate the response function $K^0_{\mu\nu}$ of non interacting CFs. This quantity is given by $K^0=D^0+E$, where (from now on, we consider $\hbar=c=e=1$)

$$D^0_{\mu\nu}(\mathbf{r}_1,t_1;\mathbf{r}_2,t_2)=-i\langle\psi_0|j_\mu(\mathbf{r}_1,t_1)j_\nu(\mathbf{r}_2,t_2)|\psi_0\rangle \tag{4.22}$$

is the free particle correlator of the mean field current (ψ_0 is the noninteracting ground state) and E is the diamagnetic term

$$E=\frac{n_{\rm e}}{m_{\rm e}}\begin{pmatrix}0&0\\0&1\end{pmatrix}. \tag{4.23}$$

In the RPA, the interactions are treated by separating out the Hartree part of both the Coulomb interaction and the Chern-Simons interaction; CFs are then treated as noninteracting objects which respond to both the external field and the self-consistent induced Hartree fields. Thus, at the RPA level the response function $K_{\mu\nu}$ reads

$$K^{-1} = [K^0]^{-1} + W, \tag{4.24}$$

where the interaction matrix $W = C + V$ is the sum of the Coulomb term

$$V(\mathbf{q}) = \begin{pmatrix} v(q) & 0 \\ 0 & 0 \end{pmatrix} \tag{4.25}$$

(where $v(q) = 2\pi e^2/(\varepsilon q)$) and the Chern-Simons term

$$C(\mathbf{q}) = \begin{pmatrix} 0 & \frac{2\pi\phi i}{q} \\ -\frac{2\pi\phi i}{q} & 0 \end{pmatrix}, \tag{4.26}$$

$C_{\mu\nu}$ is related to (4.16) via

$$H_1 = \frac{1}{2}\int d^2\mathbf{r}\; d^2\mathbf{r}'\; j_\mu(\mathbf{r}) C_{\mu\nu}(\mathbf{r},\mathbf{r}') j_\nu(\mathbf{r}'). \tag{4.27}$$

The calculation of K^0 for integer p is carried out in Appendix B. It is given by:

$$K^0(\mathbf{q}) = \frac{p}{2\pi\Delta\omega_{\rm c}} \begin{pmatrix} q^2\Sigma_0 & -iq\Delta\omega_{\rm c}\Sigma_1 \\ iq\Delta\omega_{\rm c}\Sigma_1 & \Delta\omega_{\rm c}^2(\Sigma_2+1) \end{pmatrix}, \tag{4.28}$$

where $\Delta\omega_{\rm c} \equiv e\Delta B/(m_{\rm e}c) = \Delta B/m_{\rm e}$.
After some algebra, we get from (4.28), (4.25), (4.26) and (4.24):

$$K(\mathbf{q}) = \frac{p}{2\pi\Theta} \begin{pmatrix} \frac{q^2}{\Delta\omega_{\rm c}}\Sigma_0 & iq\Xi \\ -iq\Xi & \Delta\omega_{\rm c}(\Sigma_2+1) - \frac{pq^2}{2\pi}(\Sigma+\Sigma_0)V(q) \end{pmatrix}, \tag{4.29}$$

where

$$\begin{aligned} \Theta &= 1 + 2\phi p\Sigma_1 - \phi^2 p^2(\Sigma_0+\Sigma) - \frac{pq^2}{2\pi\Delta\omega_{\rm c}}\Sigma_0 V(q), \\ \Xi &= \phi p(\Sigma+\Sigma_0) - \Sigma_1, \\ \Sigma &= \Sigma_0\Sigma_2 - \Sigma_1^2. \end{aligned} \tag{4.30}$$

Within the RPA the particle mass is not renormalized by interactions and the response function (4.29) satisfies Kohn's theorem and the f-sum rule, which state respectively that the $q \to 0$ behaviour (for any fixed $\omega \neq 0$) and the $\omega \to \infty$ behaviour of an interacting system are determined by the band mass. Simon and Halperin [97] considered a "modified" RPA and showed that the mass

renormalization can be incorporated in a calculation of the response function in a way that does not violate Kohn's theorem and the f-sum rule.

It is possible to extract the FQH energy gap from K. In the large wave-vector limit, the lowest poles of K describe the excitation of a well separated quasihole-quasiparticle pair. Therefore, they occur at a frequency which equals the FQH energy gap [94, 97]. In [97] the poles of the response function in the RPA and the modified RPA were studied numerically and it was shown there that the gap scales as the Coulomb energy $e^2/\varepsilon l_B$.

Alternatively, the energy gap can be extracted from the poles of the CF single particle Green's function: this was accomplished by Stern and Halperin [98] in the large p limit.

If we average over a frequency interval which is much larger than $\Delta\omega_c$, then the diagonal matrix elements of the unperturbed response function (4.28) are well approximated by the corresponding matrix elements of the response function in zero effective magnetic field, i.e. at $\nu = 1/2$, providing that $ql_{\Delta B}$ is much *larger* than one. The necessary conditions to approximate the RPA response function (4.29) by its value at $\Delta B = 0$ are more complicated [94].

In the next section we will need the density response K_{00} in the opposite limit $ql_{\Delta B} < 1$ and $\omega = 0$. Expanding the numerator and denominator of K_{00} to second order in q and reintroducing $\hbar$,c and e for clarity, we get from (4.30) and (B.17):

$$K_{00}(q, \omega = 0) \sim \frac{pq^2}{2\pi e^2 pq/\varepsilon + 2\pi\hbar\Delta\omega_c(\phi p + 1)^2}. \tag{4.31}$$

For strong magnetic fields B, the cyclotron energy is larger than the Coulomb energy, $E_c \equiv e^2/\varepsilon l_B \ll \hbar\omega_c$. Therefore, since $\Delta\omega_c(\phi p + 1) = \omega_c$, for large B the first term in the denominator of (4.31) is smaller than the second term and can thus be neglected. Hence, (4.31) reduces to

$$K_{00}(q, \omega = 0) \sim \frac{pq^2}{2\pi\hbar\omega_c(\phi p + 1)} = \frac{\nu q^2}{2\pi\hbar\omega_c}. \tag{4.32}$$

4.4 The role of disorder: real random electric fields and fictitious random magnetic fields

We have repeatedly stated that disorder is an essential ingredient of the QHE but we have not considered the role of randomness in Chern Simons theories so far. We will now address this issue.

A random electrostatic potential induces modulations in the density of CFs. Since the fictitious magnetic field $b(\mathbf{r})$ is proportional to the density, the impurity potential will ultimately produce static fluctuations in $b(\mathbf{r})$. In the following, for notational convenience, we will denote with $b(\mathbf{r})$ the RMF related to the small

deviations of the density $\delta n(\mathbf{r}) = n(\mathbf{r}) - n_e$ from the mean value n_e:

$$b(\mathbf{r}) = \phi\Phi_0\delta n(\mathbf{r}) \qquad (\phi = 2m). \tag{4.33}$$

The random quantity $b(\mathbf{r})$ is thus a perturbation to the constant effective field $\Delta B = B - \phi\Phi_0 n_e$. In the presence of impurities or imperfections, CFs always experience a random magnetic field (RMF) given by (4.33) in addition to ΔB.

Of course, the fictitious, static RMF (4.33) and the electrostatic potential which induces the fluctuations of the density are not independent random quantities. To put it another way, although the impurities create a scalar potential only, this field gets renormalized and acquires also a vector component due to the screening by particles and mixing with the CS field.

In general, the correlation length r_c of the fictitious RMFs can be long (i.e. $r_c \gg l_B$) or short ($r_c \ll l_B$), depending on the source of the disorder electrostatic potential. Typically, in GaAs-AlGaAs heterostructures, the most important source of randomness are ionized donor impurities distributed in a thin layer separated from the electron gas by an undoped spacer. In this case each impurity produces a bare potential $V_0(\mathbf{r}) = (e/\epsilon)(r^2 + d^2)^{-1/2}$ (where d is the width of the spacer). If we assume that the impurities are randomly distributed in the layer with a sheet density n_0, the correlator of the total external potential

$$V(\mathbf{r}) = \sum_i V_0(\mathbf{r} - \mathbf{r}_i) \qquad \Leftrightarrow \qquad V(\mathbf{q}) = \sum_i \frac{2\pi e}{\epsilon q} e^{-qd} e^{-i\mathbf{q}\cdot\mathbf{r}_i}, \tag{4.34}$$

i.e. the sum of the individual impurity potentials, is

$$\langle V(\mathbf{q})V(-\mathbf{q})\rangle = n_0|V_0(\mathbf{q})|^2 = \frac{2\pi e n_0}{\epsilon^2 q^2} e^{-2qd}. \tag{4.35}$$

The induced fluctuations of the density $\delta n(\mathbf{q})$ can be calculated within the framework of linear response theory:

$$\delta n(\mathbf{q}) = eV(\mathbf{q})K_{00}(\mathbf{q}, \omega = 0), \tag{4.36}$$

where K_{00} is the density-density component of the response function, defined in the previous section. Since the inequality $d > l_{\Delta B}$ typically holds, we can take the low-q limit (4.32) of K_{00}.

In this limit, assuming again that $\mathbf{q}$ is perpendicular to the $\hat{y}$ axis and using the Coulomb gauge, the vector potential related to the RMF can be written as

$$a_x(\mathbf{q}) = 0 \qquad a_y(\mathbf{q}) = \sum_i \frac{\phi\Phi_0\nu e^2}{\varepsilon\hbar\omega_c} e^{-qd} e^{-i\mathbf{q}\cdot\mathbf{r}_i}. \tag{4.37}$$

The correlator of the RMF in the $\mathbf{q}$-space is

$$\langle b(\mathbf{q})b(-\mathbf{q})\rangle = n_0 \left(\frac{\phi\Phi_0\nu e^2}{\varepsilon\hbar\omega_c}\right)^2 q^2 e^{-2qd}. \tag{4.38}$$

Hence

$$\langle b(\mathbf{r})b(0)\rangle = \frac{9\pi n_0}{8d^4}\left(\frac{\phi\Phi_0\nu e^2}{\varepsilon\hbar\omega_c}\right)^2\left(2-\frac{3r^2}{4d^2}\right)\left[1+\frac{r^2}{4d^2}\right]^{-\frac{7}{2}}. \tag{4.39}$$

For an ideal modulation-doped sample, the number of charged impurities in the doping layer is equal to the number of electrons, $n_0 = n_e$.
Note that (4.38) and (4.39) are valid for $q < d^{-1}$ even in the case $E_c > \hbar\omega_c$, as long as $e^2/(\varepsilon d) < \hbar\omega_c$.
Since the range d of the potential (4.34) is typically larger than the average distance between the impurities, $n_0^{1/2}d > 1$, it is reasonable to assume that the random magnetic field is Gaussian.

RMFs have been the subject of intense research over the past ten years or so, mainly due to their relevance in the framework of the theory of CFs. So far, most of the work was concerned with RMFs with zero or small mean value, which effectively describe a 2DEG near filling factor $\nu = 1/2$. Since $\Delta B = 0$ in this case, the function (4.29) must be replaced by the response function of CFs experiencing no magnetic field , $K_{00}^{\Delta B=0}$. It was shown in [94] that, at the RPA level, $K_{00}^{\Delta B=0}$ is dominated by the Coulomb interaction at small q, $q \ll k_F$, (where k_F is the CF Fermi momentum): $K_{00}^{\Delta B=0} \sim \varepsilon q/(2\pi e^2)$. Therefore, at $\nu = 1/2$ the distribution of impurities described above gives rise to a RMF with vector potential

$$a_y(\mathbf{q}) = \sum_i \frac{2\pi\phi}{q} e^{-i\mathbf{q}\cdot\mathbf{r}_i} e^{-qd}. \tag{4.40}$$

The correlator of the field is thus

$$\langle b(\mathbf{q})b(-\mathbf{q})\rangle = n_0\left(2\pi\Phi_0\phi\right)^2 e^{-2qd}. \tag{4.41}$$

Fourier transforming, we obtain

$$\langle b(\mathbf{r})b(0)\rangle = n_0\left(\frac{2\pi^2\Phi_0\phi}{d}\right)^2\left[1+\frac{r^2}{4d^2}\right]^{-\frac{3}{2}}. \tag{4.42}$$

In [37, 99] a supersymmetric NLσ-model describing fermions in a RMF with short correlation length was derived: it was shown there that this model belongs to the conventional unitary symmetry class and has thus the same critical behaviour as a system of fermions subjected to a random scalar potential and a constant magnetic field. Hence, all the states are expected to be localized when the RMF has zero mean value and a localization-delocalization transition occurs when the mean value of the RMF is sufficiently large. These results show that the approximate model of weakly interacting CFs subject to a fictitious, static RMF (in addition to the external disorder potential) is at least consistent with experiments.

Evers et al. [100, 101] studied the semiclassical motion of fermions in a long-range RMF. They showed that the nature of the transport depends crucially on

both the strength of the fluctuations of the field $\langle b^2(\mathbf{r})\rangle$ and the mean value of the total field ΔB. For $\Delta B = 0$ there is a crossover from a chaotic, Drude-like diffusion to a percolating kinetics with increasing amplitude of the fluctuations. In the latter case, most classical trajectories are cyclotron orbits drifting along the closed lines of constant $b(\mathbf{r})$ and the transport is determined by a small fraction of delocalized paths, so called "snake states", which meander around the lines of zero b. In this regime the conductivity falls off as a power-law function of the strength of b.

For large ΔB, all the classical paths are circular orbits drifting along the lines of constant magnetic field and there is only one path percolating throughout the system in the thermodynamic limit: since in this case the mixing of the orbits occurs due to nonadiabatic scattering, the conductivity falls off exponentially with ΔB.

In the limit $\Delta B \to \infty$ the particles are confined to lines of costant $b(\mathbf{r})$. This percolation picture strongly resembles the semiclassical motion of particles in a constant magnetic field and a long range electrostatic potential discussed in section 3.4.2. As in this latter system, the inclusion of quantum mechanical tunneling between classical percolating trajectories enhances the localization length but does not delocalize the states. Hence, when approaching the center of Landau bands, a localization-delocalization transition should occur also in the case of long-range RMFs.

In chapter 6 we will study the localization of states in the tails of the DOS of fermions in a RMF with large mean value. We will consider both short-range and long-range RMFs.

Chapter 5

Composite Fermions with spin

In this chapter the spin polarization of the FQHE ground states at fixed filling factors is analyzed within a model of Composite Fermions with spin. We show that several cross-overs between differently polarized ground states as a function of the perpendicular magnetic field occur, in agreement with recent experimental investigations by Kukushkin et al. [102]. The magnetic field and temperature scalings of the polarization, as well as the magnetic field dependence of the spin-flip gap, are studied. The effect of disorder and spin-orbit scattering on the spin polarization transitions is also discussed.
Part of the results presented in this chapter is published in [103].

5.1 Experiments on spin polarization in the FQHE

In the previous chapters, it has been assumed that the Zeeman splitting is sufficiently large such that the spins of all electrons in a Landau band are completely polarized [82]. However, due to the small electronic effective mass m_e ($m_e = 0.067m_0$, where m_0 is the bare electron mass) and the small g-factor ($g = -0.44$), in GaAs the Zeeman term E_z is about 70 times smaller than the cyclotron energy $\hbar\omega_c$ (for GaAs, in Kelvin, $\hbar\omega_c \approx 20B[T]K$ and $E_z \approx 0.29B[T]K$, with B in Tesla) [104].

Recently, the improved quality of samples has allowed to observe FQH structures down to few Tesla, where the Coulomb energy scale can easily mix the different spin channels. Thus, spin effects have to be taken into account in order to describe the properties of these structures.
Indeed, partly spin-polarized ground states (GS) have been proposed at various filling factors ν by Halperin [104]. An example is the state at $\nu = 2/5$ that has also been studied numerically. For this, the GS has been shown to be non-polarized [105] without Zeeman splitting. Exact diagonalization confirmed the Halperin wave function to be an excellent approximation of the true GS [106].

A possible way to change the spin polarization of the 2DEG is to tune the

Zeeman energy and the cyclotron energy independently by tilting the magnetic field with respect to the direction orthogonal to the 2DEG. The cyclotron gap is only sensitive to the orthogonal component of B since it is related to the motion of the particles in the plane, whereas E_z is sensitive to the total field B. Tilted-field experiments at $\nu = 8/5$ (the particle-hole conjugate of $2/5$) yielded reentrant behaviour of the activation gap associated with the transition from an unpolarized GS for small B to a spin-polarized one at large B [107].
A similar behaviour has been found for $\nu = 2/3$, without tilting the field, via back-gate modulation of the 2D electron density [108].

Recently, direct measurements [102] of the spin polarization γ_e of the GS as a function of a purely *perpendicular* magnetic field B have been performed via radiative recombination of the 2D electrons with holes bound to a δ-doping of acceptors. In these experiments, the filling factors of the Quantum Hall systems were kept constant by a simultaneous back-gate modulation. The data, extrapolated to zero temperature, unambiguously showed the expected cross-overs for several ν's of the principal series $\nu = p/(2p \pm 1)$ (p integer) as a function of B (see figure 5.1). With increasing B (ν fixed), $\gamma_e(B)$ showed wide plateaux corresponding to given spin polarizations. At certain magnetic fields, crossovers between successive plateaux were observed.
Especially, two interesting features came out of this experiment: (i) the spin polarization cross-overs were smooth at $T = 0$ and (ii) small plateaux occured within each cross-over region.
More recently, the temperature scaling of the polarization has been measured with different experimental techniques [109, 110, 111].

In this chapter, we aim at analyzing the experiments within a picture of Composite Fermions (CF) with spin. We explicitly address point (i) considering both the influence of disorder and of spin-orbit scattering near the spin polarization transition. The temperature scaling of the polarization is considered, as well as the magnetic field dependence of the spin-flip gap. A possible explanation for feature (ii) can be found in [112].

In the following, we consider the simplest, albeit non-trivial, model with only one adjustable parameter, namely the prefactor α in the CF effective mass $m^*(B) = m_0\alpha\sqrt{B}$. We find that the model fits a large number of experimental data quantitatively. This strongly indicates that quasi-free CF with spin are a good starting point for the theory of the FQHE, though a complete microscopic justification of the model is still lacking.

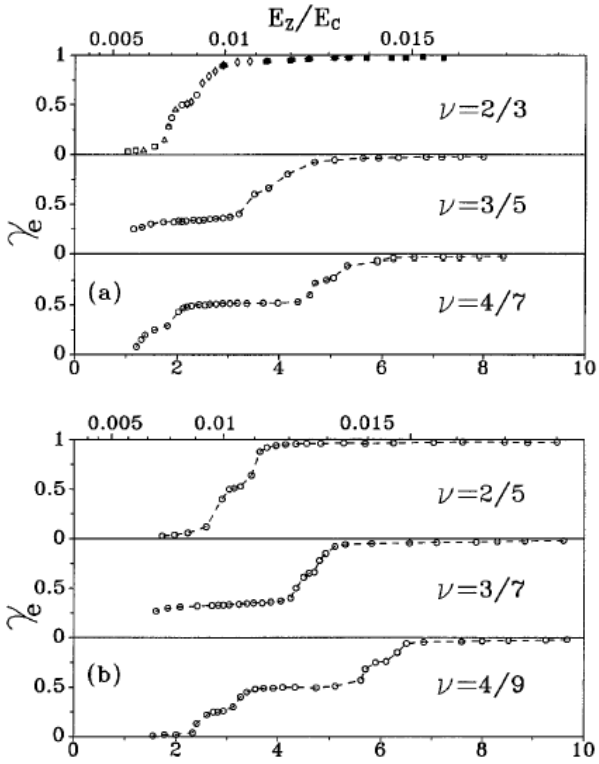

Figure 5.1: The degree of spin polarization γ_e of a GaAs-AlGaAs sample as a function of the (perpendicular) magnetic field B for some fixed filling factors ν belonging to the principal sequence. The curves show wide plateaux with constant γ_e separated by smooth crossover regions. Note the formation of additional shoulders in the crossover regions, corresponding to polarizations midway between the values of γ_e in the wide plateaux.

5.2 Polarization transitions and crossings of CFs Landau levels

In chapter 4 CFs were introduced via a singular Chern-Simons gauge transformation of the many-electron wavefunction. Since we considered the polarized limit, the transformation depended only on the positions of the electrons. For the non-fully spin-polarized states it has been noted that interacting spin-1/2 electrons in two dimensions (2D) in a perpendicular magnetic field can be described as a $U(1) \otimes U(1)$ gauge invariant liquid of spin-up and down electrons that interact with a doublet of Chern-Simons gauge fields [113, 114]. Then, the number of flux quanta associated with spin-up or down fermions can be different. However, one can show that for the principal sequence the effective magnetic field is the same for both species. This generates the states at $\nu = (p_\uparrow + p_\downarrow)/2[(p_\uparrow + p_\downarrow) \pm 1]$, where $p_{\uparrow/\downarrow}$ are the numbers of filled spin-up/down CFLL. At mean field we have equal cyclotron gaps $\hbar\Delta\omega_{c\uparrow} = \hbar\Delta\omega_{c\downarrow} \equiv \hbar\omega_c^*$. In the following, we focus on the principal sequence with $p = p_\uparrow + p_\downarrow$ (p integer).

The mean field assumption has the problem of generating the energy gaps scaling incorrectly (see section 4.2). The dimensional analysis of the spinless case by Halperin, Lee and Read [94] yields an activation cyclotron gap at fixed p,

$$\hbar\omega_c^* \propto \frac{1}{2p \pm 1} \frac{e^2}{\varepsilon l_B}, \tag{5.1}$$

since the Coulomb energy $e^2/\varepsilon l_B$ ($\approx 51\mathrm{K}\sqrt{\mathrm{B[T]}}$) is the only energy scale for electrons in the first LL, with the dielectric constant ε (≈ 12.8 for GaAs) and $l_B = (\Phi_0/2\pi B)^{1/2}$ the magnetic length. Equation (5.1) can be obtained by assuming an effective CF mass $m^* \propto \sqrt{B}$. As discussed in section 4.3, Eq. (5.1) can be derived from the study of the CF density response function or the CF single particle Green's function (see [97, 98]).
The activation gap is interpreted as the smallest energy needed to excite a CF from the GS into the first unoccupied CFLL without spin-flips. The scaling law (5.1) has been confirmed by numerical diagonalization of small 2D systems on a sphere [115].

A logarithmic divergence of m^* has been predicted in a very narrow region near $\nu = 1/2$ [98]. However, clear experimental evidence for this behaviour is still missing.

When spin is taken into account, a different energy gap can be introduced, associated with the reversal of the spin of a CF in the uppermost CFLL. In connection to this process, a new effective mass — the "polarization mass" — can be introduced [116, 117]. Both the activation and the polarization masses scale as $\sqrt{B}$ but with different prefactors, due to their different physical origin.

Estimates for the magnitudes of these gaps have been obtained without taking

into account disorder, finite thickness of the sample and LL-mixing. Thus, in experiments typically smaller energy gaps than the theoretically predicted ones are observed [89].
In order to discuss the results of the recent experiments, we consider in the following $m^*/m_0 = \alpha\sqrt{B}$. Such a dependence of m^* on B has been recently observed in experiments [118]. We use α as a fitting parameter that incorporates the mentioned corrections. We will show that the experimental results for all of the different filling factors can be described with an accuracy of about 10% by a unique choice of α.

The above considerations suggest the following form of the CF cyclotron gap

$$\hbar\omega_c^*(p,B) = \frac{\hbar e}{m_0 c}\frac{\sqrt{B}}{\alpha(2p\pm 1)}. \tag{5.2}$$

These gaps are consistent with recent numerical investigations [119], especially for $p > 2$. The Zeeman term can be easily included since it is not affected by the Chern-Simons transformation. It depends only on B. Thus,

$$E_{n_s ps}(B) = \left(n_s + \frac{1}{2}\right)\hbar\omega_c^*(p,B) + \frac{s}{2}g\mu_B B \tag{5.3}$$

are the energies of spin-up/down ($s = \pm 1$) CFLLs.

We see from (5.2) that, in contrast with the IQHE, in the fractional case *crossings* of quasiparticle LLs with opposite spin at a given filling can occur as a function of B *without* any in-plane field, i.e. in a naturally isotropic phase.

In order to find the ground state at $T = 0$ at a certain B we have to occupy the lowest p CFLLs. At $T = 0$ the chemical potential lies in the middle between two CFLLs. Since the LL degeneracy is the same for all of them, the corresponding spin polarization is $\gamma_e(B) = [p_\uparrow(B) - p_\downarrow(B)]/p$. The transitions between differently polarized GS are then given by the crossings between CFLL with different spins at the Fermi energy. For example, the critical magnetic field $B_{\rm crit}$ at which the transition to the completely spin-up polarized GS takes place is obtained as the crossing point between the $n_- = 0$ and the $n_+ = p - 1$ CFLL,

$$B_{\rm crit}(p) = \left[\frac{2(p-1)}{|g|\,\alpha(2p\pm 1)}\right]^2. \tag{5.4}$$

We recover the $\nu = 1/2$-limit for $p \to \infty$.

The allowed values of polarization for the incompressible states with CF filling p indicated in Table 5.1 do coincide with the experimentally observed ones in the large plateaux.

The comparison of (5.4) with experimental data [102] leads to a first interesting result, namely a linear relation between $|g|\alpha$ and ν which is consistent with all the experimentally investigated filling factors ν: $|g|\alpha = -0.075 + 0.787\nu$

(Fig. 5.2). From this we can determine the g-factor for a given effective mass (given by α). A similar relationship has been observed [120] for fractions belonging to the principal sequence of FQHE states around $\nu = 3/2$, but in these experiments the crossings were produced by tilting the magnetic field at a constant electron density.

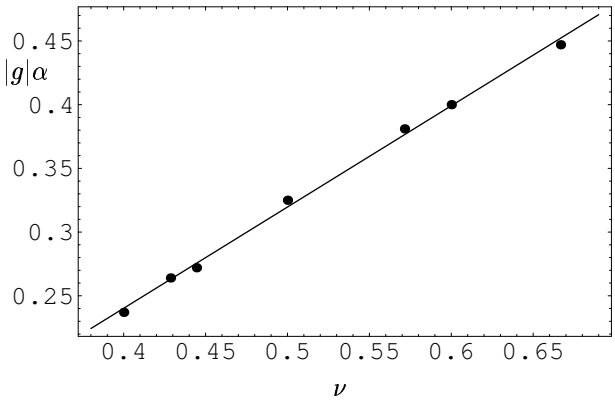

Figure 5.2: Experimental values [102] for $|g|\alpha$ extracted from (5.4). Best fit $|g|\alpha = -0.075 + 0.787\nu$.

Another interesting feature is related to the B dependence of $E_{n_s ps}(B)$ near the crossings. If we define the "slope" $S_{n_s ps}(B) = \partial_B E_{n_s ps}(B)$ it is easy to check that

$$\left| S_{n_\uparrow p\uparrow}(B_{n_\uparrow, n'_\downarrow}) - S_{n'_\downarrow p\downarrow}(B_{n_\uparrow, n'_\downarrow}) \right| = |g|\, \mu_B, \tag{5.5}$$

where $B_{n_\uparrow, n'_\downarrow}$ is the magnetic field where the two levels $E_{n_\uparrow p\uparrow}$ and $E_{n'_\downarrow p\downarrow}$ cross. Therefore the relative slopes of the two CFLL at the crossing is the same for all the possible crossings at a given filling factor. This means that any characteristic energy scale involved in processes close to the LL crossings will produce quantitatively similar effects independently on the chosen crossing point.

p	γ_e
1	1
2	0,1
3	1/3, 1
4	0, 1/2, 1

Table 5.1: Allowed values of the spin polarization γ_e for the Quantum Hall states belonging to the principal sequence $\nu = p/(2p \pm 1)$.

5.3 Smoothening of the transitions: disorder and spin-orbit effects

So far, at $T = 0$, the model predicts step-like transitions of $\gamma_e(B)$ at the magnetic fields for which the Fermi energy is at a crossing point between two spin-up/down CFLL. On the other hand, the experimental data, extrapolated to $T = 0$, show smooth cross-overs. In the following, we suggest different origins for such a behaviour.

5.3.1 The role of fictitious, inhomogeneous magnetic fields: semiclassical theory

A first contribution to the smoothening at $T = 0$ is the disorder-induced broadening of the CFLL. If the density of states (DOS) of the crossing CFLLs are broad, within a single particle picture it is easy to see that the Fermi energy lies in their overlap for the magnetic fields around the transition. The relative population of the two spin modes is then a continuous function of B even at $T = 0$, producing the observed smooth zero temperature spin polarization transition. It is therefore important to investigate the DOS of the CFLL in presence of a disorder field.

At the filling factors considered, an important source of randomness is the fluctuating magnetic field associated with the distribution of the fluxes connected to the screening charge density (see section 4.4). The fictitious RMF does depend on the Fermi energy of the 2DEG. In the experiments, the fractional filling factor of electrons is kept fixed and thus the number of exactly filled CFLLs is also fixed. Therefore, we consider the correlator introduced in section 4.4 with fixed ν,

$$\langle b(\mathbf{q})b(-\mathbf{q})\rangle = n_0 \left(\frac{2\pi\phi\nu}{\varepsilon\omega_c}\right)^2 q^2 e^{-2qd}, \tag{5.6}$$

and we use the semiclassical formula (6.20) in section 6.2. In formula (5.6) we have chosen natural units $\hbar = c = e = 1$.
We use a semiclassical method since diagrammatic evaluations of the single particle Green's function of fermions in a RMF are plagued by infrared divergencies, as discussed in chapter 6.
In our system the mean magnetic field is relatively strong (only few Landau levels are filled) and the semiclassical approximation is not fully justified but we believe that the following expression (5.8) yields a reasonable order-of-magnitude estimate of the broadening in this regime as well.

According to Eqs. (6.20) and (6.22), the semiclassical width of LLs due to

the field (5.6) is

$$\Gamma(E) = \left[n_0 \left(\frac{2\pi\phi\nu}{\varepsilon\omega_c} \right)^2 \frac{3\pi E^2}{2m^{*2}\omega_c^{*2}d^4} \, {}_2F_1\left(\frac{3}{2}, \frac{5}{2}, 3, -\frac{2E}{m^*\omega_c^{*2}d^2} \right) \right]^{1/2}, \qquad (5.7)$$

where ω_c^* is the renormalized cyclotron frequency of CFs defined in the previous section and m^* is the effective mass of the CF around the magnetic fields of interest for the spin polarization transition. The width of the n-th CFLL is then given by

$$\begin{aligned} \Gamma_n &\equiv \Gamma((n+1/2)\omega_c^*) \\ &= \left[n_0 \left(\frac{2\pi\phi\nu}{\varepsilon\omega_c} \right)^2 \frac{3\pi(n+1/2)^2}{2m^{*2}d^4} \, {}_2F_1\left(\frac{3}{2}, \frac{5}{2}, 3, -\frac{2(n+1/2)}{m^*\omega_c^* d^2} \right) \right]^{1/2}. \end{aligned} \qquad (5.8)$$

The width of LLs (5.8) shows weak magnetic field dependence. This result is in partial agreement with the experiments, since the ZTS region in [102] seems to be roughly independent on the different spin polarization transitions at a given filling fraction.

Let's now focus on the $\nu = 2/3$ state for a comparison of formula (5.7) with the experiments. Assuming that $B \approx 2T$ (around which the first polarization transition occurs) we get from (5.8), for the 0-th LL, $\Gamma_0 \approx 0.12\ K$ (with the parameters of the GaAs-AlGaAs heterostructures used in [102]). From the experimentally measured ZTS [102], we can deduce the typical energy scale involved to be of the order of $0.3\ K$.

In order to describe more closely the experiments, a deeper analysis of the DOS in the quantum limit, where $E \sim \hbar\omega_c^*$, is needed. Moreover, since the CF density response function K_{00} is affected by disorder, this quantity and the broadening of LLs due to the random fields should be determined self-consistently.

5.3.2 Spin-orbit effects

The disorder-induced broadening of the CFLLs is not the only origin of the ZTS. One can also obtain it by anticrossing of the CFLL near the critical fields. In analogy with the IQHE [121], anticrossing could be driven by spin-orbit coupling. In order to obtain the effective spin-orbit Hamiltonian for the CFLL involved in the transition, let's start with the single particle 2D Bychkov-Rashba term

$$V_{\text{Rashba}}^{\text{2D}} = \frac{\hbar e \langle E_z \rangle}{4m_0^2c^2} \, \hat{z} \cdot \vec{s} \times \vec{\Pi}. \qquad (5.9)$$

Here $\langle E_z \rangle$ is the average electric field built into the heterojunction along the growth direction z. By writing the kinetic momentum $\vec{\Pi}$ in terms of the interLL operators a, $a^\dagger$ (with $a^\dagger|n,k\rangle = \sqrt{n+1}|n+1,k\rangle$ where $|n,k\rangle$ describes the state

of the n-th LL with internal momentum k): $\Pi_x = il_{\Delta B}/\sqrt{2}\hbar(a^\dagger - a)$ and $\Pi_y = l_{\Delta B}/\sqrt{2}\hbar(a^\dagger + a)$ and the Pauli matrices s_x, s_y in terms of the rising and lowering spin operators $s_\pm = s_x \pm is_y$ we obtain the effective Hamiltonian for two close CFLL with opposite spins

$$H_{\rm SO} = E_{n_\uparrow+1,p,\uparrow}(B)\; c^\dagger_{n_\uparrow+1,\uparrow} c_{n_\uparrow+1,\uparrow} + E_{n_\downarrow,p,\downarrow}(B)\; c^\dagger_{n_\downarrow,\downarrow} c_{n_\downarrow,\downarrow} + \\ +(V_{\rm SO}\; c^\dagger_{n_\uparrow+1,\uparrow} c_{n_\downarrow,\downarrow} + \text{h.c.}) \tag{5.10}$$

with $V_{\rm SO} = \sqrt{2}\hbar^2 e\langle E_z\rangle/4m_0^2c^2l_{\Delta B}$ and $c_{n_s,s}$ the destruction operator for a particle in the state $|n_s, k\rangle$ and spin s. By diagonalizing (5.10) we get the resulting single particle split eigenmodes $\Psi_\pm$ as linear combinations of the CFLL eigenfunctions ψ_{n_s},

$$\Psi_\pm = \mathcal{N}\left[\psi_{n_\downarrow} + \left(\frac{\Delta(B)}{2V_{\rm SO}} \pm \sqrt{\left(\frac{\Delta(B)}{2V_{\rm SO}}\right)^2 + 1}\right)\psi_{n_\uparrow+1}\right] \tag{5.11}$$

where $\Delta(B) = E_{n_\uparrow+1,p,\uparrow}(B) - E_{n_\downarrow,p,\downarrow}(B)$ and $\mathcal{N}$ is a normalization factor. The new eigenenergies are

$$\epsilon_\pm(B) = \frac{E_{n_\uparrow+1,p,\uparrow}(B) + E_{n_\downarrow,p,\downarrow}(B)}{2} \pm \sqrt{\left(\frac{\Delta(B)}{2}\right)^2 + V_{\rm SO}^2}. \tag{5.12}$$

It can be seen how the eigenmodes (5.11) have expectation values of the spin that change smoothly from, say, $\downarrow$ to $\uparrow$ when B moves from the left to the right of $B_{n_\uparrow+1,n_\downarrow}$. By evaluating with these states $\gamma_{\rm e}(B)$ at $T = 0$ we obtain the cross-over behaviour shown in Fig. (5.3) for $\nu = 2/5$ (dashed line). The width of the crossover region in B is a function of $V_{\rm SO}$, which also represents the smallest energy separation (the gap) between the eigenmodes. The typical spin-orbit-induced splitting in GaAs heterostructures is of the order of 0.2-0.3 K. We obtain the right energy scale needed to produce the observed ZTS. Similar results can be obtained for the other ν's considered in [102]. In a real experiment both the disorder induced broadening of the CFLL and the spin-orbit anticrossing contribute to the ZTS.

5.4 Temperature scaling of the polarization and the spin-flip gap

Our model allows the direct analysis of the temperature scaling of the polarization for the gapped and gap-less states at fixed ν. Considering the thermal population of the CFLL (neglecting level splitting, for simplicity) we obtain

$$\gamma_{\rm e}(p, B, T) = \frac{1}{p}\sum_{n_s,s} s \cdot F(n_s, p, s, B, T) \tag{5.13}$$

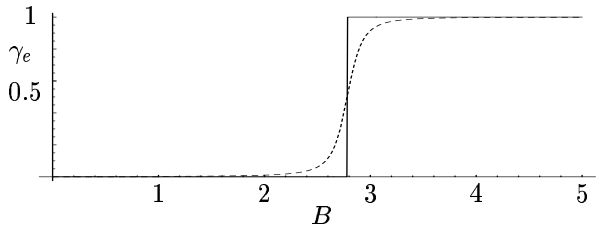

Figure 5.3: Spin polarization of the GS at $T = 0$ for $\nu = 2/5$ as a function of B (in Tesla), for $\alpha = 0.2$. Full line: with level crossing. Dashed line: with anti-crossing ($V_{\rm SO} = 0.1$ K, see text).

with $F(n_s, p, s, B, T)$ the Fermi occupation of the energy level $E_{n_s ps}$ at magnetic field B and temperature T. The Fermi distribution depends on the chemical potential $\mu_p(B, T)$, which must be determined self-consistently as a function of temperature by imposing that the sum of the spin up and spin down CF is equal to their total number. Results for $\gamma_{\rm e}(p, B, T)$ for various p's and B's are shown in Fig. 5.4.

Comparing with experiment, one observes that the data [102, 109, 110, 111] can be described within 10% by choosing α independently on the filling factor. The data obtained from the sample of Ref. [102, 109, 110] are reasonably well described by choosing $\alpha = 0.2$ (see Fig.5.4a,b) while the measurements in Ref. [111] are better fitted by $\alpha = 0.6$. An analysis of the data of Ref. [111] is presented also in Ref. [117].
In order to improve the fit, in Fig. 5.4c we have plotted the lowest five modes with $\alpha = 0.24$ and the remaining four with $\alpha = 0.16$. The slightly better agreement obtained in this way could reveal a slight dependence of α on B.

The CF model also allows the calculation of the spin-flip gap $\Delta_{\rm sf}$ as a function of B at fixed p. $\Delta_{\rm sf}$ is experimentally determined by fitting $\gamma_{\rm e}(T)$ for small temperatures as $\exp(-\Delta_{\rm sf}/2{\rm k_B T})$, for the states whose polarization vanishes at $T = 0$, or as $1 - \exp(-\Delta_{\rm sf}/2{\rm k_B T})$, for states with $\gamma_{\rm e}(T) \to 1$ for $T \to 0$. From the temperature scaling of the polarization described above, we extracted the dependence of $\Delta_{\rm sf}$ on B, depicted in Fig. 5.5 for $\nu = 2/3$ and $4/7$. Similar results are obtained for the other fractions.

In all these predicted gaps we observe reentrant behaviour for which clear minima are expected. This is consistent with several experiments [107, 108, 110] performed with both tilted magnetic fields (tuning the Zeeman splitting independently of the Coulomb energy) and with purely perpendicular fields at $\nu = 2/3$, $8/5$ and $4/3$. The recent measurements [110] show the expected reentrant behaviour but the shape of the minimum is affected by the simultaneous formation of the state responsible for the above-mentioned shoulders [112] in the polarization. We predict that the multiple minima in $\Delta_{\rm sf}$ for fractions $\nu = p/(2p \pm 1)$ with large p ($p \geq 4$) could be observed in spectroscopy experiments at very low

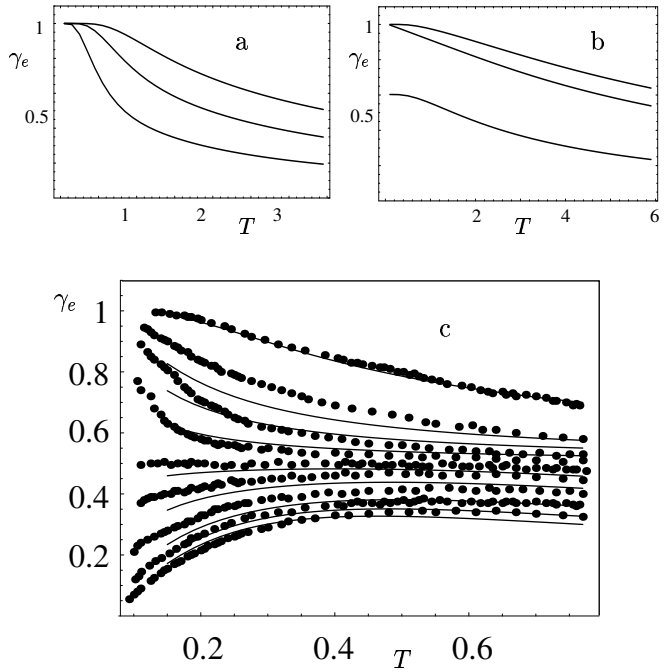

Figure 5.4: Temperature dependence (T in Kelvin) of γ_e for fixed filling factors and magnetic fields. (a) $\nu = 1/3$ $B = 2.75, 5.51, 8.9$ T (bottom to top); (b) $\nu = 1/2$ $B = 3.3, 9.3, 12$ T (bottom to top); (c) $\nu = 2/3$ $B = 1.05, 1.2, 1.4, 1.8, 2.1, 2.3, 2.4, 2.5, 3.0$ T (bottom to top). Results (a) and (b) are obtained with $\alpha = 0.2$, while in (c) $\alpha = 0.24$ for $B \leq 2.1$ T and $\alpha = 0.16$ for $B > 2.1$ T. Experimental data (bullets, data from [110]) are obtained at the same B as the theoretical curves.

T on very pure samples.

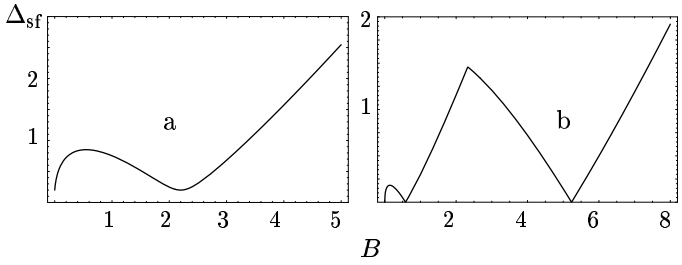

Figure 5.5: Spin-flip gap (in Kelvin) as a function of the magnetic field B (in Tesla) for fixed filling factors ($\alpha = 0.2$). (a) $\nu = 2/3$, $V_{SO} = 0.1$ K; (b) $\nu = 4/7$. In (b) level repulsion has not been included in order to emphasize the formation of the multiple minima.

Chapter 6

Density of States of Fermions in a Random Magnetic Field

In this chapter we study the density of states of particles subjected to an inhomogeneous magnetic field with large mean value and weak fluctuations. We consider both short-range and long-range fields. Due to the random field, Landau levels are broadened into narrow bands.

We start this chapter by discussing the diagrammatic approach to the problem. We show that this approach is plagued by infrared divergencies due to the long-ranged nature of the vector potential correlations. Moreover, it is not gauge-invariant. Then we briefly discuss the semiclassical method, which provides valuable information on the width of the bands corresponding to large Landau numbers.

In the second part of the chapter, we focus on the tails of the Landau bands. In these regions gauge-invariant, non-perturbative methods can be applied. We investigate the properties of the localized eigenstates in the tails and we calculate the dependence of the density of states on the energy and the mean value of the magnetic field near the centre of the bands and near the band edge (at E=0).

Part of the results presented in this chapter will be published in [122].

6.1 Failure of naive perturbative techniques

As mentioned in section 4.4, the problem of a charged quantum particle constrained to move in a static RMF has recently attracted a lot of theoretical and experimental interest. Apart from its relevance in the theory of CFs, this model is supposed to describe states with spin-charge separation in high-T_c superconductors [123]. Besides, a static RMF in 2D semiconductors can be experimentally realized in several ways. One possibility of creating a RMF is to use a type II disordered superconductor with randomly pinned Abrikosov flux lines in an external magnetic field as the substrate for the 2DEG [124]. Alternatively,

a magnetically active substrate such as a demagnetized ferromagnet with randomly oriented magnetic domains may be used [125]. Recently, static RMFs in 2DEGs were created by applying strong magnetic fields parallel to GaAs Hallbars decorated with randomly patterned magnetic films [126].

The standard way to estimate the Density of States (DOS) of fermions in a disordered potential is to calculate perturbatively the imaginary part of the self-energy of the single-particle Green's function by conventional diagrammatic techniques . In the case of a RMF, this approach is questionable since the two-point Green's function $G(\mathbf{r}, t; \mathbf{r}', t')$ is not a gauge invariant quantity. Moreover, the calculation of the self-energy is plagued by infrared divergencies [127, 128, 129, 130, 131] which are due to the long range nature of the correlator of the vector potentials (even in the case of δ-correlated RMFs). According to some authors, these divergencies are unphysical, being related to the non-gauge-invariance of the Green's function, but the question is still controversial [129, 131].

We will now calculate the broadening of Landau levels due to a Random Magnetic Field in the self-consistent Born approximation and show which diagrams diverge and why. We consider non interacting Fermions in 2D subjected to a strong, constant magnetic field B and a Gaussian, δ-correlated RMF with zero mean and correlator

$$\langle b(\mathbf{r}) b(\mathbf{r}') \rangle = \beta_0 \delta(\mathbf{r} - \mathbf{r}'). \tag{6.1}$$

The corresponding vector potential correlator is (in the momentum space):

$$\langle a_\alpha(\mathbf{q}) a_\beta(\mathbf{q}') \rangle = \frac{\beta_0}{q^2} \delta_{\alpha\beta} \delta(\mathbf{q} + \mathbf{q}'). \tag{6.2}$$

As in the case of electrostatics potentials discussed in chapter 3, the Green's function is diagonal in the Landau basis and the diagonal elements depend only on the LL index n, owing to the rotational invariance of the averaged random field:

$$G_n(z) = \frac{1}{z - E_n^0 - \Sigma_n(z)} \tag{6.3}$$

Let's assume naively that $\mathrm{Im}\Sigma \ll \hbar\omega_c$ and neglect Landau level mixing (as we did in section 2.3, when dealing with scalar potentials): the self-energy of the n-th Landau level in the SCBA is:

$$\Sigma_n(E) = \frac{r_n}{E - E_n - \Sigma_n(E)} \tag{6.4}$$

where (in the Landau gauge)

$$r_n = \int dp \frac{d\mathbf{q}}{(2\pi)^2} \frac{e^2}{m_e^2 c^2} \frac{\beta_0}{q^2} \sum_\mu |\langle n, k | \{\Pi_\mu e^{i\mathbf{q}\cdot\mathbf{r}}\} | n, p \rangle|^2 \tag{6.5}$$

where $\Pi_\mu = p_\mu + (e/c)A_\mu$ and $|n, p\rangle$ indicates the intermediate state of LL index n and internal momentum p. Again, the DOS consists of semiellipses having a

width $\Gamma_n \approx 2\sqrt{r_n}$ (see section 2.3). Remembering that $\Pi_x = i\hbar/\sqrt{2}l_B(a^\dagger - a)$ and $\Pi_y = \hbar/\sqrt{2}l_B(a^\dagger + a)$ (where $a^\dagger$ and a are inter-Landau level creation and annihilation operators and l_B is the magnetic length related to B), it can be immediately shown that the matrix element $\langle n, k|\{\Pi_\mu e^{i\mathbf{q}\cdot\mathbf{r}}\}|n, p\rangle$ vanishes for $q = 0$ and there are no infrared divergencies.

The calculation of the matrix element and the integration over p can be carried out straightforwardly to give

$$\begin{aligned} r_n &= \int \frac{d\mathbf{q}}{(2\pi)^2}\hbar^2 v_0^2 e^{-\frac{1}{2}l_B^2 q^2}(L_n^1(\frac{1}{2}l_B^2 q^2) + L_{n-1}^1(\frac{1}{2}l_B^2 q^2))^2 \\ &= \frac{\hbar^2 v_0^2}{2\pi}\int \frac{d\xi}{l_B^2} e^{-\xi}(L_n^1(\xi) + L_{n-1}^1(\xi))^2, \end{aligned} \tag{6.6}$$

where the characteristic velocity of the problem $v_0 = e\sqrt{\beta_0}/2mc$ has been introduced and $L_n^1(x)$ is the n-th Laguerre polinomial. Exploiting the relations

$$\sum_{t=0}^{n} L_s^0(\xi) = L_n^1(\xi) \tag{6.7}$$

and

$$\int_0^\infty d\xi e^{-\xi} L_s^0(\xi) L_t^0(\xi) = \delta_{s,t}, \tag{6.8}$$

we finally obtain

$$r_n = \frac{1}{\pi} m_e v_0^2 \hbar\omega_c (2n + \frac{1}{2}). \tag{6.9}$$

The broadening of Landau levels is finite and dependent on n (remember that in section 2.3 we proved that, for δ-correlated scalar potential, the width of LLs does not depend on n). Moreover, the LL widths have the same dependence on B, β_0 and n as formula (6.16) in section 6.2 (after making the substitution $E \sim (n + 1/2)\hbar\omega_c$ in (6.16)).

Unfortunately, that's not the whole story: if we take Landau level mixing into account, singular terms appear due to matrix elements between neighbouring LLs, $\langle n, k|\{\Pi_\mu e^{i\mathbf{q}\cdot\mathbf{r}}\}|n \pm 1, p\rangle$, which do not vanish in the $q \to 0$ limit [132]. As in the $B = 0$ case [127, 128, 129], those terms diverge logarithmically for $q \to 0$.

LL mixing must be always taken into account when the perturbing term is a magnetic field $b(\mathbf{r})$, no matter how weak it is. Let's suppose that the perturbing field is a very small, constant field δB: clearly, the Hilbert space spanning the n-th LL with energy $\hbar e(B + \delta B)/(m_e c)$ and degeneracy $(B + \delta B)S/\Phi_0$ cannot be obtained from perturbation theory by taking into account only the eigenstates in the unperturbed n-th LL, since the degeneracy of the old LL is smaller, BS/Φ_0.

In conclusion, divergent terms plague the calculation of the one particle Green's function of fermions subject to a δ-correlated RMF with large mean B. Of course,

the infrared singularities would be even stronger and more difficult to cure for long-range RMFs. The divergencies are ultimately due to the anomalously strong low-angle (forward) scattering, which can be traced to the contribution of the fluctuations of $\mathbf{a}(\mathbf{q})$ in the limit $q \to 0$. Note, however, that the transport relaxation time $\tau_{\rm tr}$ entering the Drude formula is finite [99], since the contribution of forward scattering is reduced by the weighting term.

6.2 Semiclassical results

In order to circumvent the difficulties described in the previous section, E. Altshuler et al. [129, 133] calculated the DOS of electrons in a RMF in the semiclassical approximation, assuming that the energy E of the particle is much larger than the cyclotron energy and Γ, where Γ is the width of LLs due to the RMF. If these conditions are fulfilled, the DOS $\rho(E)$ (proportional to the imaginary part of G) is given by the disorder averaged path integral over the closed classical trajectories $x_E(t)$

$$\rho(E) = \frac{m_{\rm e}}{2\pi}\left[1 + {\rm Re}\left\langle \oint \mathcal{D}x_E(t)\ \exp\left(\frac{i}{\hbar}\mathcal{S}[x_E(t)]\right)\right\rangle\right]. \tag{6.10}$$

The action on one particular path is

$$\mathcal{S} = \frac{e}{c}\int_s d\mathbf{r}\,(B + b(\mathbf{r})) \tag{6.11}$$

where s is the area enclosed by the trajectory. Assuming that the RMF is a small perturbation to the mean field B ($\hbar\omega_{\rm c} \gg m_{\rm e}v_0^2$, where $v_0^2 = e^2\beta_0/4m_{\rm e}^2c^2$), the classical trajectories are not affected by the RMF and are thus circles with cyclotron radius $R_{\rm c} = v/\omega_{\rm c} = \sqrt{2E/m_{\rm e}\omega_{\rm c}^2}$ (v and E are respectively the velocity and the energy of the particle); more precisely, every circle gives rise to infinitely many trajectories labelled by their winding number. For the disorder average over a Gaussian RMF the following equality holds:

$$\left\langle \exp\left(i\frac{e}{c}\int_s d\mathbf{r}\ b(\mathbf{r})\right)\right\rangle = \exp\Big(-\frac{e^2}{2c^2}\int_s d\mathbf{r}\int_s d\mathbf{r}'\ \langle b(\mathbf{r})b(\mathbf{r}')\rangle\Big). \tag{6.12}$$

Hence, after averaging, the total, effective action on a classical trajectory is the sum of two terms:

$$i\mathcal{S}_{\rm av} = i\frac{e}{c}s_{\rm or}B - \frac{e^2}{2c^2}\beta_0 s_{\rm nor}, \tag{6.13}$$

where $s_{\rm or}$ and $s_{\rm nor}$, the oriented and non-oriented areas enclosed by the trajectory respectively, are given by

$$s_{\rm or} = \frac{1}{2}\oint d\mathbf{r}\times\mathbf{r},$$

$$s_{\rm nor} = \frac{1}{4\pi} \oint \oint d\mathbf{r} d\mathbf{r}' \ln(|\mathbf{r} - \mathbf{r}'|) \tag{6.14}$$

(we recall that the non-oriented area enclosed by η-windings of a trajectory is the geometrical area multiplied by η^2). The first term of (6.13) describes the phase acquired by the particle due to the flux of B and the second term appears due to averaging over the random field $b(\mathbf{r})$.

Carrying out the sum over the circles with different winding number [129], a Gaussian DOS is obtained

$$\rho(E) = \frac{1}{2\pi l^2} \sum_{N=0}^{\infty} \sqrt{\frac{1}{\pi}} \frac{\tau(E)}{\hbar} \exp\left(- \left[E - \hbar\omega_{\rm c}(N + \frac{1}{2}) \right]^2 \frac{\tau^2(E)}{\hbar^2} \right) \tag{6.15}$$

and the width of the levels is

$$\Gamma(E) = \left[\frac{1}{\pi} E m_{\rm e} v_0^2 \right]^{1/2}. \tag{6.16}$$

We consider now the broadening of LLs due to the RMFs with the following correlators:

$$\langle b(\mathbf{q}) b(-\mathbf{q}) \rangle = \mathcal{B}_1^2 q^2 e^{-2qd} \tag{6.17}$$

and

$$\langle b(\mathbf{q}) b(-\mathbf{q}) \rangle = \mathcal{B}_2^2 e^{-2qd}, \tag{6.18}$$

which correspond to the correlators (4.38) and (4.41) introduced in chapter 4, when we considered the fictitious Chern-Simons fields experienced by CFs. However, in this section we will assume that $\mathcal{B}_1^2$ and $\mathcal{B}_2^2$ are arbitrary constants.

For weak RMFs such that $\omega_c \tau_{\rm tr} \gg 1$ ($\tau_{\rm tr}$ is the *transport* time related to the RMF), the DOS is again given by (6.10) and the averaged, effective action $\mathcal{S}_{\rm av}$ on a classical orbit can be generally written as

$$i\mathcal{S}_{\rm av} = i s_{\rm or} B - \frac{1}{2} k^2 \langle \mathcal{S}_{\rm RF}^2 \rangle, \tag{6.19}$$

where $\mathcal{S}_{\rm RF} = \oint \mathbf{a} \cdot d\mathbf{r} = \int b(\mathbf{r}) d^2\mathbf{r}$ is the contribution to the action induced by the random fields along a cyclotron orbit of winding number $k = 1$ (we assume $\hbar = e = c = 1$ to simplify the formulas). From (6.17), we get

$$\begin{aligned} \langle \mathcal{S}_{\rm RF}^2 \rangle &= \mathcal{B}_1^2 \int d^2\mathbf{q}\ q^2 e^{-2qd} \left| \int d\mathbf{r} e^{-i\mathbf{q}\mathbf{r}} \right|^2 \\ &= \mathcal{B}_1^2 (2\pi R_{\rm c})^2 \int d^2\mathbf{q} e^{-2qd} \left[J_1(qR_{\rm c}) \right]^2 \\ &= \mathcal{B}_1^2 \frac{3\pi^3}{4} \frac{Rc^4}{d^4}\ {}_2F_1\left(\frac{3}{2}, \frac{5}{2}, 3, -\frac{R_{\rm c}^2}{d^2} \right), \end{aligned} \tag{6.20}$$

where ${}_2F_1$ is the hypergeometric function. For very large energies, $R_c \gg d$ and Eq. (6.20) yields

$$\langle \mathcal{S}_{RF}^2 \rangle \sim \mathcal{B}_1^2 4\pi^2 \frac{R_c}{d}, \tag{6.21}$$

since ${}_2F_1(3/2, 5/2, 3, -x) \to 16x^{-3/2}/(3\pi)$ for $x \to \infty$. The sum over the classical trajectories can be easily carried out and the semiclassical DOS is a superposition of Gaussian functions peaked at the Landau energies, like (6.15). The width of the peaks is given by

$$\Gamma(E) = \left(\frac{\omega_c^2}{2\pi^2} \langle \mathcal{S}_{RF}^2 \rangle \right)^{1/2}. \tag{6.22}$$

In the limit $R_c \gg d$, $\Gamma(E)$ is thus proportional to $E^{1/4}$ and proportional to $\sqrt{B}$:

$$\Gamma(E) = \left(\sqrt{\frac{2E}{m_e}} \frac{2\mathcal{B}_1^2 \omega_c}{d} \right)^{1/2} \tag{6.23}$$

In the case (6.18), we obtain

$$\begin{aligned} \langle \mathcal{S}_{RF}^2 \rangle &= \mathcal{B}_2^2 \int d^2\mathbf{q} e^{-2qd} \left| \int d\mathbf{r} e^{-i\mathbf{q}\mathbf{r}} \right|^2 \\ &= \mathcal{B}_2^2 (2\pi R_c)^2 \int d^2\mathbf{q}\; q^{-2} e^{-2qd} \left[J_1(qR_c) \right]^2 \\ &= \mathcal{B}_2^2 4\pi^3 R_c^2 \left[1 - {}_2F_1\left(\frac{1}{2}, \frac{1}{2}, 2, -\frac{R_c^2}{d^2} \right) \right], \end{aligned} \tag{6.24}$$

For large energies, $R_c \gg d$, we get

$$\langle \mathcal{S}_{RF}^2 \rangle \sim \mathcal{B}_2^2 4\pi^3 R_c^2. \tag{6.25}$$

Therefore, in this limit $\Gamma(E)$ is proportional to $\sqrt{E}$ and independent on B:

$$\Gamma(E) = \left(2\pi\omega_c^2 \mathcal{B}_2^2 R_c^2 \right)^{1/2} = \left(\frac{4\pi \mathcal{B}_2^2 E}{m_e} \right)^{1/2}. \tag{6.26}$$

6.3 Landau Level tails

From now on, we will focus on the DOS in the tails of the broadened Landau Levels (LLs). As we discussed in section 3.3, in these regions the Optimum Fluctuation Method (OFM) can be applied. This method has the advantage of being non-perturbative.

The averaged DOS is:

$$\rho(E) = \int Db(\mathbf{r}) P[b(\mathbf{r})] \rho[E; b(\mathbf{r})], \tag{6.27}$$

where $P[b(\mathbf{r})]$ is the probability of the realization $b(\mathbf{r})$. Here we will consider fermions subject to a constant B and a Gaussian RMF with zero mean value and correlation function:

$$\langle b(\mathbf{r})b(\mathbf{r}')\rangle = \beta(\mathbf{r}-\mathbf{r}'). \tag{6.28}$$

We assume that $\beta(\mathbf{r}-\mathbf{r}') \to 0$ as $|\mathbf{r}-\mathbf{r}'| \to \infty$. The system is thus ergodic, i.e. the correlations between different regions decay to zero with increasing distance between the regions. We will also assume that $\beta(\mathbf{r}-\mathbf{r}')$ is solely a function of $|\mathbf{r}-\mathbf{r}'|$.

In the following we will study both RMFs with correlation length $r_c < l_B$ (we will call them short-range fields) and fields with $r_c > l_B$ (long-range RMFs). The probability of the realization $b(\mathbf{r})$ of the RMF with correlator (6.28) is

$$P[b(\mathbf{r})] = \mathcal{N}\exp\left\{-\int b(\mathbf{r})\beta^{-1}(\mathbf{r}-\mathbf{r}')b(\mathbf{r}')d\mathbf{r}d\mathbf{r}'\right\} \equiv \mathcal{N}\exp\{-S[b(\mathbf{r})]\}, \tag{6.29}$$

where $\mathcal{N}$ is a normalization constant and

$$\int d\mathbf{r}'\beta^{-1}(\mathbf{r}-\mathbf{r}')\beta(\mathbf{r}'-\mathbf{r}'') = \delta(\mathbf{r}-\mathbf{r}''). \tag{6.30}$$

For δ-correlated RMFs with correlation function (6.1), formula (6.29) reduces to

$$P[b(\mathbf{r})] \sim \exp\left\{-\frac{1}{\beta_0}\int b^2(\mathbf{r})d\mathbf{r}\right\}. \tag{6.31}$$

We can obtain asymptotically exact expressions for the DOS in the fluctuation region of the spectrum (i.e. in the tails of Landau bands) since we are able to figure out the nature of the typical quantum states which determine the spectrum in those regions. Intuitively, since the DOS in the tails is exponentially small, we expect that states are localized around low probability fluctuations of $b(\mathbf{r})$ [74, 134, 135, 136, 137, 138].

The OFM allows one to determine the structure and the shape of the localized states in the tails and to determine the shape of the corresponding configurations of the magnetic field, as well as to find the leading terms in the asymptotic expansion of the exponent of the DOS in the tails,

$$\rho(E) \sim e^{-F(E)}. \tag{6.32}$$

It is well known that, for an ergodic random field, the DOS is a self-averaging quantity, i.e. the ensemble average of the DOS (6.27) coincides with its spatial average for a given typical realization of the RMF.

Let's focus for simplicity on the left tail of the first Landau Level and consider a typical realization of $b(\mathbf{r})$: since in this tail the energies are significantly smaller than $\hbar\omega_c/2$, in the system there must be a finite density of fluctuations in which

the field $b(\mathbf{r})$ assumes large (compared to its typical values $\beta(0)^{1/2}$), negative values. In these magnetic wells, the total field $B + b(\mathbf{r})$ is significantly smaller than B (compared to the typical fluctuations of $B + b(\mathbf{r})$). However, due to the macroscopic homogeneity of the RMF, these wells must lie very far from each other; more precisely, the average distance between two neighbouring fluctuations must be much larger than the typical size of a well.

Hence, we can divide our system into many subsystems containing exactly one large fluctuation of $b(\mathbf{r})$ and consider the contribution to the DOS of each subsystem, independently of the others. Since we are interested in the leading term of the logarithm of the DOS only, we can disregard the boundary effects due to the partitioning of the system into such subsystems. The DOS in the tail thus reads

$$\rho(E) \sim \sum_{\alpha} \frac{V_\alpha}{V} \rho_\alpha(E), \tag{6.33}$$

where V_α and $\rho_\alpha(E)$ are, respectively, the volume and the DOS of the subsystem α and V is the total volume of the system.

Since the wells which determine the spectrum in the tail have very small probabilities, only those wells in which the lowest level $E_{0,\alpha}$ is equal to E must be taken into account, since a configuration in which the energy E corresponds to an excited level is much less probable. Therefore, we have

$$\rho_\alpha(E) \sim \frac{1}{V_\alpha} \delta(E - E_{0,\alpha}). \tag{6.34}$$

Furthermore, since the DOS is a self-averaging quantity, we can rewrite (6.33), where $\rho_\alpha(E)$ is given by (6.34), as an ensemble average,

$$\rho(E) \sim \frac{1}{\bar{V}} \int Db(\mathbf{r}) \exp\{-S[b(\mathbf{r})]\} \delta(E - E_0[b(\mathbf{r})]), \tag{6.35}$$

where $\bar{V}$ is the characteristic volume of an optimal fluctuation of the RMF and $E_0[b(\mathbf{r})]$ is the lowest level in the realization $b(\mathbf{r})$ of the field. As we said, the probabilities of the fluctuations which contribute to the DOS in the tail are exponentially small, i.e. they correspond to very large values of the functional $S[b(\mathbf{r})]$; therefore, the integral (6.35) is dominated by the most probable configurations and it can thus be calculated in the saddle point approximation [138]:

$$-\ln \rho(E) = \min_{b(\mathbf{r})} S[b(\mathbf{r})]|_{E_0[b(\mathbf{r})]=E}. \tag{6.36}$$

This formula will be the starting point for many of the subsequent arguments and calculations.

For very weak RMFs, $\beta(0)^{1/2} \ll B$, the width Γ_0 of the first Landau band is much smaller than $\hbar\omega_c$. In this case, the fluctuation region of the spectrum is not exhausted by the neighbourhood of the boundary of the spectrum at $E = 0$

and the saddle point approximation (6.36) can be used to evaluate the left tail of the Landau band even at energies E close to the centre of the band [74], as long as $(1/2\hbar\omega_c - E) \gg \Gamma_0$ and the DOS is *exponentially small* there (the definition of this region will be made more precise in the following section). Therefore, in section 6.3.2 we will derive a variational equation from (6.36) which will enable us to calculate the exponent of the DOS in the left tail both near the boundary and near the centre of the LL. That method can also be generalized to deal with higher LLs.

As far as the right tail of the first LL and the tails of higher LLs are concerned, the picture is in general very complicated. However, it becomes simpler when $\beta(0)^{1/2} \ll B$ and energies near the band centres are considered.

In the case of very weak RMFs, for a given Landau level n, the density of states is peaked at the Landau energy $(n + 1/2)\hbar\omega_c$ and is exponentially small elsewhere. Again, the width of the level Γ_n is much smaller than the cyclotron energy. Therefore, there are regions near the band centres where the inequalities $\Gamma_n \ll \Delta E_n = |E-(n+1/2)\hbar\omega_c| \ll \hbar\omega_c$ are fulfilled and the Optimum Fluctuation Method can be safely applied, since the DOS is exponentially small there.

The fluctuations of $b(\mathbf{r})$ which determine the spectrum near the centre of the bands are small compared to B but very *large* compared to its typical values $\beta(0)^{1/2}$: they are expected to look like shallow wells in the left tails and low humps in the right ones.

Let's concentrate on the right tail of a Landau level n. The spectrum of a particle which experiences an optimal fluctuation of $b(\mathbf{r})$ in addition to B differs only slightly from the unperturbed Landau spectrum: the magnetic perturbation breaks the degeneracy of LLs and the DOS consists of bands of discrete energy levels lying in small right neighbourhoods of the corresponding LL. The total width of the band n of this system is given by $\delta E_n \equiv E_{n,max} - (n + 1/2)\hbar\omega_c$, where $E_{n,max}$ is the highest energy level in the band.

If we now calculate the DOS of the disordered system at energy shift ΔE_n in the right tail of the n-th LL, it is clear that only those fluctuations in which $\delta E_n = \Delta E_n$ must be considered, since a fluctuation in which $\delta E_n > \Delta E_n$ is definitely stronger and thus less probable. The calculation of the DOS in the left tails is completely analogous but δE_n is now given by $\delta E_n \equiv (n+1/2)\hbar\omega_c - E_{n,min}$.

Hence, in the tails close to the center of the n-th Landau band, the leading term in the expansion of the exponent of the DOS is

$$-\ln \rho(E) = \min_{b(\mathbf{r})} S[b(\mathbf{r})]|_{\delta E_n[b(\mathbf{r})]=\Delta E_n}. \tag{6.37}$$

This picture is not valid in the regions between Landau bands near the energies $E \sim n\hbar\omega_c$, since more complicated configurations of $b(\mathbf{r})$ are expected to determine the DOS at these energies.

For very large n, the DOS in a weak RMF can be obtained by the semiclassical method introduced in the previous section.

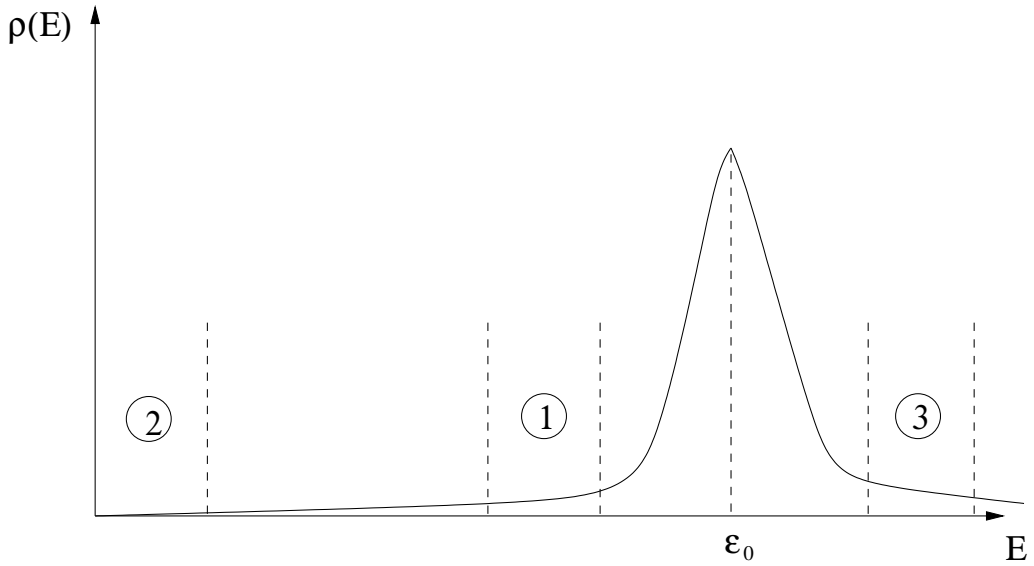

Figure 6.1: Density of states $\rho(E)$ for the lowest Landau band of an electron subject to a constant magnetic field B and a weak RMF, $\beta(0)^{1/2} \ll B$. The band is peaked at the energy $\epsilon_0 = 1/2\hbar\omega_c$. In region 1 and region 3 the DOS is exponentially small and the inequality $\Delta E_0 \ll \hbar\omega_c$ holds (where $\Delta E_0 = |E - \epsilon_0|$). The exponent of the DOS is proportional to ΔE^2 in those regions. In region 2 the exponent of $\rho(E)$ is inversely proportional to E.

6.3.1 Qualitative picture: Lifshitz argument

In the following, we will focus mainly on the left tail of the first Landau band. The generalization of our arguments to higher bands is not difficult and we will thus discuss it only very briefly.

In the case of weakly correlated RMFs, it is reasonable to assume that an optimal configuration near the band centre (which corresponds to region 1 in Fig. 6.1) looks like a magnetic circular well with very steep walls and depth $\Delta b \ll B$ (we will prove in the next subsection that this assumption is not too bad). If R is the radius of the well, then its action is given by $S \approx \Delta b^2 R^2/\beta_0$.

The Ground State energy E_0 of a fermion subjected to a constant magnetic field B plus an additional circular magnetic well can be easily evaluated. In the following we will evaluate E_0 as a function of the radius R for fixed S. The Hamiltonian is:

$$H = \frac{1}{2m_e}(\mathbf{p} + \frac{e}{c}\mathbf{A} + \frac{e}{c}\mathbf{a})^2, \tag{6.38}$$

where, in the Coulomb gauge, $\mathbf{A} = 1/2B\hat{z} \times \mathbf{r}$,

$$\mathbf{a} = \begin{cases} -1/2\Delta b\hat{z} \times \mathbf{r} & r < R \\ -\frac{\Delta\Phi}{2\pi}\frac{\hat{z}\times\mathbf{r}}{r^2} & r > R \end{cases} \tag{6.39}$$

and $\Delta\Phi = \Delta b \pi R^2$.

The angular momentum is a good quantum number:

$$\Psi(\mathbf{r}) = \frac{1}{\sqrt{2\pi}} e^{i\mu\phi} R(r) \tag{6.40}$$

and the radial wave function $R(r)$ satisfies the equation:

$$-\frac{\hbar^2}{2m_\mathrm{e}}\left(\frac{\partial^2 R}{\partial r^2} + \frac{1}{r}\frac{\partial R}{\partial r} - \frac{\tilde{\mu}^2}{r^2}R\right) + \left(\frac{\hbar\omega_\mathrm{c}}{2}\tilde{\mu} + \frac{m_\mathrm{e}\omega_\mathrm{c}^2 r^2}{8} - E\right)R = 0 \tag{6.41}$$

where

$$\omega_\mathrm{c} = \begin{cases} eB/m_\mathrm{e}c & r < R \\ e(B-\Delta b)/m_\mathrm{e}c & r > R \end{cases} \tag{6.42}$$

and

$$\tilde{\mu} = \begin{cases} \mu & r < R \\ \mu - \Delta\Phi/\Phi_0 & r > R \end{cases} \tag{6.43}$$

Now we can solve equation (6.41) inside the well and outside the well and match the solutions at $r = R$. The general solution of Eq. (6.41) for constant ω_c and $\tilde{\mu}$ is:

$$R(\xi) = e^{-\frac{\xi}{2}}\xi^{-\frac{1}{2}+\frac{1}{2}(1+|\tilde{\mu}|)}[C_1 U(-\zeta + \frac{1}{2}(1+|\tilde{\mu}|), 1+|\tilde{\mu}|, \xi) + \tag{6.44}$$

$$+C_2\Phi(-\zeta + \frac{1}{2}(1+|\tilde{\mu}|), 1+|\tilde{\mu}|, \xi)] \tag{6.45}$$

where Φ and U are confluent hypergeometric functions, $\xi = m_\mathrm{e}\omega_\mathrm{c} r^2/2\hbar$ and $\zeta = E/\hbar\omega_\mathrm{c} - \tilde{\mu}/2$.

The coefficient C_1 must be set equal to 0 inside the well because U diverges at $r = 0$; as regards the region $r > R$, we set $C_2 = 0$ because Φ diverges exponentially for large R (unless $-\zeta + \frac{1}{2}(1+|\tilde{\mu}|)$ is a negative, integer number; however, this condition does not yield a continuous eigenfunction on $(0,\infty)$ if $\Delta b \neq 0$).

To calculate the eigenvalues, we must impose the requirements that the wave-function and its derivative be continuous at $r = R$. For a magnetic circular well the angular momentum μ of the ground state is $\mu = 0$ and the lowest level is thus a solution of the following, implicit equation for E:

$$\frac{l_{Bo}^2}{l_{Bi}^2}\left[-\frac{1}{2} + (-\zeta_\mathrm{i} + 1/2)\frac{\Phi(-\zeta_\mathrm{i}+\frac{3}{2}, 2, R^2/2l_{Bi}^2)}{\Phi(-\zeta_\mathrm{i}+\frac{1}{2}, 1, R^2/2l_{Bi}^2)}\right] + \frac{1}{2} - \frac{|\tilde{\mu}_\mathrm{o}|l_{Bo}^2}{R^2} +$$
$$+\frac{-\zeta_\mathrm{o} + 1/2(1+|\tilde{\mu}_\mathrm{o}|)}{1+|\tilde{\mu}_\mathrm{o}|}\frac{U(-\zeta_\mathrm{o}+\frac{1}{2}(3+|\tilde{\mu}_\mathrm{o}|), 2+|\tilde{\mu}_\mathrm{o}|, R^2/2l_{Bo}^2)}{U(-\zeta_\mathrm{o}+\frac{1}{2}(1+|\tilde{\mu}_\mathrm{o}|), 1+|\tilde{\mu}_\mathrm{o}|, R^2/2l_{Bo}^2)} = 0 \tag{6.46}$$

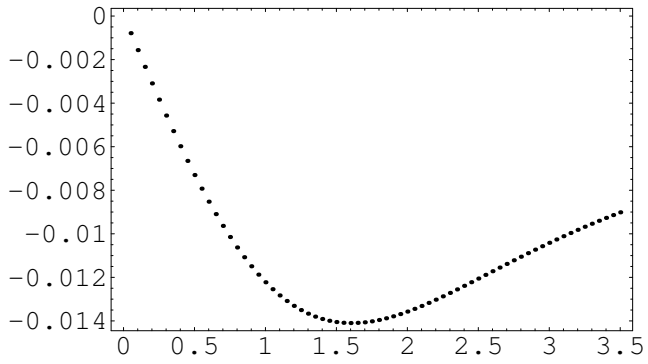

Figure 6.2: Diagram of $\Delta E_0 = E_0 - 1/2\hbar\omega_c$ as a function of the radius R of the magnetic well for fixed action S (ΔE_0 and R in units of $\hbar\omega_c$ and l_B respectively).

where the indexes "i" and "o" indicate the regions inside and outside the well respectively and $|\tilde{\mu}_o| = \Delta\Phi/\Phi_0$.

This equation has been solved numerically: the energy shift ΔE_0 as a function of the radius of the well for fixed S is shown in fig. 6.2. The minimum in the ground state energy (i.e., the minimum of ΔE_0) corresponds to the optimal fluctuation with radius $R_{\rm opt}$ and depth $\Delta b_{\rm opt}$.

Then we have solved Eq. (6.46) for different values of B and S. We have found that, for shallow wells $\Delta b \ll B$, $R_{\rm opt}$ is proportional to l_B (see fig. 6.3) and $\Delta E_0(l_{\rm opt})$ is proportional to $\Delta b_{\rm opt}$ and does not depend on B:

$$R_{\rm opt} \propto l_B \propto B^{-1/2}, \qquad \Delta E_0 \propto \Delta b_{\rm opt}. \tag{6.47}$$

Therefore, for given energy E, the action of the optimum fluctuation in which $E_0 = E$ is:

$$S(\Delta E_0) \sim \frac{R_{\rm opt}^2 \Delta b_{\rm opt}^2}{\beta_0} = K_1 \frac{l_B^2 \Delta E_0^2}{\beta_0} \tag{6.48}$$

$$\Rightarrow \rho(E) \sim \exp\left(-K_1 \frac{l_B^2 \Delta E_0^2}{\beta_0}\right) \tag{6.49}$$

(where $K_1 = \alpha(m_e c/\hbar e)^2$ and α is a numerical factor) and the variance of the distribution is proportional to B. Therefore, our simple arguments are expected to be valid when $(\beta_0/K_1 l_B^2)^{1/2} \ll \Delta E_0 \ll \hbar\omega_c$.

A completely analogous argument holds for the right tail of the first LL, near the band centre (region 3 in Fig. 6.1). In this case the optimal fluctuations are magnetic circular humps with height $\Delta b \ll B$ and the system is described by the Hamiltonian (6.41), provided that the replacements $\Delta b \to -\Delta b$ and $\Delta\Phi \to -\Delta\Phi$ are made in formulas (6.42) and (6.43) respectively. It is not difficult to show

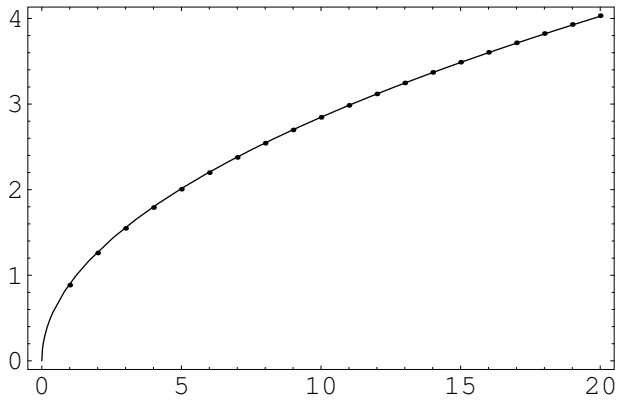

Figure 6.3: Diagram of $R_{\rm opt}$ as a function of B (arbitrary units).

that the angular momentum of the highest energy state $E_{0,max}$ in the first band of the new energy spectrum is $\mu = 0$. Therefore $E_{0,max}$ is the *lowest* level satisfying Eq. (6.46) and the leading exponential term of the DOS in the right tail shows the same dependence on the energy shift and B as Eq. (6.49).

In the case of long-range RMFs, the analysis of the DOS near the band centre is simpler: the localization radius of a typical optimum state (of the order of l_B) is much shorter than the radius of an optimal potential well (of the order of the correlation length $r_{\rm c}$), and the energy E of this state is thus given to a very good approximation by the first LL energy in the field $B - \Delta b$: $E = \hbar e(B-\Delta b)/(m_{\rm e}c)$. Therefore, the energy shift is proportional to Δb and the RMF acts as an effective random electrostatic potential. Since for long-range RMFs the radius of the well is the largest length scale, the probability distribution (6.29) can be approximately rewritten as

$$P[\Delta b] \sim \exp\left[-\frac{\Delta b^2}{\beta(0)}\right]. \tag{6.50}$$

Hence,

$$-\ln\rho(E) \sim \frac{\Delta E_0^2}{\epsilon_\beta^2}, \tag{6.51}$$

with $\epsilon_\beta = \hbar e\beta(0)^{1/2}/m_{\rm e}c$, and the exponent of the DOS does not depend on B, as long as the inequality $l_B \ll r_{\rm c}$ is fulfilled. Eq. (6.51) is valid if $\epsilon_\beta \ll \Delta E_0 \ll \hbar\omega_{\rm c}$.

The above analysis is valid both for electrons in a real, static RMF and for non-interacting CFs in a fictitious RMF. If we focus on CFs subjected to the Gaussian RMF described by the correlator (5.6) and we assume that $d \gg l_B$ (as is usually the case in GaAs-AlGaAs heterostructures), we can use formula (6.50).

From the correlator (4.38) we get

$$\beta(0) \sim \frac{n_0}{d^4} \left(\frac{\phi \Phi_0 \nu e^2}{\varepsilon \hbar \omega_c} \right)^2 , \tag{6.52}$$

where ϕ is an even integer and $\nu = 1/(\phi + 1)$, since we are considering the 0-th CFLL. For $\phi = 2$, the 0-th CFLL corresponds to the filling factor $\nu = 1/3$. We obtain from (6.50)

$$\rho(E) \sim \exp \left[-\frac{(B \Delta E_0)^2}{K_2} \right] , \tag{6.53}$$

where K_2 does not depend on B. Therefore, in the case of CFs, the exponent of the DOS is proportional to B^2, since the static Chern-Simons correlator (5.6) does depend on B.

Note that the fluctuations of the screened electrostatic potential due to donor impurities should also be taken into account when calculating the DOS of CFs in the tails. Since the probability distribution of a long-range, Gaussian stochastic potential is given by

$$P[\Delta V] \sim \exp \left[-\frac{\Delta V^2}{W_1} \right] \tag{6.54}$$

(where $W_1 = W(0)$ and $W(r)$ is the potential correlator) and $\Delta E_0 \sim \Delta V$, we obtain again a ΔE_0^2-dependence of the exponent of the DOS near the band center (assuming that the potential is weak). Clearly, these arguments are valid if $W_1 \ll \Delta E_0$. The exponent is independent on B, provided that the correlation radius of $V(\mathbf{r})$ is much larger than l_B.

Considerations similar to those presented above do yield a ΔE_n^2-dependence of the exponent of the DOS also in the tails of higher Landau bands, in the regions where $\Gamma_n \ll \Delta E_n \ll \hbar \omega_c$, In these regions of the spectrum, the DOS of non-interacting fermions in a RMF thus resembles the DOS of independent fermions in a Gaussian electrostatic potential, see section 3.3 and Refs. [74, 75].

As far as the prefactors in the exponent and the preexponential factors are concerned, more powerful approaches are needed to evaluate them. We will briefly discuss this point in the next subsection.

Near the band edge at $E \sim 0$ (corresponding to region 2 in Fig. 6.1), the energy dependence of the DOS is completely different. Let's consider first short-range RMFs: in this case states with arbitrarily small energies are expected to be localized in very large regions of area A, inside which $b \approx 0$ and outside which $b \approx B$. The action of these fluctuations is $S \sim \exp(-AB^2/\beta_0)$. Since these wells are very large, the ground state energy should depend weakly on the conditions on the boundary ∂A. Hence, we can assume that the wave function vanishes at the boundary ∂A. In this case, for a given energy E, the regions with the smallest area A (and thus the highest probability) for which the ground state

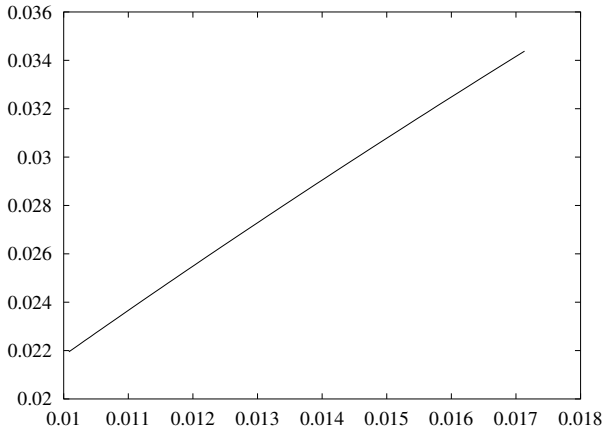

Figure 6.4: Diagram of the ground state energy E_{GS} in a magnetic well with $B = 0$ inside as a function of R^{-2}, where R is the radius of the well (E_{GS} and R in units of $\hbar\omega_c$ and l_B respectively).

energy coincides with E are 2D balls (by virtue of the isoperimetric inequality). The ground state wavefunction of a particle confined into a circular region of radius R is $J_0(\sqrt{\epsilon}r)$, where $\epsilon = 2m_eE/\hbar^2$, and its energy is $E \sim c_0\hbar^2/(2m_eR^2)$, with $c_0 \sim 5.78$. Therefore $R \propto E^{1/2}$ and the DOS is a non-analytic function of E:

$$\rho(E) \sim \exp\left(-K_3\frac{B^2}{\beta_0 E}\right), \tag{6.55}$$

with $K_3 = c_0\pi\hbar^2/2m_e$. The above argument is analogous to the argument used by Lifshitz to estimate the tail of the DOS of a particle subject to a Poissonian random potential generated by short-range, repulsive impurities in zero magnetic field [136, 138, 139].

One could argue that imposing that the wavefunction vanishes at ∂A is too crude an approximation for a magnetic well, even for large R. Therefore we calculated the exact ground state energy of the system as a function of the radius of the well: the results, plotted in fig. 6.4, show clearly that E_{GS} is inversely proportional to R^2.

Let's now consider RMFs with correlation length $r_c \geq l_B$: intuitively, for any correlation length r_c, there is a right neighbourhood of $E = 0$ such that, for each energy belonging to this interval, the optimum well has a radius much larger than the correlation length, $R \gg r_c$, or, equivalently, $E \ll \hbar^2/(m_e r_c^2)$. The larger the correlation length, the closer to the band edge the energies of the optimal states must be in order to fulfil that inequality. In this region, the action of $b(\mathbf{r})$ can be written as (6.55), where $\beta_0 \equiv \int \beta(\xi)d^2\xi$, and the DOS is given by (6.55). Hence, in the limit $E \to 0$, the length scale r_c becomes irrelevant and the behaviour of

the tail is "universal".

In the case of CFs, the picture is more complicated far from the center of the band, since CFs experience a stochastic electrostatic potential in addition to the RMF. Furthermore, the scalar potential and the RMF are not independent random quantities (see section 4.4).

Note the difference with respect to the tails of the DOS in a Gaussian random potential $V(\mathbf{r})$. In that case, the band edge is $-\infty$ and the behaviour of the tail is universal in the limit $E \to -\infty$. In contrast to the RMF case, states are localized inside deep, narrow wells in the region of large, negative energies and the radius of the wave function is thus the smallest length scale of the problem (unless $V(\mathbf{r})$ is assumed to be δ-correlated, an unphysical approximation in this region). At extremely negative energies, $E \to -\infty$, the kinetic energy becomes irrelevant and the tail is dominated by the potential energy, i.e. it is purely classical:

$$\ln \rho(E) \sim -E^2/2W(0), \tag{6.56}$$

where $W(r)$ is the potential correlator (see for instance [138, 140]).

6.3.2 Derivation of the saddle point equation

In this section we will derive the variational equations which determine the actual shape of the optimal fluctuations, following an approach which was originally developed by Houghton and Schäfer [137] in order to study the tails of the density of states in a random, electrostatic potential. Their approach is equivalent to Zittartz-Langer approach [135]. We will show that the qualitative conclusions of the previous section concerning the energy dependence of the DOS in the fluctuation region of Landau bands are correct.

Saddle point methods have already been used to study the DOS of fermions subject to some kind of magnetic disorder. In [141], the formal technique developed by Friedberg and Luttinger [136] was applied to a system of randomly distributed flux tubes of fixed strength. In the band edge near $E = 0$, they found an exponential DOS with exponent inversely proportional to the energy, as in (6.55). In [128], a field theoretical approach was used to calculate the DOS in a RMF with zero mean value near $E = 0$ but no definite conclusions were drawn about the actual shape of the tail. Furthermore, there are now many numerical studies of the spectrum of fermions in RMFs with different r_c and B [142].

Recently this subject has attracted the interest of the community of mathematical physicists [143, 144]. In particular, in the paper of Ueki [143], the upper and lower bounds for the logarithm of the *integrated* DOS of some simple Gaussian RMFs with zero mean have been evaluated.

As far as we know, nobody has tackled the problem of the tails of the DOS in a RMF with large B analytically so far.

In the following we will focus on the left tail of the first LL. According to formula (6.36), we must search for the maximum of the probability distribution (6.29) under the constraint $E_0 = E$. For the moment we choose a weaker constraint

$$\det\{H[b(\mathbf{r})] - E\} = 0, \tag{6.57}$$

or, equivalently, $E_n = E$ for some energy level E_n and we take the limit $E \to E_0$ later. Due to the constraint, the optimum fluctuation $\bar{b}(\mathbf{r})$ of the RMF must satisfy the following variational equation:

$$\int \beta^{-1}(\mathbf{s}-\mathbf{s}')\bar{b}(\mathbf{s}')d\mathbf{s}' + \mu \frac{\delta \det\{H[b(\mathbf{r})] - E\}}{\delta b(\mathbf{s})}\bigg|_{b=\bar{b}} = 0, \tag{6.58}$$

where μ is a Lagrange multiplier. Exploiting the relation

$$\det\{H[b(\mathbf{r}) - E\} = \exp(\mathrm{tr}\ln\{H[b(\mathbf{r})] - E\}), \tag{6.59}$$

the functional derivative can be evaluated and equation (6.58) becomes:

$$\int \beta^{-1}(\mathbf{s}-\mathbf{s}')\bar{b}(\mathbf{s}')d\mathbf{s}' + \mu\ \det\{H[b(\mathbf{r})] - E\} \sum_n \frac{1}{E_n - E}\frac{\delta E_n[b(\mathbf{r})]}{\delta b(\mathbf{s})}\bigg|_{b=\bar{b}} = 0. \tag{6.60}$$

If we write $\det\{H - E\}$ as the product of its eigenvalues $\prod_{n=0}^{\infty}(E_n - E)$ and we assume that the ground state energy $E_0[\bar{b}(\mathbf{r})]$ is equal to E, $E \to E_0$, we find

$$\int \beta^{-1}(\mathbf{s}-\mathbf{s}')\bar{b}(\mathbf{s}')d\mathbf{s}' + \mu \prod_{n=1}^{\infty}(E_n - E)\frac{\delta E_0[b(\mathbf{r})]}{\delta b(\mathbf{s})}\bigg|_{b=\bar{b}} = 0. \tag{6.61}$$

If we choose the Coulomb gauge, we can write the Hamiltonian explicitly as a function of $b(\mathbf{r})$. In this gauge, the vector potential related to $b(\mathbf{r})$ is given by

$$\mathbf{a}(\mathbf{r}) = \frac{1}{2\pi}\int \frac{\hat{z}\times(\mathbf{r}-\mathbf{r}')}{|\mathbf{r}-\mathbf{r}'|^2} b(\mathbf{r}')d\mathbf{r}' \tag{6.62}$$

and the operator equality $\hat{\mathbf{p}}\cdot\mathbf{a}(\hat{\mathbf{r}}) = \mathbf{a}(\hat{\mathbf{r}})\cdot\hat{\mathbf{p}}$ holds. For small deviations $\delta b(\mathbf{r})$ from the optimal configuration, $b = \bar{b} + \delta b$, we have, using perturbation theory,

$$E_0[\bar{b} + \delta b] - E_0[\bar{b}] \sim \frac{e}{m_e c}\langle\Psi_0|\Pi\cdot\delta\mathbf{a}|\Psi_0\rangle, \tag{6.63}$$

where $\mathbf{\Pi} \equiv \mathbf{p} + (e/c)\mathbf{A}(\mathbf{r}) + (e/c)\mathbf{a}(\mathbf{r})$. Here Ψ_0 and $\mathbf{a}$ are the ground state wave function and the vector potential related to $\bar{b}$ respectively and $\delta\mathbf{a}$ is the vector potential related to δb (in the Coulomb gauge).
The functional derivative $\delta E_0/\delta b(\mathbf{s})$ can now be calculated easily:

$$\begin{aligned}\frac{\delta E_0}{\delta b(\mathbf{s})}\bigg|_{b=\bar{b}} &= \frac{e}{m_e c}\langle\Psi_0|\mathbf{\Pi}\cdot\mathbf{a}_\Phi(\mathbf{r}-\mathbf{s})|\Psi_0\rangle \\ &= \frac{e}{c}\int \mathbf{j}_0\cdot\mathbf{a}_\Phi(\mathbf{r}-\mathbf{s})d^2\mathbf{r},\end{aligned} \tag{6.64}$$

where

$$\mathbf{a}_\Phi(\mathbf{r}-\mathbf{s}) = \frac{1}{2\pi}\frac{\hat{z}\times(\mathbf{r}-\mathbf{s})}{|\mathbf{r}-\mathbf{s}|^2} \tag{6.65}$$

is the vector potential of a singular flux tube of unit strength located at $\mathbf{s}$ and $\mathbf{j}_0 = \Psi_0^*\mathbf{\Pi}\Psi_0/2m_\mathrm{e}$ is the current flowing in the ground state. The variational equation (6.61) becomes:

$$\bar{b}(\mathbf{s}) = -\mu'(E)\frac{e}{c}\int d^2\mathbf{s}'\beta(\mathbf{s}-\mathbf{s}')\int d^2\mathbf{r}\;\mathbf{j}_0\cdot\mathbf{a}_\Phi(\mathbf{r}-\mathbf{s}'), \tag{6.66}$$

where $\mu'(E) \equiv \mu\prod_{n=1}^{\infty}(E_n - E)$.

If $\beta(\mathbf{s}-\mathbf{s}')$ is a function of the distance $|\mathbf{s}-\mathbf{s}'|$ only, then it is natural to assume that the optimum fluctuation is rotationally invariant and that the angular momentum of the ground state is zero (i.e. the eigenstate is real); then eq. (6.66) simplifies to

$$\bar{b}(\mathbf{s}) = -\mu'(E)\frac{e^2}{m_\mathrm{e}c^2}\int d^2\mathbf{s}'\beta(\mathbf{s}-\mathbf{s}')\langle\Psi_0|(\mathbf{A}+\mathbf{a})\cdot\mathbf{a}_\Phi(\hat{\mathbf{r}}-\mathbf{s}')|\Psi_0\rangle. \tag{6.67}$$

In the δ-correlated case (6.1), Eq. (6.67) can be written as:

$$\bar{b}(\mathbf{s}) = -\mu'(E)\beta_0 e^2/(m_\mathrm{e}c^2)\langle\Psi_0|(\mathbf{A}+\mathbf{a})\cdot\mathbf{a}_\Phi(\hat{\mathbf{r}}-\mathbf{s})|\Psi_0\rangle. \tag{6.68}$$

Equation (6.67), together with the Schrödinger equation

$$\frac{1}{2m_\mathrm{e}}\Pi^2\Psi_0 = E\Psi_0, \tag{6.69}$$

determines the optimal $b(\mathbf{r})$ and $\Psi_0(\mathbf{r})$. For zero angular momentum states, (6.69) reduces to

$$\frac{1}{2m_\mathrm{e}}\left[p^2 + \frac{e^2}{c^2}(\mathbf{A}(\mathbf{r})+\mathbf{a}(\mathbf{r}))^2\right]\Psi_0 = E\Psi_0. \tag{6.70}$$

If we consider the left tail (the right tail, respectively) of the n-th Landau band at energies close to the band center, we must take the limit $E \to E_{n,min}$ (resp. $E \to E_{n,max}$) in (6.60) (see formula (6.37)). Therefore, the two coupled equations which determine the optimal fluctuations are given again by (6.66) and (6.69), provided that the ground state wavefunction Ψ_0 is replaced with the state $\Psi_{n,min}$ corresponding to $E_{n,min}$ (resp. $E_{n,max}$) in (6.66) and (6.69).

As far as the right tail of the first LL is concerned, we expect that the angular momentum of $\Psi_{0,max}$ is zero (see the previous subsection). Hence, the optimal $\bar{b}(\mathbf{r})$ and $\Psi_{0,max}$ satisfy (6.67) and (6.70). Furthermore, $\Psi_{0,max}$ is the lowest energy state of the Hamiltonian (6.70), since the excited states of (6.70) are related to higher LLs.

So far we have not considered the fluctuations of the magnetic field around the saddle point configuration satisfying (6.66). Those fluctuations must be taken into account in order to determine the pre-exponential factor in the DOS. It turns out that this problem is much more difficult to solve than the analogous problem for electrostatic randomness, which was solved in [74, 75] near the centre of Landau bands. At the moment we are working on it. However, only the leading exponential term in the DOS can be extracted from experiments and this term can be fully determined within the Optimum Fluctuation Method.

6.3.3 Discussion of the results

We have solved equations (6.67) and (6.69) iteratively both in the limit $r_c \ll l_B$ and in the limit $r_c \ll l_B$ (short-range and long-range RMFs, respectively).

For each value of E, a rectangular magnetic well was first used in eq. (6.69); then the value of Ψ_0 so obtained and the same rectangular well were substituted in (6.67). The value of μ' was varied until the ground state energy in the new magnetic well $b(\mathbf{s})$ coming out of (6.67) was equal to E. The new Ψ_0 obtained from (6.69) and the "old" $b(\mathbf{s})$ were then substituted in (6.67) and so on. Near the band center, this iteration process converges very rapidly, while the convergence of the process is much slower near the band edge.

To simplify the calculations, we have considered RMFs with Gaussian correlators:

$$\beta(\mathbf{r}-\mathbf{r}') = \frac{\beta'}{2\pi r_c^2} \exp\left(-\frac{|\mathbf{r}-\mathbf{r}'|^2}{2r_c^2}\right). \tag{6.71}$$

In the short-range case, the optimal fluctuations near the band center are shallow wells (compared to B) with steep walls. A typical optimum well is plotted in fig. 6.5 for $r_c = 0.1 l_B$: it corresponds to an energy shift $\Delta E/0.5\ \hbar\omega_c \simeq 3.6 \cdot 10^{-2}$. In fig. 6.6 the ground state wavefunction in this fluctuation is shown. In fig. 6.7 we have plotted the action of the optimum fluctuation as a function of the energy shift ΔE (for $r_c = 0.1 l_B$): the dependence of S on ΔE^2 is linear, in agreement with our predictions in section 6.3.1.

In the case of long-range fields, the optimal fluctuations near the band centre are shallow wells as in Fig. 6.8 (for $r_c = 10 l_B$). The radius of the ground state is much smaller than the size of the well, see fig. 6.9. The parabolic dependence of the action of the optimum well on the energy shift ΔE was checked in the long-range case too.

As far as the region near the band edge is concerned, three typical optimal wells for short-range RMFs are shown in fig. 6.10. The energies of the ground states in these configurations are about 1-2 hundredths of the first LL energy $1/2\hbar\omega_c$. Inside the wells, the total field $B + b$ is zero. In fig. 6.11, the optimal wells corresponding to a short-range ($r_c^{SR} = 0.1 l_B$) and a long-range field ($r_c^{LR} = 10 l_B$) are plotted. The ground state energy in both wells is about

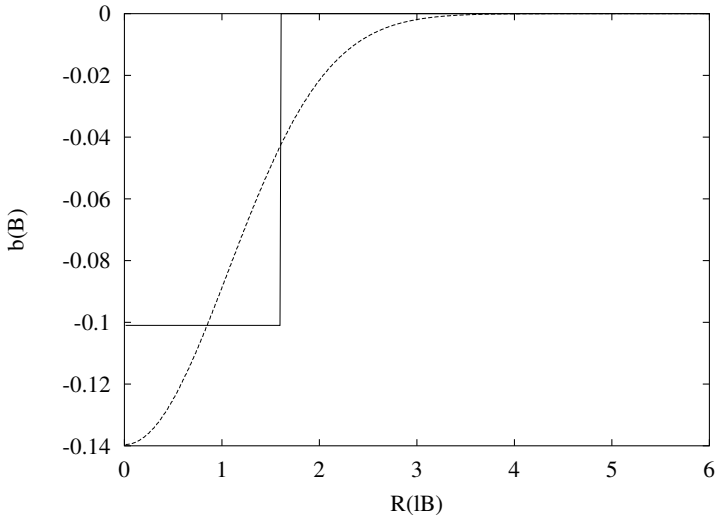

Figure 6.5: Plot of the optimum magnetic well and the trial rectangular well for $\Delta E = 3.6 \cdot 10^{-2}\hbar\omega_c$. Magnetic fields are in units of B ($r_c = 0.1 l_B$).

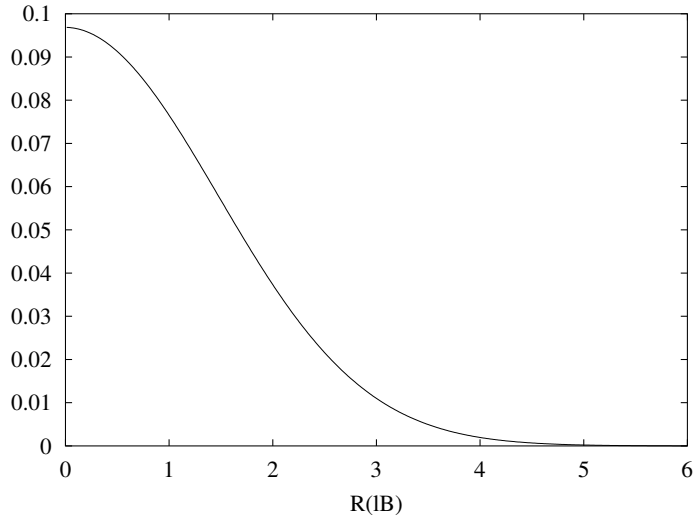

Figure 6.6: Plot of the ground state wavefunction in the optimum well depicted in Fig. 6.5 (correlation length $r_c = 0.1 l_B$).

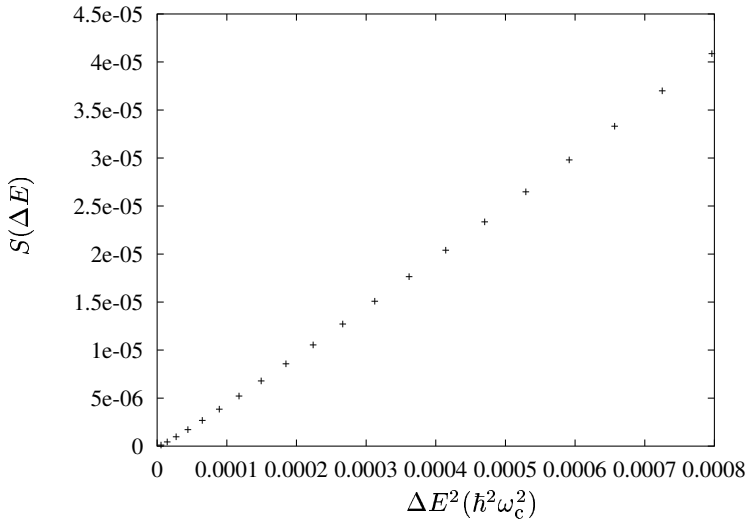

Figure 6.7: Plot of the action S of the optimum fluctuation as a function of ΔE^2. The energy shifts ΔE are in units of $\hbar\omega_c$ ($r_c = 0.1l_B$).

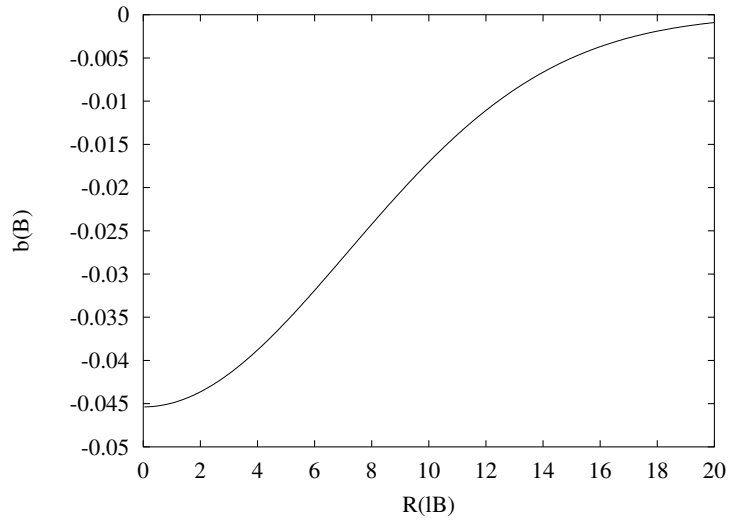

Figure 6.8: Plot of the optimum magnetic well for a long-range RMF ($r_c = 10l_B$) near the band centre. The energy shift is $\Delta E = 2.6 \cdot 10^{-2}\hbar\omega_c$.

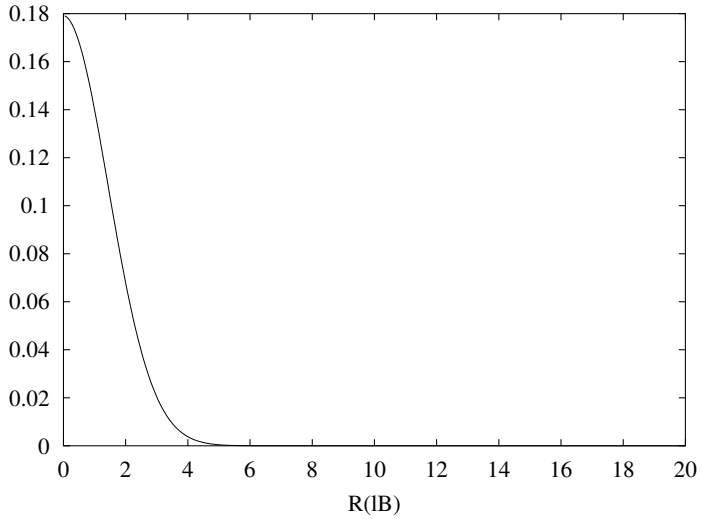

Figure 6.9: Plot of the ground state wavefunction in the optimum well plotted in Fig. 6.8 (correlation length $r_c = 10l_B$).

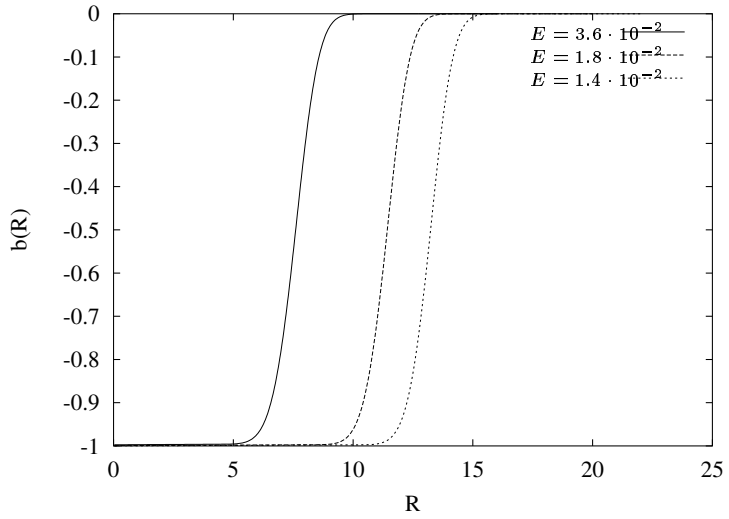

Figure 6.10: Plot of three optimal magnetic wells with different ground state energies E. E and b(R) are given in units of $\hbar\omega_c$ and B respectively ($r_c = 0.1l_B$).

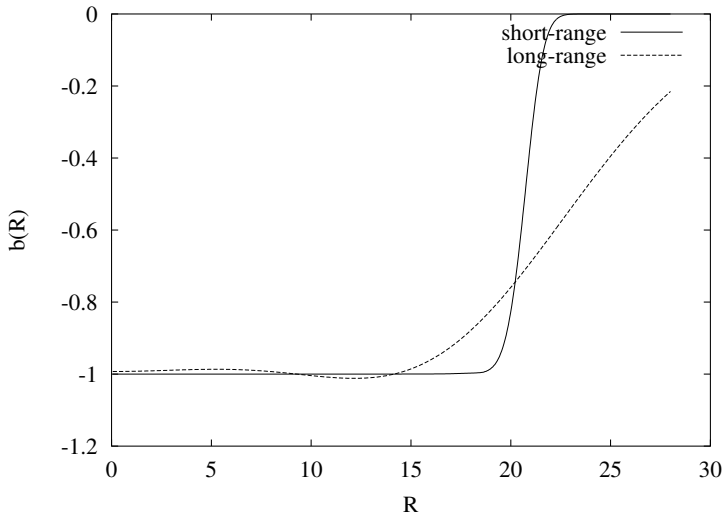

Figure 6.11: Plot of the optimal magnetic wells for short-range ($r_c = 0.1 l_B$) and long-range ($r_c = 10 l_B$) RMFs at energy $E \sim 7 \cdot 10^{-3} \hbar\omega_c$. Magnetic fields are in units of B.

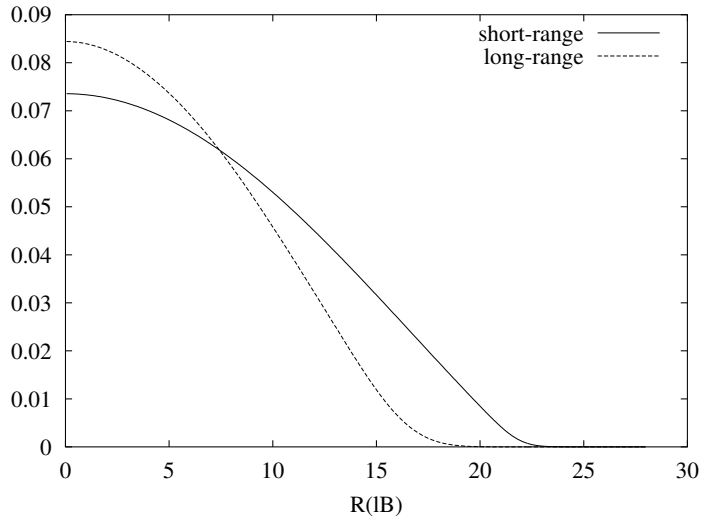

Figure 6.12: Plot of the ground states of the optimal wells depicted in Fig. 6.11. The energy of the states is approximately $E \sim 5 \cdot 10^{-3} \hbar\omega_c$.

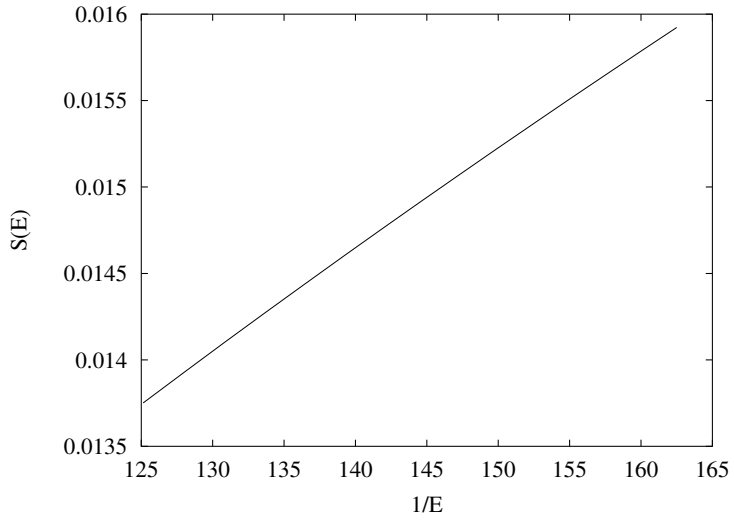

Figure 6.13: Plot of the action S of the optimum fluctuation as a function of $1/E$ near the band edge. E is given in units of $\hbar\omega_c$ ($r_c = 0.1 l_B$).

$5 \cdot 10^{-3}\hbar\omega_c$. The walls of the fluctuation corresponding to the short-range RMF are steeper than the walls of the "long-range" fluctuation but the radii of the wells are already larger than r_c^{LR}. For smaller energies the radius of the typical well would become much larger than r_c^{LR} and the length scales r_c^{LR} and r_c^{SR} would become totally irrelevant. In fig. 6.13 a plot of the action of the optimum fluctuation near the band edge as a function of the inverse of the energy E is shown (for $r_c = 0.1 l_B$): the dependence of S on $1/E$ is linear, again in agreement with our qualitative arguments in section 6.3.1.

Chapter 7

Conclusions

"De paz y de piedad
era la ciencia perfecta"
Juan de la Cruz

In this thesis we analyzed some topics concerning the properties of disordered low-dimensional systems in a magnetic field.

In part 1 we studied the averaged localization length of fermions in a quasi 1D system as a function of a magnetic field applied perpendicular to the wire. For this purpose, we considered a spectral correlation function, the autocorrelation function of spectral determinants (ASD), which is easier to study than the averaged two-terminal conductance since it does not necessitates the use of the full supersymmetric method. The localization length was derived as the crossover length scale from correlated to uncorrelated energy level statistics, as studied with the ASD. It was shown that its symmetry dependence coincides exactly with the localization length as defined by the exponential decay of the averaged two-terminal conductance.

Then, the ASD was used to get analytical information on the localization length in the crossover region, which was shown to be governed by the magnetic phase shifting rate, and thus strongly dependent on the geometry of the wire and the ratios of the elastic mean free path, the wire width, and the magnetic length.

In the future we would like to use the ASD as a tool to address the problem of localization in the recently discovered novel symmetry classes of disordered systems. Very recently, intriguing results on this topic have been obtained within the supersymmetric approach by Lamacraft, Simons and Zirnbauer [36] and it would be interesting to compare such results with those coming out of the ASD.

In the second part we turned to Composite Fermions. In chapter 5 we showed that a simple model of non-interacting spinful CFs with renormalized mass and g-factor yields a number of spin-polarization transitions of Quantum Hall systems

at fixed, fractional filling factor as a function of the external magnetic field. The results were shown to agree with recent experimental measurements.

Finally, in chapter 6 we studied the density of states of fermions in a random magnetic field with large mean value. After showing that conventional diagrammatic techniques become questionable in the presence of a RMF, we focused on the tails of broadened Landau bands. In these regions states are deeply localized inside low probability fluctuations of the RMF. This property of the eigenstates enabled us to calculate the leading exponential factor of the density of states in the tails by means of a saddle point method, the Houghton-Schäfer method, which is equivalent to the Optimum Fluctuation Method.

In the future, we plan to take into account fluctuations around the saddle point solution in order to calculate the preexponential factor in the DOS.

Appendix A

Evaluation of the eigenvalues of the Laplace-Beltrami Operator

The general definition of the Laplace-Beltrami Operator in an arbitrary parametrization of the matrix field Q is

$$\Delta_Q = \frac{1}{\sqrt{\bar{g}}} \sum_{i,k} \partial_k g^{ik} \sqrt{\bar{g}} \partial_i, \tag{A.1}$$

where the matrix g is the metric tensor, being defined by the quadratic form $ds^2 = 1/4 Tr dQ^2$ of the representation

$$ds^2 = d\mathbf{x}^T g d\mathbf{x}, \tag{A.2}$$

where $\mathbf{x}$ is the vector of parameters of the representation.

For $B \neq 0$, Q is an element of $U(2)/(U(1) \times U(1))$, obtained by enforcing the conditions $Q^2 = 1$, $Q^T C = CQ$, and $Q^+ = Q$, $[Q, \tau_3] = 0$. It can be parameterized as

$$Q = \begin{pmatrix} \cos\theta & e^{i\chi} \sin\theta \\ e^{-i\chi} \sin\theta & -\cos\theta \end{pmatrix}, \tag{A.3}$$

where $\theta \in [0, \pi]$ and $\chi \in [0, 2\pi]$. Thus,

$$ds^2 = d\theta^2 + \sin^2\theta d\chi^2. \tag{A.4}$$

and

$$g = \begin{pmatrix} 1 & 0 \\ 0 & \sin^2\theta \end{pmatrix}. \tag{A.5}$$

From Eqs. (A.1) and (A.5) follows:

$$\Delta_Q = \partial_{\lambda_D}(1 - \lambda_D^2)\partial_{\lambda_D} + \frac{1}{1 - \lambda_D^2} d\chi^2, \tag{A.6}$$

where $\lambda_D = \cos(\theta)$.

Note that the autocorrelation function depends on the energy difference ω through the coupling $\mathrm{Tr}\Lambda Q = 2 * 2\lambda_D$, so that only the part of the Laplacian which does not commute with $\mathrm{Tr}\Lambda Q$,

$$\Delta_Q^R = \partial_{\lambda_D}(1 - \lambda_D^2)\partial_{\lambda_D}. \tag{A.7}$$

enters in the frequency dependence of the autocorrelation function of spectral determinants, Eq. (2.39). Since $U(2)/(U(1) \times U(1)) = S_2$, the two sphere, this is equivalent to a the treatment of spherically symmetric potentials, and the Laplacian can be identified with the square of the angular momentum, $-\Delta_Q = \mathbf{L}^2$. $L_z = i\partial_\chi/(1 - \lambda_D^2)$ commutes with the Hamiltonian,

$$\bar{H} = -1/(2m_e)L^2 + i\alpha\frac{\pi}{4}\frac{\omega}{\Delta}z, \tag{A.8}$$

since $z = \cos\theta_D$ commutes with L_z. Therefore, $\omega \neq 0$ does not break the azimuthal symmetry of rotations around the z-axis.

For $B = 0$, Q is an element of the symplectic symmetric space, $Sp(2)/(Sp(1) \times Sp(1))$, obtained by enforcing the conditions $Q^2 = 1$, $Q^T C = CQ$, and $Q^+ = Q$. Thus

$$Q = \begin{pmatrix} c\mathbb{1} & A \\ A^+ & -c\mathbb{1} \end{pmatrix}. \tag{A.9}$$

with

$$A = \begin{pmatrix} a & b \\ b^* & -a^* \end{pmatrix}, \tag{A.10}$$

where $\mid a \mid^2 + \mid b \mid^2 + c^2 = 1$.

A matrix Q with the above symmetries can be represented as

$$Q = U^{-1}Q_c^0 U, \tag{A.11}$$

where

$$Q_c^0 = \begin{pmatrix} \cos\theta_C & i\sin\theta_C\tau_2 \\ i\sin\theta_C\tau_2 & -\cos\theta_C \end{pmatrix}, \tag{A.12}$$

and

$$U = V_C U_D. \tag{A.13}$$

In Eq. (A.13) U_D is given by

$$U_D = V_D^{-1}T_D^0 V_D, \tag{A.14}$$

and

$$V_{C,D} = \begin{pmatrix} \exp(i\phi_{C,D}\tau_3) & 0 \\ 0 & \mathbb{1} \end{pmatrix}, \tag{A.15}$$

$$T_D^0 = \begin{pmatrix} \cos\theta_D/2 & i\sin\theta_D/2 \\ i\sin\theta_D/2 & \cos\theta_D/2 \end{pmatrix}. \tag{A.16}$$

$\tau_i, i = 1, 2, 3$ are the Pauli matrices. Such a representation was first given by Altland, Iida and Efetov [145] to study the crossover between the spectral statistics of Gaussian distributed random matrices as the time reversal symmetry is broken, within the supersymmetric nonlinear sigma model. Here, in order to study the ASD, we need to consider only the compact block of the representation given there. We find that

$$ds^2 = \mathrm{Tr}\, dQ^2/4 = d\theta_C^2 + \cos^2\theta_C d\theta_D^2 + \sin^2\theta_C \phi_C^2 + \cos^2\theta_C \sin^2\theta_D d\phi_D^2 \quad \text{(A.17)}$$

and thereby the part of the Laplace operator which does not commute with $Tr\lambda Q = 4\lambda_C\lambda_D$ is given by Eq. (2.41),

$$\begin{aligned} \Delta_Q^R &= \partial_{\lambda_C}(1-\lambda_C^2)\partial_{\lambda_C} + 2\frac{1-\lambda_C^2}{\lambda_C}\partial_{\lambda_C} \\ &+ \frac{1}{\lambda_C^2}\partial_{\lambda_D}(1-\lambda_D^2)\partial_{\lambda_D}, \end{aligned} \quad \text{(A.18)}$$

where $\lambda_i = \cos\theta_i, i = C, D$.

For moderately strong spin-orbit scattering $1/\tau_{SO} > \Delta_C$, in the functional integral representation of the spectral determinants by Grassman vectors the a spin degree of freedom $\alpha = 2$ is introduced and the matrix C is substituted by $i\sigma_2\tau_1$[19], due to the time reversal of the spinor. The spin-orbit scattering reduces the Q matrix to unity in spin space. Thus, the matrix C has effectively the form τ_1. The condition $Q^T C = CQ$ leads therefore to a new symmetry class, where the spin symmetry is broken but the time reversal symmetry remains intact. Then, Q are 4×4- matrices on the orthogonal symmetric space $O(4)/(O(2) \times O(2))$ [33].

A matrix Q with the above symmetries can be represented as,

$$Q = V^{-1} Q_0 V, \quad \text{(A.19)}$$

with

$$Q_c^0 = \begin{pmatrix} \cos\hat{\theta} & \sin\hat{\theta} \\ \sin\hat{\theta} & -\cos\hat{\theta} \end{pmatrix}, \quad \text{(A.20)}$$

where

$$\hat{\theta} = \begin{pmatrix} \theta_1 & \theta_2 \\ \theta_2 & \theta_1 \end{pmatrix}, \quad \text{(A.21)}$$

with $\theta_i \in [0, \pi], i = 1, 2$, and

$$V = \begin{pmatrix} V_1 & 0 \\ 0 & V_2 \end{pmatrix}, \quad \text{(A.22)}$$

where

$$V_i = \exp(i\chi_i\tau_3), \quad \text{(A.23)}$$

with $\chi_i \in [0, 2\pi], i = 1, 2$.

Hence,

$$ds^2 = \text{Tr } Q^2/4 = \sum_{i=1,2} d\theta_i^2 + d\chi^T \hat{g_\chi} \chi, \tag{A.24}$$

where

$$\hat{g_\chi} = \begin{pmatrix} \sin^2\theta_1 + \sin^2\theta_2 & -\sin^2\theta_1 + \sin^2\theta_2 \\ -\sin^2\theta_1 + \sin^2\theta_2 & \sin^2\theta_1 + \sin^2\theta_2 \end{pmatrix}. \tag{A.25}$$

The part of the Laplace operator which does not commute with Tr $\lambda Q = 4\lambda_1\lambda_2$ is thus given by Eq. (2.45),

$$\Delta_Q^R = \sum_{l=1,2} \partial_{\lambda_l}(1 - \lambda_l^2)\partial_{\lambda_l}, \tag{A.26}$$

where $\lambda_i = \cos\theta_i, i = 1, 2$.

Appendix B

Non-interacting response function of CFs subject to a costant B

In this appendix we will calculate the response function K^0 of a system of CFs with p completely filled Landau levels following [96]. We will work in the Landau gauge $\mathbf{A} = (-\Delta B y, 0, 0)$.
From (4.22) follows that the components of $D^0_{\mu\nu}$ are:

$$D^0_{\mu\nu}(\mathbf{r}_1, t_1; \mathbf{r}_2, t_2) = -i\langle\psi_0|\Psi^\dagger(\mathbf{r}_1, t_1) j_\mu \Psi(\mathbf{r}_1, t_1)\Psi^\dagger(\mathbf{r}_2, t_2) j_\nu \Psi(\mathbf{r}_2, t_2)|\psi_0\rangle, \quad \text{(B.1)}$$

where ψ_0 is the noninteracting ground state,with p filled LLs.
We will now focus on the density-density component of D^0. Expressing the fermion operators in (B.1) in terms of Landau functions (3.9), the Fourier transform of D^0_{00} can be written as:

$$D^0_{00}(\mathbf{q}, \omega) = \sum_{n_1, n_2} \int dk_1 dk_2 \langle k_1, n_1|e^{i\mathbf{q}\cdot\mathbf{r}}|k_2, n_2\rangle\langle k_2, n_2|e^{-i\mathbf{q}\cdot\mathbf{r}}|k_1, n_1\rangle \times$$
$$\times D^0(n_1, n_2, \omega), \quad \text{(B.2)}$$

where

$$D^0(n_1, n_2) = \int d\omega' G^0_{n_1}(\omega' - \omega) G^0_{n_2}(\omega'). \quad \text{(B.3)}$$

In (B.3), $G^0_n(\omega)$ is the non-interacting Green's functions of fermions subjected to ΔB in the Landau representation. Assuming that $\mathbf{q} = (q, 0)$ (as we did in section 4.3), we have

$$D^0_{00}(\mathbf{q}, \omega) = \sum_{n_1=0}^{p-1} \sum_{n_2=p}^{\infty} C_{n_1,n_2} \int d\mathbf{r}_1 d\mathbf{r}_2 dk_1 dk_2 e^{i(q+k_1-k_2)(x_2-x_1)}$$

$$\times \prod_{i=1,2} H_{n_1}\left(\frac{y_i + k_1 l_{\Delta B}^2}{l_{\Delta B}}\right) e^{-\frac{1}{l_{\Delta B}^2}(y_i + k_1 l_{\Delta B}^2)^2}$$
$$\times \prod_{j=1,2} H_{n_2}\left(\frac{y_j + k_2 l_{\Delta B}^2}{l_{\Delta B}}\right) e^{-\frac{1}{l_{\Delta B}^2}(y_j + k_2 l_{\Delta B}^2)^2}$$
$$\times \left(\frac{1}{\omega - (\omega_{n_1} - \omega_{n_2}) + i\epsilon} - \frac{1}{\omega + (\omega_{n_1} - \omega_{n_2}) - i\epsilon}\right), \qquad \text{(B.4)}$$

where $C_{n_1,n_2} = (4\pi^2 2^{n_1} n_1!\, 2^{n_2} n_2!\, l_{\Delta B}^4)^{-1}$. The integration over x_1 and x_2 yields $\delta(q + k_1 - k_2)$. In order to calculate the remaining integrals, it is useful to introduce new integration variables:

$$\xi_i \equiv \frac{y_i}{l_{\Delta B}} + \frac{(k_1 + k_2) l_{\Delta B}}{2} \qquad \text{and} \qquad \eta \equiv \frac{(k_1 - k_2) l_{\Delta B}}{2}. \qquad \text{(B.5)}$$

Then

$$e^{-\frac{1}{l_{\Delta B}^2}(y_i + k_1 l_{\Delta B}^2)^2} e^{-\frac{1}{l_{\Delta B}^2}(y_i + k_2 l_{\Delta B}^2)^2} = e^{-(\xi_i^2 + \eta^2)} \qquad \text{(B.6)}$$

and

$$H_{n_1}\left(\frac{y_i + k_1 l_{\Delta B}^2}{l_{\Delta B}}\right) = H_{n_1}(\xi_i + \eta), \qquad H_{n_2}\left(\frac{y_i + k_2 l_{\Delta B}^2}{l_{\Delta B}}\right) = H_{n_2}(\xi_i - \eta). \qquad \text{(B.7)}$$

Moreover

$$\int dk_1 dk_2 dy_1 dy_2 = l_{\Delta B} \int d\xi_1 d\xi_2 d\eta d(k_1 + k_2) \qquad \text{(B.8)}$$

and $\delta(q + k_1 - k_2) = (l_{\Delta B}/2)\delta(\eta + l_{\Delta B} q/2)$. Carrying out the integration over $(k_1 + k_2)$, we get

$$D_{00}^0(\mathbf{q}, \omega) = \sum_{n_1=0}^{p-1} \sum_{n_2=p}^{\infty} l_{\Delta B}^2 C_{n_1,n_2} \int d\xi_1 \xi_2 d\eta e^{-(\xi_1^2 + \xi_2^2 + 2\eta^2)} \times$$
$$\times H_{n_1}(\xi_1 - \eta) H_{n_1}(\xi_2 - \eta) H_{n_2}(\xi_1 + \eta) H_{n_2}(\xi_2 + \eta)$$
$$\times \left(\frac{\delta(\eta + l_{\Delta B} q/2)}{\omega - (\omega_{n_2} - \omega_{n_1}) + i\epsilon} - \frac{\delta(-\eta + l_{\Delta B} q/2)}{\omega + (\omega_{n_2} - \omega_{n_1}) - i\epsilon}\right). \qquad \text{(B.9)}$$

Finally, exploiting the identity

$$\int_{-\infty}^{+\infty} e^{-x^2} H_{n_1}(x + y) H_{n_2}(x + z) = 2^{n_2} \sqrt{\pi}\, l_{\Delta B}!\, z^{n_2 - n_1} L_{n_1}^{n_2 - n_1}(-2yz), \qquad \text{(B.10)}$$

where $n_2 \geq n_1$, we obtain

$$D_{00}^0(\mathbf{q}, \omega) = \frac{p}{2\pi l_{\Delta B}^2} \sum_{n_1=0}^{p-1} \sum_{n_2=p}^{\infty} \frac{2\Delta\omega_c n_1!(n_2 - n_1) e^{-Y} Y^{n_2 - n_1}}{n_2![\omega_c - \Delta\omega_c (n_2 - n_1)^2]} [L_{n_1}^{n_2 - n_1}]^2$$
$$= \frac{1}{2\pi\Delta\omega_c} q^2 \Sigma_0, \qquad \text{(B.11)}$$

where $Y = l_{\Delta B}^2 q^2/2$ and

$$\Sigma_0 \equiv \frac{1}{p}\sum_{n_1=0}^{p-1}\sum_{n_2=p}^{\infty}\frac{n_1!(n_2-n_1)e^{-Y}Y^{n_2-n_1-1}}{n_2![(\omega/\Delta\omega_{\rm c})^2-(n_2-n_1)^2]}[L_{n_1}^{n_2-n_1}(Y)]^2. \tag{B.12}$$

Similar (albeit slightly more complicated) calculations yield:

$$D_{10}^0(\mathbf{q},\omega) = -D_{01}^0(\mathbf{q},\omega) = \frac{ipq}{2\pi}\Sigma_1 \tag{B.13}$$

$$D_{11}^0(\mathbf{q},\omega) = \frac{p\Delta\omega_{\rm c}}{2\pi}\Sigma_2, \tag{B.14}$$

where

$$\begin{aligned}\Sigma_1 &\equiv \frac{1}{p}\sum_{n_1=0}^{p-1}\sum_{n_2=p}^{\infty}\frac{n_1!(n_2-n_1)e^{-Y}Y^{n_2-n_1-1}}{n_2![(\omega/\Delta\omega_{\rm c})^2-(n_2-n_1)^2]}[L_{n_1}^{n_2-n_1}]^2\Lambda(n_1,n_2,Y)\\ \Sigma_2 &\equiv \frac{1}{p}\sum_{n_1=0}^{p-1}\sum_{n_2=p}^{\infty}\frac{n_1!(n_2-n_1)e^{-Y}Y^{n_2-n_1-1}}{n_2![(\omega/\Delta\omega_{\rm c})^2-(n_2-n_1)^2]}[L_{n_1}^{n_2-n_1}]^2[\Lambda(n_1,n_2,Y)]^2\end{aligned} \tag{B.15}$$

and

$$\begin{aligned}\Lambda(n_1,n_2,Y) = \frac{1}{2}[&YL_{n_1-1}^{n_2-n_1+1}(Y)(1-\delta_{n_1,0}) - (n_1+1)L_{n_1+1}^{n_2-n_1-1}(Y) +\\ &-n_2L_{n_1}^{n_2-n_1-1}(Y) + YL_{n_1}^{n_2-n_1+1}(Y)].\end{aligned}$$

Since the diamagnetic term E is

$$E = \frac{e^2 n_{\rm e}}{m_{\rm e}}\begin{pmatrix}0&0\\0&1\end{pmatrix} = \frac{p\Delta\omega_{\rm c}}{2\pi}\begin{pmatrix}0&0\\0&1\end{pmatrix}, \tag{B.16}$$

the total non-interacting response function $K^0 = D^0 + E$ is given by (4.28).

It is easy to calculate the small q, ω limit of Σ_i: since $Y \propto q^2$, in this limit the sums in (B.12) and (B.15) are restricted to a limited range of n_1 and n_2: $n_2 - n_1 = 1, 2$ and $n_1 < p$, $n_2 \geq p$. Hence, to lowest order in q and ω

$$\begin{aligned}\Sigma_0 &\sim -1 - (\omega/\Delta\omega_{\rm c})^2 + (3/8)pl_{\Delta B}^2 q^2,\\ \Sigma_1 &\sim -1 - (\omega/\Delta\omega_{\rm c})^2 + (3/4)pl_{\Delta B}^2 q^2,\\ \Sigma_2 &\sim -1 - (\omega/\Delta\omega_{\rm c})^2 + pl_{\Delta B}^2 q^2.\end{aligned} \tag{B.17}$$

Appendix C

Acknowledgments

First of all I would like to thank my supervisor, Prof. Bernhard Kramer, for introducing me into the subject and for encouraging me to develop my own ideas. He also gave me the opportunity to participate in a number of international workshops, as well as the possibility to carry on a fruitful collaboration with my former supervisor in Genoa.

Then I wish to express my gratitude to Stefan Kettemann for his continuous support and for many enlightening discussions.

I also acknowledge very useful discussions with Mikhail Raikh, Vladimir Fal'ko, Tomi Ohtsuki, Roberto Raimondi, Arturo Tagliacozzo and Rudolf Morf.

I would like to thank warmly all my colleagues and friends in Hamburg, especially Alex, Sebastian, Siawoosh, Maxim, Virgilio, Till, Stefan D., Kai, Grzegorz, Jun-Ichiro, Karel and Assia. I am indebted to my former colleagues Andrea and Ole and to Alex for introducing me to the mysteries of the German language.

A special mention goes to my friend and colleague Eros for his quick mind, wit and humour. I shared quite a few enjoyable moments with him.

I would also like to thank my old friends in Genoa and around the world: Marco, Dario, Ale Esposito, Guido, Ilaria, Barre, Claudio and especially my best friend Luca.

Finally, I am very grateful to my family for their moral support and encouragement.

Bibliography

[1] N. M. Ashcroft and N. D. Mermin, *Solid State Physics*, Rinehart and Winston, Philadelphia (1976).

[2] E. Abrahams, P. W. Anderson, D. C. Licciardello, V. Ramakrishnan, Phys. Rev. Lett **42** 673(1979).

[3] L. P. Gor'kov, A. I. Larkin, D. E. Khmel'nitskii, Pis'ma Zh. Eksp. Teor. Fiz. **30** , 248 (1979) [JETP Lett. **30**, 228 (1979)].

[4] P.A. Lee, T.V. Ramakrishnan, Rev. of Mod. Phys. **57**, 287 (1985); B. Kramer and A. MacKinnon, Rep. Prog.Phys. **56**, 1469 (1993); C. W. J. Beenakker, Rev. Mod. Phys. **69**, 731 (1997).

[5] F. Wegner, Z. Phys. B **25**, 327 (1976).

[6] J. Rammer, *Quantum Transport Theory*, Perseus Books, Reading (1998).

[7] B. L. Altshuler, D. E. Khmelmitskii, A. I. Larkin, and P. A. Lee, Phys. Rev. **B 22**, 5142 (1980).

[8] A. Kawabata, Solid State Commun. **34**, 431 (1980).

[9] B. L. Altshuler, A. G. Aronov, Pis'ma Zh. Eksp. Teor. Fiz. **33**, 515 (1981)[JETP Lett. **33**,499 (1981)].

[10] V. K. Dugaev, D. E. Khmel'nitskii, Sov. Phys. JETP **59**, 1038 (1984).

[11] C. W. J. Beenakker, H. van Houten, Phys. Rev. **B 37**, 6544 (1988).

[12] B. L. Altshuler, A. G. Aronov, D.E. Khmelnitskii, J. Phys. C **15**, 7367 (1982).

[13] B. L. Altshuler, A.G. Aronov in *Electron-electron Interactions in Disordered Systems*, North Holland (1985).

[14] J. Rammer and A. Schmid, Phys. Rev. B **34**, 1352 (1986).

[15] S. Hikami, A. I. Larkin and Y. Nagaoka, Prog. Theor. Phys. **63**, 707 (1980).

[16] G. Bergmann, Solid State Commun. **42**, 815 (1982).

[17] *Feynman Lectures III* (edited by R. P. Feynman, R. B. Leighton and M. Sands), Addison-Wesley, London-Reading (1971).

[18] K. B. Efetov, *Supersymmetry in Disorder and Chaos*, Cambridge University Press, Cambridge (1997).

[19] K. B. Efetov, A. I. Larkin, D. E. Khmel'nitskii, Zh. Eksp. Teor. Fiz. **79**, 1120(1980) [Sov. Phys. JETP **52**, 568(1980)].

[20] K. B. Efetov, Adv. Phys. **32**, 53 (1983).

[21] K. B. Efetov, A. I. Larkin, Zh. Eksp Teor. Fiz. **85**, 764(1983) [Sov. Phys. JETP **58**, 444].

[22] M. E. Gershenson et al., Phys. Rev. Lett. **79**, 725(1997); Phys. Rev. B **58**, 8009 (1998).

[23] S.Kettemann and R.Mazzarello, Phys.Rev.B **65**, 085318 (2002).

[24] S. Kettemann, Phys. Rev. **B 59**, 4799 (1999); S. Kettemann, Phys. Rev. B Rapid Commun. **62**, R13282 (2000).

[25] S. Kettemann and A. Tsvelik, Phys. Rev. Lett. **82**, 3689 (1999).

[26] L. P. Gor'kov, O. N. Dorokhov, and F. V. Prigara, Zh. Eksp. Teor. Fiz. **84**, 1440 (1983)[Sov. Phys. JETP **57**, 838 (1983)]. B. L. Alt'shuler, B. I. Shklobskii, Zh. Eksp. Teor. Fiz. **91**, 127 (1986) [Sov. Phys. JETP **64**,127 (1986)].

[27] B. L. Altshuler, I. Kh. Zharekeshev, S. A. Kotochigova, and B. I. Shklovskii, Zh. Eksp. Teor. Fiz. **94**, 343 (1988) [Sov. Phys. JETP **67**, 625 (1988)]; S. N. Evangelou and E. N. Economou, Phys. Rev. Lett. **68**, 361 (1992); E. Hofstetter and M. Schreiber, Phys. Rev. Lett. **73**, 3137 (1994); I. Kh. Zharekeshev and B. Kramer, Phys. Rev. Lett. **79**, 717(1997).

[28] A. Altland, D. Fuchs, Phys. Rev. Lett. **74**, 4269(1995).

[29] T. Guhr, A. Mller-Groeling, and H.A. Weidenmller, Phys. Rep. 299, 189 (1998).

[30] A. D. Mirlin, Phys. Rep. **326**, 259 (2000).

[31] F. Haake, *Quantum Signatures of Chaos*, Springer-Verlag, Berlin (2001).

[32] S. Helgason, *Differential Geometry and Symmetric Spaces* Academic Press, New York (1962).

[33] F. Wegner, Z. Phys. B **36**, l209 (1979); F. Wegner, Nucl. Phys. B **316**, 663 (1989); S. Hikami, Prog. Theor. Phys. **64**, 1466 (1980).

[34] M. R. Zirnbauer, J. Math. Phys. **37**, 4986 (1996).

[35] M. Titov, P. W. Brouwer, A. Furusaki, C. Mudry, Phys. Rev. B **63**, 235318 (2001).

[36] A. Lamacraft, B. D. Simons, and M. R. Zirnbauer, cond-mat/0402588.

[37] D. Taras- Semchuk, K. B. Efetov, Phys. Rev. Lett. **85**, 1060 (2000); Phys. Rev. B **64**, 115301 (2001).

[38] Ya. M. Blanter, A. D. Mirlin, B. A. Muzykantskii, Phys. Rev. B **B 63**, 235315 (2001).

[39] S. Kettemann, Phys. Rev. B **69**, 035339 (2004); S. Kettemann, B. Kramer, and T. Ohtsuki, cond-mat/0307044; B. Kramer, S. Kettemann, and T. Ohtsuki, Physica E **20**, 172 (2003).

[40] F. Haake, M. Kus, H.-J. Sommers, H. Schomerus, and K. Zychowski, J. Phys. A **29**, 3641 (1996).

[41] S. Kettemann, D. Klakow, U. Smilamsky, J. Phys. A ,3643(1997).

[42] F. J. Dyson, J. Math. Phys. **3**, 1199 (1962).

[43] M. R. Zirnbauer Phys. Rev. Lett. **69**,1584 (1992), A. D. Mirlin, A. Muller-groeling, M. R. Zirnbauer, Ann. Phys. (New York) **236**, 325 (1994); P. W. Brouwer, K. Frahm, Phys. Rev. **B 53** ,1490 (1996); B. Rejaei, Phys. Rev. **B 53**, R13235 (1996).

[44] N. F. Mott, E. A. Davis, *E*lectronic Processes in Non-crystalline Materials, Clarendon Press, Oxford (1971).

[45] A. V. Andreev and B. D. Simons Phys. Rev. Lett. 75, 2304-2307 (1995).

[46] J. P. Bouchaud, J. Phys. 1 (France) **1**, 985 (1991).

[47] I. V. Lerner, Y. Imry, Europhys. Lett. **29**, 49(1995).

[48] M. Leadbeater, V. I. Falko, C. J. Lambert, Phys. Rev. Lett. 81, 1274 (1998).

[49] J.-L. Pichard, M. Sanquer, K. Slevin, and P. Debray, Phys. Rev. Lett. 65, 1812 (1990); H. Schomerus and C.W. Beenakker, Phys. Rev. Lett. 84, 3927 (2000); M. Weiss, T. Kottos, T. Geisel, Phys. Rev. **B 63**, R081306(2001).

[50] A. Miller and E. Abrahams, Phys. Rev. **120** , 745 (1960).

[51] B. I. Shklovskii and A. L. Efros, *Electronic Properties of Doped Semiconductors*, Springer-Verlag, New York (1984).

[52] V. Ambegaokar, B. I. Halperin and J. S. Langer, Phys. Rev. **B4** , 2612 (1971).

[53] M. Pollak, J. Non-Crystal. Solids **11** , 1 (1972).

[54] B. I. Shklovskii and A. L. Efros, Zh. Eksp. Teor. Fiz. **60** , 867 (1971) [Sov. Phys. JETP **33** , 468 (1971)].

[55] N. F. Mott, J. Non-Crystal. Solids **1** , 1 (1968).

[56] P. A. Lee, Phys. Rev. Lett.**53** , 2042 (1984); R. A. Serota, R. K. Kalia and P. A. Lee, Phys. Rev. **B 33** , 8441 (1986).

[57] M. E. Raikh and I. M. Ruzin, Zh. Eksp. Teor. Fiz. **95** , 1113 (1989) [Sov. Phys. JETP **68** , 642 (1989)].

[58] J. Kurkijarvi, Phys. Rev. **B 8** , 922 (1973).

[59] M. E. Raikh and A. L. Efros, Pis'ma Zh. Eksp. Teor. Fiz. **45** , 225 (1987) [JETP Lett. **45** , 280 (1987)].

[60] A. I. Larkin and D. E. Khmel'nitskii, Zh. Eksp. Teor. Fiz. **83** , 140 (1982) [Sov. Phys. JETP **56** , 647 (1982)].

[61] Yu. B. Khavin, M. E. Gershenson, A. L. Bogdanov, Phys. Rev. Lett. **81**, 1066 (1998).

[62] K. von Klitzing, G. Gorda and M. Pepper, Phys. Rev. Lett. **45**, 494 (1980).

[63] D. C. Tsui, H. L. Stoermer and A. C. Gossard, Phys. Rev. Lett. **48**, 1559 (1982).

[64] W.Pan, H. L. Stoermer, D. C. Tsui, L. N. Pfeiffer, K. W. Baldwin and K. W. West, Phys. Rev. Lett. **90**, 016801 (2003).

[65] H. L. Störmer, Physica B **177**, 401 (1992).

[66] R. E. Prange, Phys. Rev. B **23**, 4802, (1981).

[67] R. B. Laughlin, Phys. Rev. B **23**, 5632 (1981).

[68] B. I. Halperin, Phys. Rev. B **25**, 2185 (1982).

[69] H. Levine, S. B. Libby and A. M. M. Pruisken, Phys. Rev. Lett. **51**, 1915 (1983).

[70] E. Fradkin, *Field Theories of Condensed Matter Systems*, Addison-Wesley, New York (1994).

[71] T. Ando, J. Phys. Soc. Jpn., **37**, 1233 (1974); T. Ando, Y. Matsumoto, Y. Uemura, J. Phys. Soc. Jpn., **39**, 279 (1975).

[72] M. Janssen, O. Viehweger, U. Fastenrath, and J. Hajdu, *Introduction to the Theory of the Integer Quantum Hall Effect*, VCH, Weinheim, 1994.

[73] F. Wegner, Z. Phys. B **51**, 279 (1983).

[74] L. B. Ioffe and A. Larkin, Sov. Phys. JETP **54**, 556 (1981).

[75] I. Affleck, J. Phys. C **17**, 2323 (1984).

[76] M. R. Zirnbauer, Ann. Phys. **3**, 513 (1994).

[77] M. R. Zirnbauer, hep-th/9905054; M. J. Bhaseen, I. I. Kogan, O. A. Solovev, N. Taniguchi, and A. M. Tsvelik, Nucl. Phys. B **580**, 688 (2000).

[78] B. Kramer, Y. Ono and T. Ohtsuki, Surf. Sci. **196**, 127 (1988).

[79] G. V. Mil'nikov and I. M. Sokolov, JETP Lett. **48**, 536 (1988).

[80] B. Huckestein and B. Kramer, Phys. Rev. Lett. **64**, 1437 (1990).

[81] B. Miek, Europhys. Lett. **13**, 453 (1990).

[82] R. B. Laughlin, Phys. Rev. Lett. **50**, 1395 (1983).

[83] A. Comtet (Ed.), T. Jolicoeur (Ed.), S. Ouvry (Ed.), and F. David (Ed.), *Topological Aspects of Low Dimensional Systems*, Springer-Verlag, Berlin, and Les Editions de Physique, Les Ulis, 2000.

[84] O. Heinonen (Ed.), *Composite Fermions*, World Scientific, Singapore (1998).

[85] F. D. M. Haldane and E. H. Rezayi, Phys. Rev. Lett. **54**, 237 (1985).

[86] S. A. Trugman and S. Kivelson, Phys. Rev. B **31**, 5280 (1985); V. L. Pokrovskii and A. L. Talapov, J. Phys. C **18**, L691 (1985).

[87] J. K. Jain, Phys. Rev. Lett. **63**, 199 (1989).

[88] B. I. Halperin, Phys. Rev. Lett. **52**, 1583 (1984).

[89] G. S. Boebinger, A. M. Chang, H. L. Stormer, and D. C. Tsui, Phys. Rev. Lett. **55**, 1606 (1985); G. S. Boebinger, H. L. Stormer, D. C. Tsui, A. M. Chang, J. C. M. Hwang, A. Y. Cho, C. W. Tu, and G. Weimann, Phys. Rev. B **36**, 7919 (1987); R. L. Willett, H. L. Stormer, D. C. Tsui, A. C. Gossard, and J. H. English, Phys. Rev. B **37**, 8476 (1988).

[90] F. D. M. Haldane, Phys. Rev. Lett. **51**, 605 (1983).

[91] A. Lopez and E. Fradkin, Phys. Rev. B **44**, 5246 (1991).

[92] , S. Das Sarma and A. Pinczuk (Ed.), *Perspectives in Quantum Hall Effects*, Wiley, New York (1997).

[93] J. H. Smet, S. Jobst, K. von Klitzing, D. Weiss, W. Wegscheider, and V. Umansky, Phys. Rev. Lett. **83**, 2620 (1999).

[94] B. I. Halperin, P. A. Lee, and N. Read, Phys. Rev. B **47**, 7312 (1993).

[95] A. L. Fetter, C. B. Hanna and R. B. Laughlin, Phys. Rev. B **39**, 9679 (1989).

[96] Y.-H. Chen, F. Wilczek, E. Witten and B. I. Halperin, Int. J. Mod. Phys. **3**, 1001 (1989).

[97] S. H. Simon and B. I. Halperin, Phys. Rev. B **48**, 17368 (1993).

[98] A. Stern and B. I. Halperin, Phys. Rev. B **52**, 5890 (1995).

[99] A. G. Aronov, A. D. Mirlin and P. Wölfle, Phys. Rev. B **49**, 16609 (1994).

[100] D. G. Polyakov, F. Evers, A. D. Mirlin and P. Wölfle, Physica B **256**, 441 (1998); F. Evers, A. D. Mirlin, D. G. Polyakov, and P. Wölfle, Phys. Rev. B **60**, 8951 (1999).

[101] P. Wölfle, in: *Advances in Solid State Physics 40*, ed. by B. Kramer p. 78 (Vieweg Verlag, Wiesbaden 2000).

[102] I. V. Kukushkin, K. v.Klitzing, and K. Eberl, Phys. Rev. Lett. **82**, 3665 (1999).

[103] E.Mariani, R.Mazzarello, M.Sassetti and B.Kramer, Ann.Phys. **11**, 926 (2002).

[104] B. I. Halperin, Helv. Phys. Acta **56**, 75 (1983).

[105] T. Chakraborty and F. C. Zhang, Phys. Rev. B **29**, 7032 (1984); F. C. Zhang and T. Chakraborty, Phys. Rev. B **30**, 7320 (1984).

[106] X. C. Xie, Y. Guo, and F. C. Zhang, Phys. Rev. B **40** , 3487 (1989); P. Beran and R. Morf, Phys. Rev. B **43**, 12654 (1991).

[107] J. P. Eisenstein, H. L. Stormer, L. N. Pfeiffer, and K. W. West, Phys. Rev. Lett. **62**, 1540 (1989).

[108] J. P. Eisenstein, H. L. Stormer, L. N. Pfeiffer, and K. W. West, Phys. Rev. B **41**, 7910 (1990).

[109] I. V. Kukushkin, K. v.Klitzing, K. G. Levchenko, and Yu. E. Lozovik, JETP Letters **70**, 730 (1999).

[110] I. V. Kukushkin, J. H. Smet, K. v.Klitzing, and K. Eberl, Phys. Rev. Lett. **85**, 3688 (2000).

[111] S. Melinte, N. Freytag, M. Horvatic, C. Berthier, L. P. Levy, V. Bayot, and M. Shayegan, Phys. Rev. Lett. **84**, 354 (2000).

[112] E. Mariani, N. Magnoli, F. Napoli, M. Sassetti and B. Kramer, Phys. Rev. B **66**, 241303 (2002).

[113] A. Lopez and E. Fradkin, Phys. Rev. B **51**, 4347 (1995).

[114] S. S. Mandal and V. Ravishankar, Phys. Rev. B **54** , 8688 (1996).

[115] N. d'Ambrumenil and R. H. Morf, Phys. Rev. B **40**, 6108 (1989).

[116] K. Park and J. K. Jain, Phys. Rev. Lett. **80**, 4237 (1998).

[117] R. Shankar, Phys. Rev. B **63**, 085322 (2001); G. Murthy, cond-mat 0004334; G. Murthy, cond-mat 0008259.

[118] I. V. Kukushkin, J. H. Smet, K. von Klitzing, and W. Wegscheider, Nature **415**, 409 (2002).

[119] S. S. Mandal and J. K. Jain, cond-mat/0103631.

[120] R. R. Du, A. S. Yeh, H. L. Stormer, D. C. Tsui, L. N. Pfeiffer, and K. W. West, Phys. Rev. Lett. **75**, 3926 (1995).

[121] V. I. Falko, Phys. Rev. B **46**, 4320 (1992).

[122] R. Mazzarello, S. Kettemann and B. Kramer, to be submitted.

[123] L. B. Ioffe and A. I. Larkin, Phys. Rev. B, **39**, 8988 (1989); N. Nagaosa and P. A. Lee, Phys. Rev. Lett. **64**, 2450 (1990).

[124] S. J. Bending, K. von Klitzing and K. Ploog, Phys. Rev. Lett. **65**, 1060 (1990); A. Geim, S. J. Bending, and I. V. Grigorieva, Phys. Rev. Lett. **69**, 2252 (1992); A. Geim, S. J. Bending, I. V. Grigorieva, and M. G. Blamire, Phys. Rev. B **49**, 5749 (1994).

[125] F. B. Mancoff, R. M. Clarke, C. M. Marcus, S. C. Zhang, K. Campman, and A. C. Gossard, Phys. Rev. B **51**, 13269 (1995).

[126] M. Ando, A. Endo, S. Katsumoto, and Y. Iye, Physica B **284**, 1900 (2000).

[127] B. L. Altshuler and L. B. Ioffe, Phys. Rev. Lett. **69** , 2979 (1992).

[128] D. V. Khveshchenko and S. V. Meshkov, Phys. Rev. B **47**, 12051 (1993).

[129] E. Altshuler, A. G. Aronov, A. D. Mirlin, and P. Wölfle, Europhys. Lett. **29**, 239 (1995);

[130] D. V. Khveshchenko, Phys. Rev. Lett. **77**, 1817 (1996).

[131] A. Shelankov, Phys. Rev. B **62**, 3196 (2000).

[132] R. Mazzarello, unpublished.

[133] A. D. Mirlin, E. Altshuler, and P. Wölfle, Ann. Phys. **5**, 281 (1996).

[134] I. M. Lifshitz, Sov. Phys. Usp. **7**, 549 (1965) .

[135] J. Zittartz and J. S. Langer, Phys. Rev. **148**, 741 (1966).

[136] R. Frieberg and J. M. Luttinger, Phys. Rev. B **12**, 4460 (1975).

[137] A. Houghton and L. Schaefer, J. Phys. A **12**, 1309 (1979).

[138] I. M. Lifshitz, S. A. Gredeskul, and L. A. Pastur, *Introduction to the Theory of Disordered Systems* (Wiley, New York, 1997).

[139] H. Leschke and S. Warzel, Phys. Rev. Lett. **92**, 086402 (2004).

[140] H. Leschke, P. Müller, and S. Warzel, Markov Processes and Related Fields **9**, 729 (2003).

[141] G. Gavazzi, J. M. Wheatley and A. J. Schofield, Phys. Rev. B **47**, 15170 (1993).

[142] T. Ohtsuki, Y. Ono, and B. Kramer, Journ. Phys. Soc. Japan **2**, 685 (1994); A. Barelli, R. Fleckinger, and T. Ziman, Phys. Rev. B **49**, 3340 (1994).

[143] N. Ueki, Ann. Henri Poincare' **1**, 473 (2000).

[144] S. Nakamura, Ann. Henri Poincare' **1**, 823 (2000); S. Nakamura, Commun. Math. Phys. **214**, 565 (2000); S. Nakamura, Proc. Indian Acad. Sci. **112**, 183 (2002).

[145] A. Altland, S. Iida, K. B. Efetov, *J. Phys. A* **26** (1993) 3545.